



HELSINKI UNIVERSITY OF TECHNOLOGY
Department of Electrical and Communications Engineering
Communications Laboratory

Mohammad Azizul Hasan

**Performance Evaluation of
WiMAX/IEEE 802.16 OFDM Physical
Layer**

Thesis submitted in partial fulfillment of the requirements for the degree of
Master of Science in Technology, Espoo, June 2007

Supervisor: Prof. Riku Jäntti

Instructor: Lic. Tech. Boris Makarevitch

| | |
|---|------------------------|
| Author: Mohammad Azizul Hasan | |
| Name of the Thesis: Performance Evaluation of WiMAX/IEEE 802.16 OFDM Physical Layer | Number of pages: 96 |
| Date: 08-06-2007 | |
| Department: Department of Electrical and Communications Engineering | |
| Professorship: S-72 Communications Engineering | |
| Supervisor: Prof. Riku Jäntti | |
| Instructor: Lic. Tech. Boris Makarevitch | |
| Abstract | |
| <p>Fixed Broadband Wireless Access (BWA) is a promising technology which can offer high speed voice, video and data service up to the customer end. Due to the absence of any standard specification, earlier BWA systems were based on proprietary standard. IEEE 802.16 WirelessMAN standard specifies a Medium Access Control (MAC) layer and a set of PHY layers to provide fixed and mobile Broadband Wireless Access (BWA) in broad range of frequencies. The WiMAX forum has adopted IEEE 802.16 OFDM PHY layer for the equipment manufacturer due to its robust performance in multipath environment. The thesis investigates the simulation performance of IEEE 802.16 OFDM PHY layer. The Stanford University Interim (SUI) channel models are selected for the wireless channel in the simulation. The evaluation was done in simulation developed in MATLAB. Perfect channel estimation is assumed.</p> | |
| Keywords: BWA, IEEE 802.16, WirelessMAN, FEC, OFDM | |

Acknowledgements

This thesis is carried out in the Communications Laboratory, Department of Electrical and Communications Engineering, Helsinki University of Technology, Espoo, Finland. I would like to take the opportunity to thank people who guided and supported me during this work.

I wish to express my deepest gratitude to my supervisor Professor Riku Jäntti for showing great interest in my work and for the guidance that he has given me. I also wish thank my instructor Lic. Tech. Boris Makarevitch for his valuable advice and guidance.

Thanks to my siblings and friends for their encouragement and mental support during my stay in Finland.

I am very grateful to my parents who have always given me their unconditional caring and support.

Mohammad Azizul Hasan

8th June, Espoo, Finland

Table of Contents

| | |
|---|-------------|
| Acknowledgements | iii |
| List of Figures | vi |
| List of Tables..... | viii |
| List of Abbreviations | ix |
| List of Symbols..... | xi |
| | |
| Chapter 1: Introduction | 1 |
| 1.1 Motivation..... | 1 |
| 1.2 Objective..... | 2 |
| 1.2 Structure of the thesis | 3 |
| | |
| Chapter 2: IEEE802.16: Evolution and Architecture..... | 4 |
| 2.1 Evolution of IEEE family of standard for BWA | 4 |
| 2.1.1 IEEE 802.16-2001 | 5 |
| 2.1.2 IEEE 802.16a-2003 | 6 |
| 2.1.4 IEEE 802.16-2004 | 7 |
| 2.1.5 IEEE 802.16e-2005..... | 7 |
| 2.2 IEEE 802.16 Protocol Layers | 8 |
| 2.3 Network Architecture and Deployment Topology: | 9 |
| 2.5 WiMAX forum and adaptation of IEEE 802.16..... | 12 |
| | |
| Chapter 3: IEEE 802.16 Physical Layer | 14 |
| 3.1 IEEE 802.16 PHY Layer:..... | 14 |
| 3.1.1 Supported Band of Frequency | 14 |
| 3.2 IEEE 802.16 PHY interface variants..... | 15 |
| 3.2.1 WirelessMAN-SC™ | 15 |
| 3.2.3 WirelessMAN-SCa™ | 16 |
| 3.2.3 WirelessMAN-OFDM™ | 16 |
| 3.2.4 WirelessMAN-OFDMA™: | 16 |
| 3.2.5 WirelessHUMAN™: | 17 |
| 3.4 WirelessMAN OFDM PHY Layer..... | 17 |
| 3.4.1 Flexible Channel Bandwidth: | 18 |
| 3.4.2 Robust Error Control Mechanism | 18 |
| 3.4.3 Adaptive Modulation and Coding..... | 18 |
| 3.4.4 Adaptive Antenna System | 19 |
| 3.4.5 Transmit Diversity:..... | 19 |
| 3.3 OFDM | 20 |
| 3.3.1 OFDM BASIC:..... | 20 |
| 3.3.2 OFDM SYSTEM IMPLEMENTATION | 22 |
| 3.3.3 CYCLIC PREFIX ADDITION | 23 |
| 3.3.4 OFDM SYSTEM DESIGN CONSIDERATIONS..... | 24 |
| 3.3.5 BENEFITS AND DRAWBACKS of OFDM: | 25 |
| 3.3.6 APPLICATION | 26 |
| | |
| Chapter 4: Simulation Model | 27 |
| 4.1 OFDM Symbol Parameter..... | 27 |

| | |
|---|-----------|
| 4.2 Physical Layer Setup | 28 |
| 4.2.1 Scrambler | 29 |
| 4.2.2 Reed-Solomon Encoder..... | 30 |
| 4.2.3 Convolutional Encoder | 30 |
| 4.2.4 Interleaver | 32 |
| 4.2.5 Constellation Mapper..... | 32 |
| 4.2.6 IFFT | 33 |
| 4.2.7 Cyclic Prefix Insertion:..... | 33 |
| 4.3 Channel Model: | 33 |
| 4.3.1 Stanford University Interim (SUI) Channel Models..... | 35 |
| 4.3.2 SUI channel models Implementation:..... | 39 |
| Chapter 5: Simulation Results | 41 |
| 5.1 The Simulator..... | 41 |
| 5.2 Physical layer performance results..... | 42 |
| 5.2.1 Scatter Plots | 42 |
| 5.2.2 BER Plots | 52 |
| 5.2.3 BLER Plots..... | 55 |
| 5.2.4 Effect of Forward Error Correction..... | 58 |
| 5.2.5 Effect of Reed-Solomon Encoding | 62 |
| 5.2.6 Effect of Bit interleaver | 66 |
| 5.2.7 Spectral Efficiency..... | 71 |
| Chapter 6: Conclusion and Future Work..... | 73 |
| 6.1 Conclusion | 73 |
| 6.2 Future Works..... | 74 |
| Reference | 75 |
| Appendix..... | 78 |

List of Figures

| | |
|---|----|
| Figure 2.1: IEEE 802.16 Protocol Stack | 9 |
| Figure 2.2: A typical IEEE 802.16 Network..... | 10 |
| Figure 2.3 : Application scenario..... | 12 |
| Figure 3.1: Block diagram of a generic MCM transmitter..... | 21 |
| Figure 3.2: Comparison between conventional FDM and OFDM [21]..... | 21 |
| Figure 3.3: Basic OFDM transmitter and receiver..... | 23 |
| Figure 3.4 : Cyclic Prefix in OFDM..... | 24 |
| Figure 4.1 Simulation Setup | 29 |
| Figure 4.2: Channel Encoding Setup..... | 29 |
| Figure 4.3: Channel Decoding Setup | 29 |
| Figure 4.4: PRBS generator for randomization..... | 30 |
| Figure 4.5: Convolutional encoder of rate $\frac{1}{2}$ | 31 |
| Figure 5.1: Scatter Plots for BPSK modulation (RS-CC 1/2) in SUI-1 channel model..... | 43 |
| Figure 5.2: Scatter Plots for QPSK modulation (RS-CC 1/2) in SUI-1 channel model.... | 44 |
| Figure 5.3: Scatter Plots for QPSK modulation (RS-CC 3/4) in SUI-1 channel model.... | 45 |
| Figure 5.4: Scatter Plots for 16-QAM modulation (RS-CC 1/2) in SUI-1 channel model. | 46 |
| Figure 5.5: Scatter Plots for 16-QAM modulation (RS-CC 3/4) in SUI-1 channel model. | 47 |
| Figure 5.6: Scatter Plots for 64-QAM modulation (RS-CC 2/3) in SUI-1 channel model. | 48 |
| Figure 5.7: Scatter Plots for 64-QAM modulation (RS-CC 3/4) in SUI-1 channel model. | 49 |
| Figure 5.8: Scatter Plots for 64-QAM modulation (RS-CC 2/3) in different SUI channel model | 50 |
| Figure 5.9: Scatter plot for 16-QAM with different CP length on SUI-5 channel model.... | 51 |
| Figure 5.10: BER vs. SNR plot for different coding profiles on SUI-1 channel..... | 52 |
| Figure 5.11: BER vs. SNR plot for different coding profiles on SUI-2 channel..... | 53 |
| Figure 5.12: BER vs. SNR plot for different coding profiles on SUI-3 channel..... | 53 |
| Figure 5.13: BER vs. SNR plot for 16-QAM 1/2 on different SUI channel..... | 55 |
| Figure 5.14: BLER vs. SNR plot for different modulation and coding profile on SUI-1..... | 56 |
| Figure 5.15: BLER vs. SNR plot for different modulation and coding profile on SUI-2..... | 56 |
| Figure 5.16: BLER vs. SNR plot for different modulation and coding profile on SUI-3..... | 57 |
| Figure 5.17: BLER vs. SNR plot for 64-QAM 2/3 modulation and coding profile on different SUI channel..... | 58 |
| Figure 5.18: Effect of FEC in QPSK 1/2 on SUI-3 channel model | 59 |

| | |
|--|----|
| Figure 5.19: Effect of FEC in QPSK 1/2 on SUI-3 channel model | 59 |
| Figure 5.20: Effect of FEC in 16-QAM 1/2 on SUI-3 channel model..... | 60 |
| Figure 5.21: Effect of FEC in 16-QAM 1/2 on SUI-3 channel model..... | 60 |
| Figure 5.22: Effect of FEC in 64-QAM 2/3 on SUI-3 channel model..... | 61 |
| Figure 5.23: Effect of FEC in 64-QAM 2/3 on SUI-3 channel model..... | 61 |
| Figure 5.24: Effect of Reed Solomon encoding in QPSK 1/2 on SUI-3 channel model | 63 |
| Figure 5.25: Effect of Reed Solomon encoding in QPSK 1/2 on SUI-3 channel model | 63 |
| Figure 5.26: Effect of Reed Solomon encoding in 16-QAM 1/2 on SUI-3 channel model.. | 64 |
| Figure 5.27: Effect of Reed Solomon encoding in 16-QAM 1/2 on SUI-3 channel model.. | 64 |
| Figure 5.28: Effect of Reed Solomon encoding in 64-QAM 2/3 on SUI-3 channel model | 65 |
| Figure 5.29: Effect of Reed Solomon encoding in 64-QAM 2/3 on SUI-3 channel model | 65 |
| Figure 5.30: Effect of Block interleaver in BPSK 1/2 on SUI-2 channel model..... | 67 |
| Figure 5.31: Effect of Block interleaver in BPSK 1/2 on SUI-2 channel model..... | 67 |
| Figure 5.32: Effect of Block interleaver in QPSK 1/2 on SUI-2 channel model | 68 |
| Figure 5.33: Effect of Block interleaver in QPSK 1/2 on SUI-2 channel model | 68 |
| Figure 5.34: Effect of Block interleaver in 16-QAM 1/2 on SUI-2 channel model | 69 |
| Figure 5.35: Effect of Block interleaver in 16-QAM 1/2 on SUI-2 channel model | 69 |
| Figure 5.36: Effect of Block interleaver in 64-QAM 2/3 on SUI-2 channel model | 70 |
| Figure 5.37: Effect of Block interleaver in 64-QAM 2/3 on SUI-2 channel model | 70 |
| Figure 5.38 Spectral efficiency of different modulation and coding profile on SUI-1 channel model | 71 |
| Figure 5.39: Spectral efficiency of QPSK 3/4 on SUI-1, 2 and 3 channel model. | 72 |

List of Tables

| | |
|--|----|
| Table 2.1: Comparison of IEEE standard for BWA | 7 |
| Table 3.1: Air Interface Nomenclature and Description[1]..... | 17 |
| Table 3.2: Mandatory channel coding per modulation | 19 |
| Table 4.1:OFDM Symbol Parameters | 28 |
| Table 4.2:Puncturing configuration of the convolutional code..... | 31 |
| Table 4.3: Terrain type for SUI channel..... | 36 |
| Table 4.4: General characteristics of SUI channels..... | 36 |
| Table 4.5: Delay spread of SUI channels..... | 37 |
| Table 4.6:Tap power(omni directional antenna) of SUI channels..... | 38 |
| Table 4.7: 90% K factor (omni directional antenna) of SUI channels | 38 |
| Table 5.1: SNR required at BER level 10-3 for different modulation and coding profile .. | 54 |
| Table 5.2:SNR required at BLER level 10-2 for different modulation and coding profile .. | 57 |
| Table 5.3: Performance improvement due to RS Coding..... | 62 |
| Table 5.4: Performance improvement due to bit interleaving | 66 |

List of Abbreviations

| | |
|----------|---|
| AAS | Adaptive Antenna System |
| ADC | Analog to Digital Conversion |
| ADSL | Asymmetric Digital Subscriber Line |
| ATM | Asynchronous Transfer Mode |
| BER | Bit Error Rate |
| BLER | Block Error Rate |
| BPSK | Binary Phase Shift Keying |
| BS | Base Station |
| BWA | Broadband Wireless Access |
| BTC | Block Turbo Coding |
| CC | Convolutional Code |
| CP | Cyclic Prefix |
| CPE | Customer Premises Equipment |
| CPS | Common Part Sublayer |
| CS | Convergence Sublayer |
| DAC | Digital to Analog Conversion |
| DAMA | Demand Assignment Multiple Access |
| DFS | Dynamic Frequency Selection |
| DFT | Discrete Fourier Transform |
| DL | Downlink |
| DSL | Digital Subscriber Line |
| ETSI | European Telecommunications Standards Institute |
| FDD | Frequency Division Duplexing |
| FDM | Frequency Division Multiplexing |
| FEC | Forward Error Correction |
| FFT | Fast Fourier Transform |
| HIPERMAN | High PERFORMANCE Metropolitan Area Network |
| ICI | Inter-Carrier Interference |
| IDFT | Inverse Discrete Fourier Transform |

| | |
|-------------|---|
| IEEE | Institute of Electrical and Electronics Engineers |
| ISI | Inter-Symbol Interference |
| LAN | Local Area Network |
| LOS | Line of Sight |
| MAC | Medium Access Control |
| MCM | Multi-Carrier Modulation |
| NLOS | Non Line of Sight |
| N-WEST | National Wireless Electronics Systems Testbed |
| OFDM | Orthogonal Frequency Division Multiplexing |
| OFDMA | Orthogonal Frequency Division Multiple Access |
| PCI | Peripheral Component Interconnect |
| PMP | Point-to Multipoint |
| PTP | Point-to-Point |
| QAM | Quadrature Amplitude Modulation |
| QoS | Quality of Service |
| QPSK | Quadrature Phase-Shift keying |
| SDU | Service Data Unit |
| SNR | Signal to Noise Ratio |
| SS | Subscriber Stations |
| STBC | Space Time Block Code |
| SUI | Stanford University Interim |
| TDD | Time Division Duplexing |
| TDM | Time Division Multiplexing |
| TDMA | Time Division Multiple Access |
| UL | Uplink |
| WAN | Wide Area Network |
| WiMAX | Worldwide Interoperability for Microwave Access |
| WirelessMAN | Wireless Metropolitan Network |

List of Symbols

| | |
|-------------------|--|
| τ_{\max} | Maximum delay spread |
| N_{used} | Number of Used Subcarrier |
| n | Sampling Factor |
| G | Ratio of Guard time to useful symbol time |
| N_{FFT} | Smallest power of 2 greater than N_{used} |
| F_s | Sampling Frequency |
| Δf | Subcarrier Spacing |
| T_b | Useful Symbol Time |
| T_g | CP Time |
| T_s | OFDM Symbol Time |
| N | The number of overall bytes after encoding |
| K | The number of data bytes before encoding |
| T | The number of data bytes which can be corrected |
| N_{cbps} | The number of coded bits per the allocated subchannels per OFDM symbol |
| N_{cpc} | The number of coded bits per subcarriers |
| M | The complex constant of the complex Gaussian set |
| σ^2 | The variance of the complex Gaussian set |
| f_m | Doppler frequency |

Chapter 1

Introduction

This chapter provides a brief introduction on the motivation of this thesis work and its objective as well. At last the structure of the document is provided.

1.1 Motivation

Broadband Wireless Access (BWA) has emerged as a promising solution for last mile access technology to provide high speed internet access in the residential as well as small and medium sized enterprise sectors. At this moment, cable and digital subscriber line (DSL) technologies are providing broadband service in this sectors. But the practical difficulties in deployment have prevented them from reaching many potential broadband internet customers. Many areas throughout the world currently are not under broadband access facilities. Even many urban and suburban locations may not be served by DSL connectivity as it can only reach about three miles from the central office switch [3]. On the other side many older cable networks do not have return channel which will prevent to offer internet access and many commercial areas are often not covered by cable network. But with BWA this difficulties can be overcome. Because of its wireless nature,

it can be faster to deploy, easier to scale and more flexible, thereby giving it the potential to serve customers not served or not satisfied by their wired broadband alternatives.

IEEE 802.16 standard for BWA and its associated industry consortium, Worldwide Interoperability for Microwave Access (WiMAX) forum promise to offer high data rate over large areas to a large number of users where broadband is unavailable. This is the first industry-wide standard that can be used for fixed wireless access with substantially higher bandwidth than most cellular networks [2]. Wireless broadband systems have been in use for many years, but the development of this standard enables economy of scale that can bring down the cost of equipment, ensure interoperability, and reduce investment risk for operators.

The first version of the IEEE 802.16 standard operates in the 10–66GHz frequency band and requires line-of-sight (LOS) towers. Later the standard extended its operation through different PHY specification to 2-11 GHz frequency band enabling non line of sight (NLOS) connections, which require techniques that efficiently mitigate the impairment of fading and multipath [4]. Taking the advantage of OFDM technique the PHY is able to provide robust broadband service in hostile wireless channel.

The OFDM-based physical layer of the IEEE 802.16 standard has been standardized in close cooperation with the European Telecommunications Standards Institute (ETSI) High PERFORMANCE Metropolitan Area Network (HiperMAN) [5]. Thus, the HiperMAN standard and the OFDM-based physical layer of IEEE 802.16 are nearly identical. Both OFDM-based physical layers shall comply with each other and a global OFDM system should emerge [4]. The WiMAX forum certified products for BWA comply with the both standards.

1.2 Objective

The objective of this thesis is to implement and simulate the IEEE 802.16 OFDM physical layer using Matlab in order to have better understanding of the standard and the

system performance. This involves studying, through simulation, the various PHY modulation, coding schemes and interleaving in the form of bit-error-rate (BER) and block-error-rate (BLER) performance under reference channel models.

1.2 Structure of the thesis

The first chapter is an introduction of the thesis work. The rest of the chapters are organized as follows:

Chapter 2 discusses the evolution and architecture of the IEEE 802.16 standard for BWA.

Chapter 3 provides an overview of the IEEE 802.16 physical layer and OFDM technique.

Chapter 4 deals with the PHY layer simulation model and SUI channel model employed by this thesis.

Chapter 5 provides results obtained from the PHY layer simulation.

Chapter 6 concludes with a summary of the research done and recommendation for future work.

Chapter 2

IEEE 802.16: Evolution and Architecture

This chapter discusses the evolution of the IEEE 802.16 standard for BWA to form the basis for further discussion. The protocol layers of the standard have been overviewed to get the idea of interaction between different protocol stack. The chapter ends up with a brief discussion of the IEEE 802.16 based network architecture, deployment topology, application scenarios and its affiliation with WiMAX forum.

2.1 Evolution of IEEE family of standard for BWA

In late 90's many telecommunication equipment manufacturers were beginning to develop and offer products for BWA. But the Industry was suffering from an interoperable standard. With the need of a standard, The National Wireless Electronics Systems Testbed (N-WEST) of the U.S National Institute of Standards and Technology (NIST) called a meeting to discuss the topic in August 1998 [6]. The meeting ended up with a decision to organize within IEEE 802. The effort was welcomed in IEEE 802, which led to formation of the 802.16 Working Group. Since then, the Working Group members have been working a lot to develop standards for fixed and mobile BWA. IEEE

Working Group 802.16 on Broadband Wireless Access (BWA) standard is responsible for development of 802.16 and the included WirelessMan™ air interface, along with associated standards and amendments.

The IEEE 802.16 standard contains the specification of Physical (PHY) and Medium Access Control (MAC) layer for BWA. The first version of the standard IEEE802.16-2001 [7] was approved on December 2001 and it has gone through many amendments to accommodate new features and functionalities. The current version of the standard IEEE 802.16-2004 [1], approved on September 2004, consolidates all the previous versions of the standards. This standard specifies the air interface for fixed BWA systems supporting multimedia services in licensee and licensed exempt spectrum [1]. The Working Group approved the amendment IEEE 802.16e-2005 [8] to IEEE802.16-2004 on February 2006. To understand the development of the standard to its current stage, the evolution of the standard is presented here.

2.1.1 IEEE 802.16-2001

This first issue of the standard specifies a set of MAC and PHY layer standards intended to provide fixed broadband wireless access in a point-to-point (PTP) or point-to-multipoint (PMP) topology [7]. The PHY layer uses single carrier modulation in the 10 – 66 GHz frequency range.

Transmission times, durations and modulations are assigned by a Base Station (BS) and shared with all nodes in the network in the form of broadcast Uplink and Downlink maps. Subscribers need only to hear the base station that they are connected and do not need to listen any other node of the network. Subscriber Stations (SS) has the ability to negotiate for bandwidth allocation on a burst to-burst basis, providing scheduling flexibility.

The standard employs QPSK, 16-QAM and 64-QAM as modulation scheme. These can be changed from frame to frame and from SS to SS, depending on the robustness of the connection. The standard supports both Time Division Duplexing (TDD) and Frequency Division Duplexing (FDD) as duplexing technique.

An important feature of 802.16-2001 is its ability to provide differential Quality of Service (QoS) in the MAC Layer. A Service Flow ID does QoS check. Service flows are characterized by their QoS parameters, which can then be used to specify parameters like maximum latency and tolerated jitter [10]. Service flows can be originated either from BS or SS. 802.16-2001 works only in (Near) Line of Sight (LOS) conditions with outdoor Customer Premises Equipment (CPE).

2.1.2 IEEE 802.16a-2003

This version of the standard amends IEEE 802.16-2001 by enhancing the medium access control layer to support multiple physical layer specifications and providing additional physical layer specifications. This was ratified by IEEE 802.16 working group in January 2003[9]. This amendment added physical layer support for 2-11 GHz. Both licensed and license-exempt bands are included. Non Line of Sight (NLOS) operation becomes possible due to inclusion of below 11 GHz range, extending the geographical reach of the network. Due to NLOS operation multipath propagation becomes an issue. To deal with multipath propagation and interference mitigation features like advanced power management technique and adaptive antenna arrays were included in the specification [9]. The option of employing Orthogonal Frequency Division Multiplexing (OFDM) was included as an alternative to single carrier modulation.

Security was improved in this version; many of privacy layer features became mandatory while in 802.16-2001 they were optional. IEEE 802.16a also adds optional support for mesh topology in addition to PMP.

2.1.3 IEEE 802.16c-2002

In December 2002, IEEE Standards Board approved amendment IEEE 802.16c [6]. In this amendment detailed system profiles for 10-66 GHz were added and some errors and inconsistencies of the first version of the standard were corrected.

2.1.4 IEEE 802.16-2004

802.16-2001, 802.16a-2003 and 802.16c-2002 were all together consolidated and a new standard was created which is known as 802.16-2004. In the beginning, it was published as a revision of the standard under the name 802.16REVd, but the changes were so genuine that the standard was reissued under the name 802.16-2004 at September 2004. In this version, the whole family of the standard is ratified and approved.

Table 2.1: Comparison of IEEE standard for BWA

| | IEEE 802.16-2001 | IEEE 802.16a | IEEE802.16-2004 | IEEE 802.16e-2005 |
|-------------------------------|--|--|---|--|
| Completed | December 2001 | January 2003 | June 2004 | December 2005 |
| Spectrum | 10-66 GHz | 2-11 GHz | 2-11 GHz | 2-6 GHz |
| Popagation/channel conditions | LOS | NLOS | NLOS | NLOS |
| Bit Rate | Up to 134 Mbps (28 MHz channelization) | Up to 75 Mbps (20 MHz channelization) | Up to 75 Mbps (20 MHz channelization) | Up to 15Mbps (5 MHz channelization) |
| Modulation | QPSK, 16-QAM (optional in UL), 64-QAM (optional) | BPSK, QPSK, 16-QAM, 64-QAM, 256-QAM (optional) | 256 subcarriers OFDM, BPSK, QPSK, 16-QAM, 64-QAM, 256-QAM | Scalable OFDMA, QPSK, 16-QAM, 64-QAM, 256-QAM (optional) |
| Mobility | Fixed | Fixed | Fixed/Nomadic | Portable/mobile |

2.1.5 IEEE 802.16e-2005

This amendment was included in the current applicable version of standard IEEE 802.16-2004 in December 2005. This includes the PHY and MAC layer enhancement to enable combined fixed and mobile operation in licensed band.

2.2 IEEE 802.16 Protocol Layers

The IEEE 802.16 standard is structured in the form of a protocol stack with well defined interfaces. As shown in Figure 2.1, the MAC layer is formed with three sublayers:

- .. Service Specific Convergence Sublayer (CS)
- .. MAC Common Part Sublayer (CPS) and
- .. Privacy Sublayer.

The MAC CS receives higher level data through CS Service Access Point (SAP) and provides transformation and mapping into MAC Service Data Unit (SDU). MAC SDUs are then received by MAC CPS through MAC SAP. The specification targeted two types of traffic transported through IEEE 802.16 networks: Asynchronous Transfer Mode (ATM) and Packets. Thus, Multiple CS specifications are available for interfacing with various protocols.

The MAC CPS is the core part of the MAC layer, defining medium access method. The CPS provides functions related to duplexing and channelization, channel access, PDU framing, network entry and initialization. This provides the rules and mechanism for system access, bandwidth allocation and connection maintenance. QoS decisions for transmission scheduling are also performed within the MAC CPS.

The Privacy layer lies between the MAC CPS and the PHY layer. Security is a major issue for public networks. This sub layer provides the mechanism for encryption and decryption of data transferring to and from PHY layer and is also used for authentication and secure key exchange. Data, PHY control, statistics are transferred between the MAC CPS and the PHY through the PHY SAP.

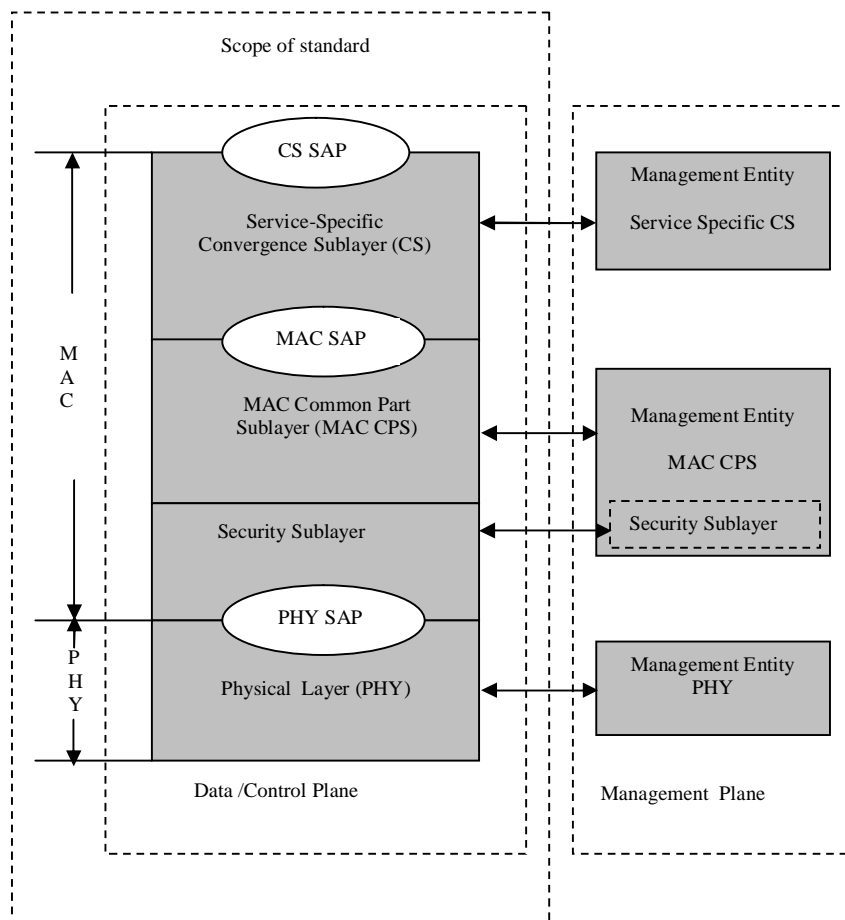


Figure 2.1: IEEE 802.16 Protocol Stack

The PHY layer includes multiple specifications, which make the standard adaptable to different frequency ranges. The flexibility of the PHY enables the system designers to tailor their system according to the requirements. The PHY specifies some mandatory features to be implemented with the system including some optional features.

2.3 Network Architecture and Deployment Topology:

An IEEE 802.16 network is consists of fixed infrastructural sites. In fact, the IEEE 802.16 network is resembled to cellular phone network. Each cell consists of a Base

Station (BS) and one or more subscribe station (SS), depending on the implementation of the topology. Therefore, the BS provides Point to Point (PTP) service or Point to Multi-point (PMP) service in order to serve multiple SSs. BSs provide connectivity to core networks. The SS can be a roof mounted or wall mounted customer premises equipment (CPE) or a stand alone hand held device like Mobile phone, personal digital assistant (PDA) or peripheral component interconnect (PCI) card for PC or Laptop. In case of a outside CPE, the users inside the building are connected to a conventional network like Ethernet Local Area Network (IEEE 802.3 for LAN) or Wireless LAN (IEEE 802.11b/g for WAN) which have access to the CPE. A group of cells can be grouped together to form a network, where BSs are connected through a core network, as shown in Figure 2.2. The IEEE 802.16 network also support mesh topology, where SSs are able to communicate among them selves without the need of a BS [1].

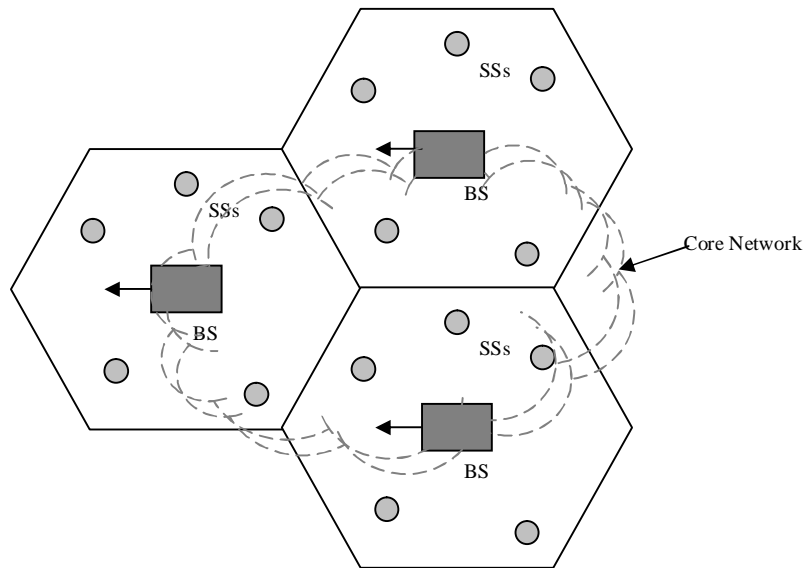


Figure 2.2: A typical IEEE 802.16 Network

BSs typically employ one or more wide beam antennas that may be partitioned into several smaller sectors, where all sectors sum to a complete 360 degree coverage. CPEs typically employ highly directional antennas that are pointed towards the BS. Depending on the need, IEEE 802.16 network can be deployed in different forms.

2.4 Application of IEEE 802.16 based network:

IEEE 802.16 supports ATM, IPv4, IPv6, Ethernet and Virtual Local Area Network (VLAN) services [1]. SO, it can provide a rich choice of service possibilities to voice and data network service providers. It can be used for a wide selection of wireless broadband connection and solutions.

- .. Cellular Backhaul: IEEE 802.16 wireless technology can be an excellent choice for back haul for commercial enterprises such as hotspots as well as point-to-point back haul applications due to its robust bandwidth and long range.
- .. Residential Broadband: Practical limitations like long distance and lack off return channel prohibit many potential broadband customers reaching DSL and cable technologies [3]. IEEE 802.16 can fill the gaps in cable and DSL coverage.
- .. Underserved areas: In many rural areas, especially in developing countries, there is no existence of wired infrastructure. IEEE 802.16 can be a better solution to provide communication services to those areas using fixed CPE and high gained antenna.
- .. Always Best Connected: As IEEE 802.16e supports mobility [8], so the mobile user in the business areas can access high speed services through their IEEE 802.16/WiMAX enabled handheld devices like PDA, Pocket PC and smart phone.

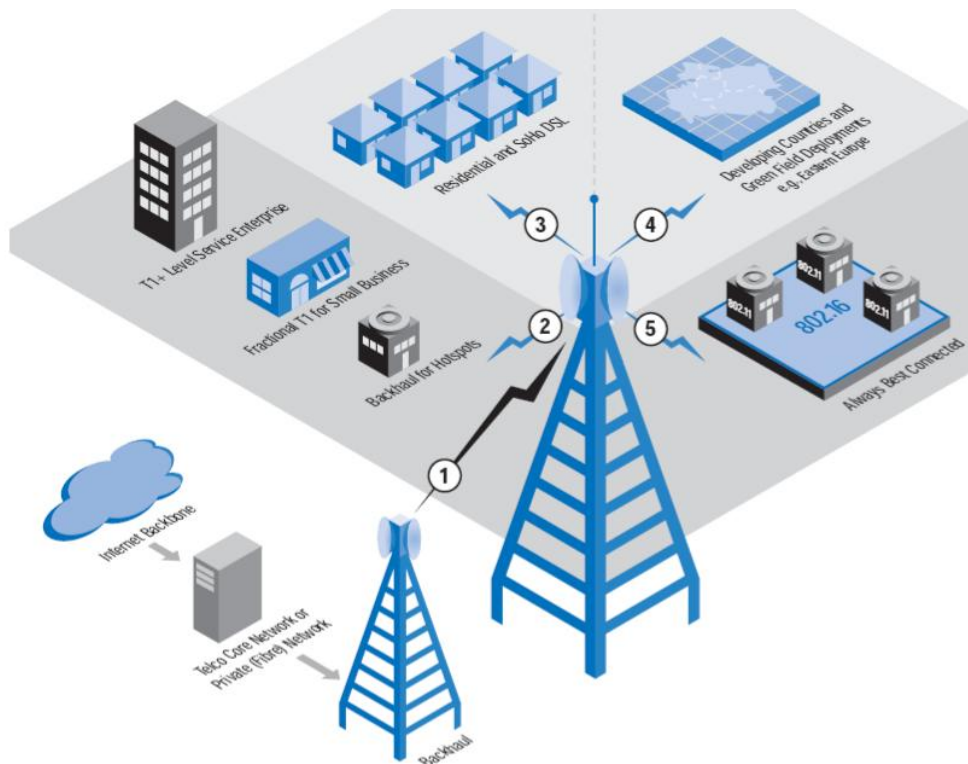


Figure 2.3: Application scenarios [3]

2.5 WiMAX forum and adaptation of IEEE 802.16

The Worldwide Interoperability for Microwave Access (WiMAX) forum is an alliance of telecommunication equipments and components manufacturers and service providers, formed to promote and certify the compatibility and interoperability of BWA products employing the IEEE 802.16 and ETSI HiperMAN [17] wireless specifications. WiMAX Forum Certified™ equipment is proven interoperable with other vendors' equipment that is also WiMAX Forum Certified™ [33]. So far WiMAX forum has setup certification laboratories in Spain, Korea and China. Additionally, the WiMAX forum creates what it calls system profiles, which are specific implementations, selections of options within the standard, to suit particular ensembles of service offerings and subscriber populations [19].

WiMAX forum has adopted two version of the IEEE 802.16 standard to provide different types of access:

- .. Fixed/Nomadic access: The WiMAX forum has adopted IEEE802.16-2004 and ETSI HyperMAN standard for fixed and nomadic access [17]. This uses Orthogonal Frequency Division Multiplexing and able to provide supports in Line of Sight (LOS) and Non Line of Sight (NLOS) propagation environment. Both outdoor and indoor CPEs are available for fixed access. The main focus of the WiMAX forum profiles are on 3.5 GHz and 5.8 GHz frequency band.

- .. Portable/Mobile Access: The forum has adopted the IEEE 802.16e version of the standard, which has been optimized for mobile radio channels. This uses Scalable OFDM Access and provides support for handoffs and roaming [17]. IEEE 802.16e based network is also capable to provide fixed access. The WiMAX Mobile WiMAX profiles will cover 5, 7, 8.75, and 10 MHz channel bandwidths for licensed worldwide spectrum allocations in the 2.3 GHz, 2.5 GHz, 3.3 GHz and 3.5 GHz frequency bands [18]. The first certified product is expected to be available by the end of 2007.

Chapter 3:

IEEE 802.16 Physical Layer

This chapter discusses about the different variants of the IEEE 802.16 PHY layer with their capabilities and conditions of operation. The OFDM based physical layer has been overviewed with its various mechanisms. Finally the chapter concludes with a discussion on OFDM technology and its design considerations.

3.1 IEEE 802.16 PHY Layer:

The IEEE 802.16 standard supports multiple physical specifications due to its modular nature. The first version of the standard only supported single carrier modulation. Since that time, OFDM and scalable OFDMA have been included to operate in NLOS environment and to provide mobility. The standard has also been extended for use in below 11 GHz frequency bands along with initially supported 10-66 GHz bands.

3.1.1 Supported Band of Frequency

The IEEE 802.16 supported licensed and unlicensed bands of interest are as follows:

- .. **10-66 GHz licensed band:** In this frequency band, due to shorter wave length, line of sight operation is required and as a result the effect of multipath propagation is neglected. The standard promises to provide data rates up to 120 Mb/s in this frequency band [6]. The abundant availability of bandwidth is also another reason to operate in this frequency range. Unlike the lower frequency ranges where frequency bands are often less than 100MHz wide, most frequency bands above 20GHz can provide several hundred megahertz of bandwidth [19]. Additionally, channels within these bands are typically 25 or 28 MHz wide. [6]
- .. **2-11 GHz licensed and licensed exempt:** In this frequency bands, both licensed and licensed exempt bands are addressed. Additional physical functionality supports have been introduced to operate in Near LOS and NLOS environment and to mitigate the effect of multipath propagation. In fact, many of the IEEE 802.16 PHY's most advantageous capabilities are found in this frequency range. Operation in licensed exempt band experiences additional interference and co-existence issue. The PHY and MAC address mechanism like dynamic frequency selection (DFS) to detect and avoid interference [1](for licensed exempt band). Though service provision in this frequency band is highly depends on design goals, vendors typically cite target aggregate data rates of up to 70Mb/s in a 14 MHz channel [18]

3.2 IEEE 802.16 PHY interface variants

The standard has assigned a unique name to each physical interface. They have been described below along with their supported features in brief

3.2.1 WirelessMAN-SC™

This is the only PHY specification defined to operate in 10-66 GHz frequency band. It employs single carrier modulation with adaptive burst profiling, in which transmission parameters, including the modulation and coding schemes, may be tuned individually to each subscriber station (SS) on a frame by frame basis. The standard both supports Frequency Division Duplexing (FDD) and Time division Duplexing(TDD) to separate

uplink and downlink. The standard also supports half duplex FDD SS , which may be less expensive as they do not transmit and receive simultaneously [28]. This duplexing technique is common to all the PHY specifications. Access in uplink direction is done by combination of time division multiple access (TDMA) and Demand Assignment Multiple Access (DAMA), exactly the uplink channel is divided into several time slots. Communication on the downlink in PTM Architecture is employed using Time Division Multiplexing (TDM). It also specifies the randomization, forward error correction (FEC), modulation and coding schemes.

3.2.3 WirelessMAN-SCa™

This is also based on single carrier modulation targeted for 2-11 GHz frequency range. Access is done by TDMA technique both in uplink and downlink, additionally TDM also supported in downlink.

3.2.3 WirelessMAN-OFDM™

This is based on orthogonal frequency division multiplexing (OFDM) with a 256 point transform to support multiple SS in 2-11 GHz frequency band. Access is done by TDMA. The WiMAX forum has adopted this PHY specification for BWA. Because of employing OFDM and other features like multiple forward error correction method, this is the most suitable candidate to provide fixed support in NLOS environment. We have chosen this PHY specification for our simulation model. From next sections our discussion will be on this PHY layer.

3.2.4 WirelessMAN-OFDMA™:

This PHY specification uses OFDM access (OFDMA) with at least a single support of specified multi-point transform (2048, 1024, 512 or 128) to provide combined fixed and Mobile BWA. Operation is limited to below 11 GHz licensed band [8]. In this specification multiple access is provided by addressing a subset of the multiple carriers to individual receivers [6].

3.2.5 WirelessHUMAN™:

This specification is targeted for license exempt band below 11 GHz. Any of the air interfaces specified for 2-11 GHz can be used for this. This supports only TDD for duplexing [1].

Table 3.1 : Air Interface Nomenclature and Description[1]

| Designation | Band of operation | Duplexing Technique | Notes |
|------------------------|-------------------------------------|---------------------|--|
| WirelessMAN-SC™ | 10-66 GHz | TDD, FDD | Single Carrier |
| WirelessMAN-SCa™ | 2-11 GHz Licensed band | TDD, FDD | Single Carrier technique for NLOS |
| WirelessMAN- OFDM™ | 2-11 GHz Licensed band | TDD, FDD | OFDM for NLOS operation |
| WirelessMAN- OFDMA™ | 2-11 GHz Licensed band | TDD, FDD | OFDM Broken into subgroups to provide multiple access in a single frequency band. |
| WirelessHUMAN™ | 2-11 GHz Licensed Exempt Band | TDD | May be SC, OFDM, OFDMA. Must include Dynamic Frequency Selection to mitigate interference |

3.4 WirelessMAN OFDM PHY Layer

This version of the 256-point OFDM based air interface specification seems to be favored by the WiMAX forum for reasons such as lower peak to average ratio, faster fast fourier transform (FFT) calculation, and less stringent requirements for frequency synchronization compared to 2048-point WirelessMAN OFDMA. The size of the FFT point determines the number of subcarriers. Of these 256 subcarriers, 192 are used for

user data, 56 are nulled for guard band and 8 are used as pilot subcarriers for various estimation purposes. The PHY allows to accept variable CP length of 8, 16, 32 or 64 depending on the expected channel delay spread. In the following sub sections, we will discuss about the other mechanism of the PHY layer.

3.4.1 Flexible Channel Bandwidth:

The channel bandwidth can be an integer multiple of 1.25 MHz, 1.5 MHz, 1.75 MHz, 2MHz and 2.75 MHz with a maximum of 20 MHz [1]. But the WiMAX forum has initially narrowed down the large choice of possible bandwidth to a few possibilities to ensure interoperability between different vendor's products [2].

3.4.2 Robust Error Control Mechanism

Forward Error Correction (FEC) is done on two phases through the outer Reed-Solomon (RS) code and inner Convolutional code (CC). The RS coder corrects burst error at the byte level. It is particularly useful for OFDM links in the presence of multipath propagation. The CC corrects independent bit errors. The puncturing functionality in CC made the concatenated codes rate compatible as per specification. The support of Turbo coding is left as an optional feature to increase the coverage and/or capacity [2] with the expense of increased decoding latency and complexity.

3.4.3 Adaptive Modulation and Coding

The specified modulation scheme in the downlink (DL) and uplink (UL) are binary phase shift keying (BPSK), quaternary PSK (QPSK), 16 quadrature amplitude modulation (QAM) and 64-QAM to modulate bits to the complex constellation points. The FEC options are paired with the modulation schemes to form burst profiles. The PHY specifies seven combinations of modulation and coding rate, which can be allocated selectively to each subscriber, in both UL and DL [4]. There are trade-offs between data rate and robustness, depending on the propagation conditions. Table 3.2 Shows the combination of those modulation and coding rate.

Table 3.2: Mandatory channel coding per modulation

| Modulation | Uncoded Block Size (bytes) | Coded Block Size (bytes) | Overall coding rate | RS code | CC code rate |
|------------|----------------------------|--------------------------|---------------------|-------------|--------------|
| BPSK | 12 | 24 | 1/2 | (12,12,0) | 1/2 |
| QPSK | 24 | 48 | 1/2 | (32,24,4) | 2/3 |
| QPSK | 36 | 48 | 3/4 | (40,36,2) | 5/6 |
| 16-QAM | 48 | 96 | 1/2 | (64,48,8) | 2/3 |
| 16-QAM | 72 | 96 | 3/4 | (80,72,4) | 5/6 |
| 64-QAM | 96 | 144 | 2/3 | (108,96,6) | 3/4 |
| 64-QAM | 108 | 144 | 3/4 | (120,108,6) | 5/6 |

3.4.4 Adaptive Antenna System

The PHY optionally supports and provides a signaling structure that enables the use of adaptive antenna system (AAS). The feature enables the transmission of DL and UL burst using directed beams, each intended for one or more SSs. In addition, the feature allows SS to deliver channel quality feedback to the BS [2].

3.4.5 Transmit Diversity:

Space time block codes (STBC) can be implemented in the DL to provide transmit diversity. The feature is optional to implement. In [2], Alamouti STBC [20] has been proposed as a good candidate to implement this feature providing diversity in time and space.

3.3 OFDM

In this section, we will discuss about the OFDM method and its design consideration.

3.3.1 OFDM BASIC:

The idea of OFDM comes from Multi-Carrier Modulation (MCM) transmission technique. The principle of MCM describes the division of input bit stream into several parallel bit streams and then they are used to modulate several sub carriers as shown in Figure 3.1. Each sub-carrier is separated by a guard band to ensure that they do not overlap with each other. In the receiver side, bandpass filters are used to separate the spectrum of individual sub-carriers. OFDM is a special form of spectrally efficient MCM technique, which employs densely spaced orthogonal sub-carriers and overlapping spectrums. The use of bandpass filters are not required in OFDM because of the orthogonality nature of the sub-carriers. Hence, the available bandwidth is used very efficiently without causing the Inter-Carrier Interference (ICI). In Figure 3.1, the effect of this is seen as the required bandwidth is greatly reduced by removing guard band and allowing sub-carrier to overlap. It is still possible to recover the individual sub-carrier despite their overlapping spectrum provided that the orthogonality is maintained. The Orthogonality is achieved by performing Fast Fourier Transform (FFT) on the input stream. Because of the combination of multiple low data rate sub-carriers, OFDM provides a composite high data rate with long symbol duration. Depending on the channel coherence time, this reduces or completely eliminates the risk of Inter-Symbol Interference (ISI), which is a common phenomenon in multi-path channel environment with short symbol duration. The use of Cyclic Prefix (CP) in OFDM symbol can reduce the effect of ISI even more [24], but it also introduces a loss in SNR and data rate.

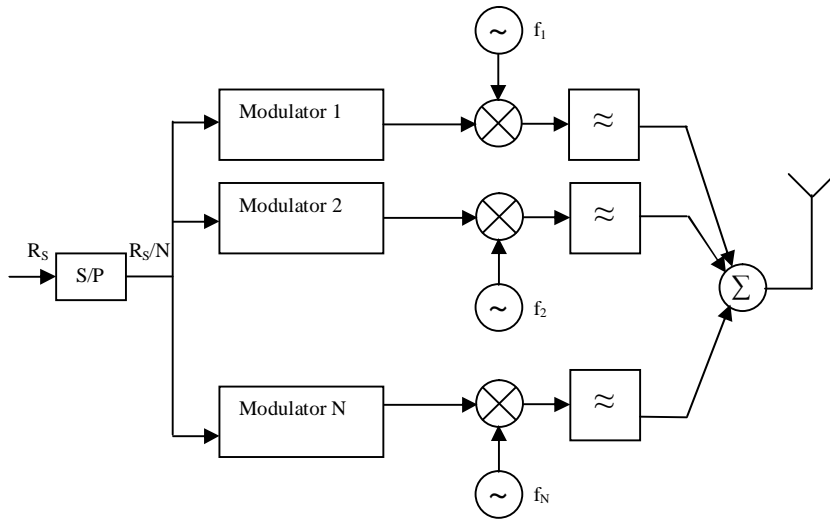


Figure 3.1: Block diagram of a generic MCM transmitter.

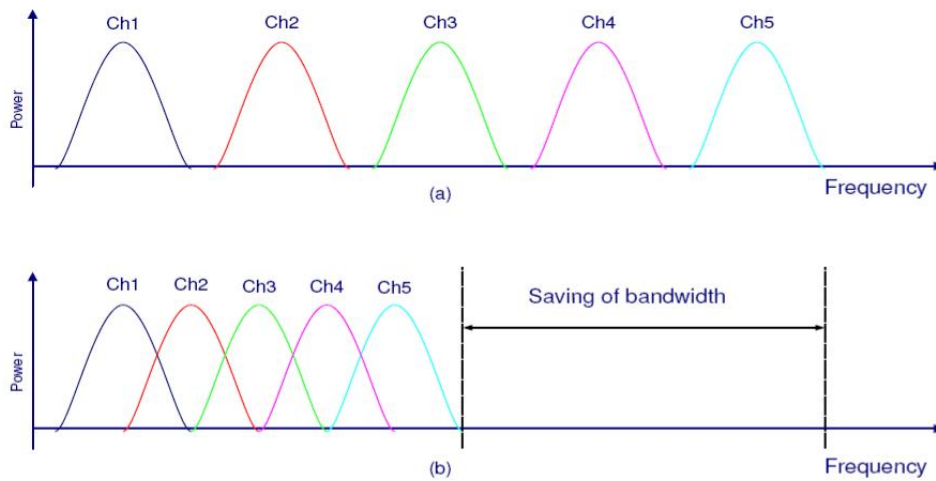


Figure 3.2: Comparison between conventional FDM and OFDM [21]

3.3.2 OFDM SYSTEM IMPLEMENTATION

The principle of OFDM was already around in the 50's and 60's as an efficient MCM technique. But, the system implementation was delayed due to technological difficulties like digital implementation of FFT/IFFT, which were not possible to solve on that time. In 1965, Cooley and Tukey presented the algorithm for FFT calculation [22] and later its efficient implementation on chip makes the OFDM into application.

The digital implementation of OFDM system is achieved through the mathematical operations called Discrete Fourier Transform (DFT) and its counterpart Inverse Discrete Fourier Transform (IDFT). These two operations are extensively used for transforming data between the time-domain and frequency-domain. In case of OFDM, these transforms can be seen as mapping data onto orthogonal subcarriers.

In order to perform frequency-domain data into time domain-data, IDFT correlates the frequency domain input data with its orthogonal basis functions, which are sinusoids at certain frequencies. In other ways, this correlation is equivalent to mapping the input data onto the sinusoidal basis functions. In practice, OFDM systems employ combination of fast fourier transform (FFT) and Inverse fast fourier transform (IFFT) blocks which are mathematical equivalent version of the DFT and IDFT.

At the transmitter side, an OFDM system treats the source symbols as though they are in the frequency-domain. These symbols are feed to an IFFT block which brings the signal into the time-domain. If the N numbers of subcarriers are chosen for the system, the basis functions for the IFFT are N orthogonal sinusoids of distinct frequency and IFFT receive N symbols at a time. Each of N complex valued input symbols determines both the amplitude and phase of the sinusoid for that subcarrier. The output of the IFFT is the summation of all N sinusoids and makes up a single OFDM symbol. The length of the OFDM symbol is NT where T is the IFFT input symbol period. In this way, IFFT block provides a simple way to modulate data onto N orthogonal subcarriers.

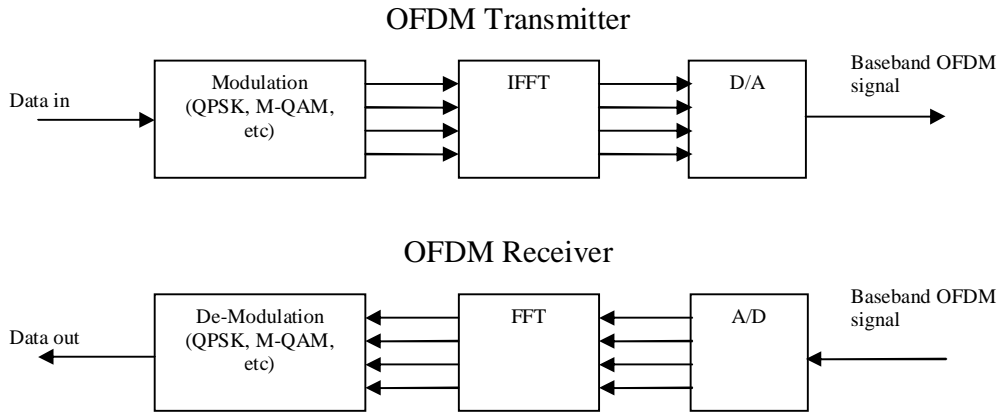


Figure 3.3: Basic OFDM transmitter and receiver

At the receiver side, The FFT block performs the reverse process on the received signal and bring it back to frequency-domain. The block diagram in Figure 3.3 depicts the switch between frequency-domain and time domain in an OFDM system.

3.3.3 CYCLIC PREFIX ADDITION

The subcarrier orthogonality of an OFDM system can be jeopardized when passes through a multipath channel [23]. CP is used to combat ISI and ICI introduced by the multipath channel. CP is a copy of the last part of OFDM symbol which is appended to the front of transmitted OFDM symbol [24]. The length of the CP (T_g) must be chosen as longer than the maximum delay spread of the target multipath environment. Fig 3.4 depicts the benefits arise from CP addition, certain position within the cyclic prefix is chosen as the sampling starting point at the receiver, which satisfies the criteria

$$\tau_{\max} < T_x < T_g$$

where τ_{\max} is the maximum multi-path spread. Once the above condition is satisfied, there is no ISI since the previous symbol will only have effect over samples within $[0, \tau_{\max}]$. And it is also clear from the figure that sampling period starting from T_x will encompass the contribution from all the multi-path components so that all the samples experience the same channel and there is no ICI.

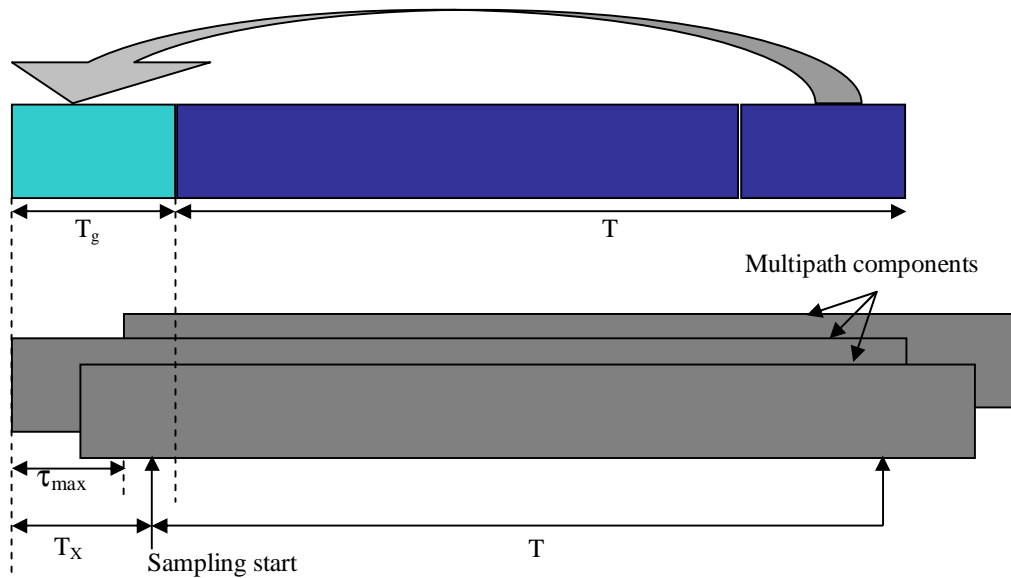


Figure 3.4: Cyclic Prefix in OFDM

3.3.4 OFDM SYSTEM DESIGN CONSIDERATIONS

OFDM system design issues aim to decrease the data rate at the subcarriers, hence, the symbol duration increases and as a result, the multipath effects are reduced effectively. The insertion of higher valued CP will bring good results against combating multipath effects but at the same time it will increase loss of energy. Thus, a tradeoff between these two parameters must be done to obtain a reasonable system design.

3.3.4.1 SYSTEM DESIGN REQUIREMENTS:

OFDM system depends on the following four requirements: [23]

- .. Available bandwidth: The bandwidth limit will play a significant role in the selection of number of sub-carriers. Large amount of bandwidth will allow obtaining a large number of subcarriers with reasonable CP length.
- .. Required bit rate: The system should be able to provide the data rate required for the specific purpose.
- .. Tolerable delay spread: An user environment specific maximum tolerable delay spread should be known beforehand in determining the CP length.

- .. Doppler values: The effect of Doppler shift due to user movement should be taken into account.

3.3.4.2 SYSTEM DESIGN PARAMETERS:

The design parameters are derived according to the system requirements. The design parameters for an OFDM system are as follows [24]

- .. Number of subcarriers: We stated earlier that the selection of large number of subcarriers will help to combat multipath effects. But, at the same time, this will increase the synchronization complexity at the receiver side.
- .. Symbol duration and CP length: A perfect choice of ratio between the CP length and symbol duration should be selected, so that multipath effects are combated and not significant amount bandwidth is lost due to CP.
- .. Subcarrier spacing: Subcarrier spacing will be depend on available bandwidth and number of subcarriers used. But, this must be chosen at a level so that synchronization is achievable.
- .. Modulation type per subcarrier: The performance requirement will decide the selection of modulation scheme. Adaptive modulation can be used to support the performance requirements in changing environment.
- .. FEC coding: A suitable selection of FEC coding will make sure the robustness of the channel to the random errors.

3.3.5 BENEFITS AND DRAWBACKS of OFDM:

In the earlier section, we have stated that how an OFDM system combats the ISI and reduces the ICI. Besides those benefits, there are some other benefits as follows:

- .. High spectral efficiency because of overlapping spectra
- .. Simple implementation by fast fourier transform

- .. Low receiver complexity as the transmitter combat the channel effect to some extends.
- .. Suitable for high-data-rate transmission
- .. High flexibility in terms of link adaptation
- .. Low complexity multiple access schemes such as orthogonal frequency-division multiple access (OFDMA)
- .. It is possible to use maximum likelihood detection with reasonable complexity[25]

On the other side, few drawbacks of OFDM are listed as follows

- .. An OFDM system is highly sensitive to timing and frequency offsets [24]. Demodulation of an OFDM signal with an offset in the frequency can lead to a high bit error rate.
- .. An OFDM system with large number of subcarriers will have a higher peak to average power ratio (PAPR) compared to single carrier system. High PAPR of a system makes the implementation of Digital to analog (DAC) and Analog to Digital Conversion (ADC) extremely difficult [23].

3.3.6 APPLICATION

OFDM has gained a big interest since the beginning of the 1990s [26] as many of the implementation difficulties have been overcome. OFDM has been in use or proposed for a number of wired and wireless applications. Digital Audio Broadcasting (DAB) was the first commercial use of OFDM technology [23]. OFDM has also been used for the Digital Video Broadcasting [27]. OFDM under the acronym of Discrete Multi Tone (DMT) has been selected for asymmetric digital subscriber line (ADSL) [32]. The specification for Wireless LAN standard such as IEEE 802.11a/g [29, 30] and ETSI HIPERLAN2 [31] has employed OFDM as their PHY technologies. IEEE 806.16 standard for Fixed/Mobile BWA has also accepted OFDM for PHY technologies.

Chapter 4

Simulation Model

This chapter discusses the simulation model employed by this research. As we have stated before, our research goal is to evaluate performance of IEEE 802.16 OFDM physical layer. This task involves modeling of the physical layer as well as the propagation environment. Simulation was chosen to be the primary tool for our study. We have employed Matlab™ 6.0 to develop the simulator. Before going for the physical layer setup, let us first define the OFDM symbol parameter used in our study.

4.1 OFDM Symbol Parameter

There are two types of OFDM parameters (primitive and derived) that characterize OFDM symbol completely. The later one can be derived from the former one because of fixed relation between them. In our MATLAB implementation of the physical layer, the primitive parameters are specified as '*OFDM_params*' and primitive parameters are calculated as '*IEEE802.16 paparams*' which can be accessed globally. The used OFDM parameters are listed in Table 4.1.

Table 4.1:OFDM Symbol Parameters

| Type | Parameters | Value |
|-----------|--|-------------------------|
| Primitive | Nominal Channel Bandwidth, BW | 1.75 MHz |
| | Number of Used Subcarrier, N_{used} | 200 |
| | Sampling Factor, n | 8/7 |
| | Ratio of Guard time to useful symbol time, G | 1/4 ,1/8, 1/16, 1/32 |
| Derived | N_{FFT} (smallest power of 2 greater than N_{used}) | 255 |
| | Sampling Frequency, F_s | Floor(n.BW/8000) X 8000 |
| | Subcarrier Spacing, Δf | F_s/N_{FFT} |
| | Useful Symbol Time, T_b | $1/\Delta f$ |
| | CP Time, T_g | $G.T_b$ |
| | OFDM Symbol Time, T_s | T_b+T_g |
| | Sampling Time | T_b/N_{FFT} |

4.2 Physical Layer Setup

The structure of the baseband part of the implemented transmitter and receiver is shown in Figure 4.1. This structure corresponds to the physical layer of the IEEE 802.16-2004 WirelessMAN-OFDM air interface. In this setup, we have just implemented the mandatory features of the specification, while leaving the implementation of optional features for future work. Channel coding part is composed of three steps- randomization, Forward Error Correction (FEC) and interleaving. FEC is done in two phases through the outer Reed-Solomon (RS) and inner Convolutional Code (CC). The complementary operations are applied in the reverse order at channel decoding in the receiver end. The complete channel encoding setup is shown in Figure 4.2 while corresponding decoding setup is shown in Figure 4.3. Through the rest of the sections, the individual block of the setup will be discussed with implementation technique.

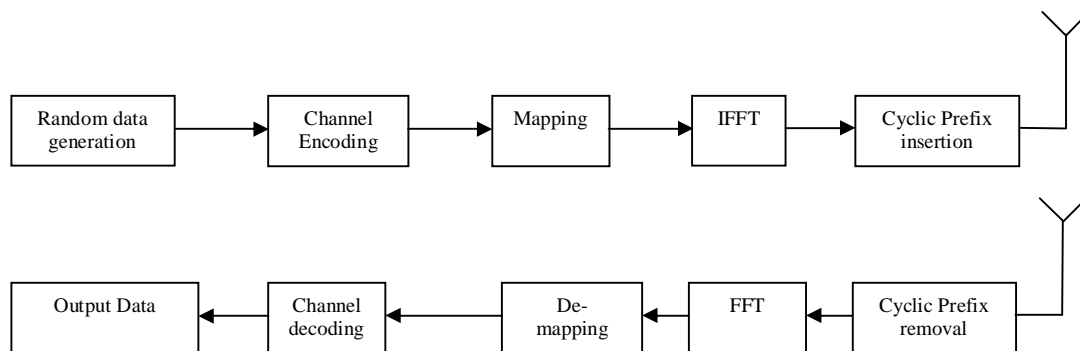


Figure 4.1: Simulation Setup

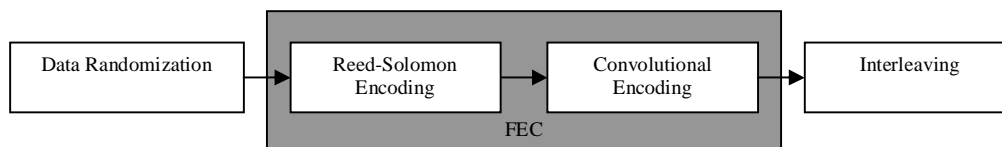


Figure 4.2: Channel Encoding Setup

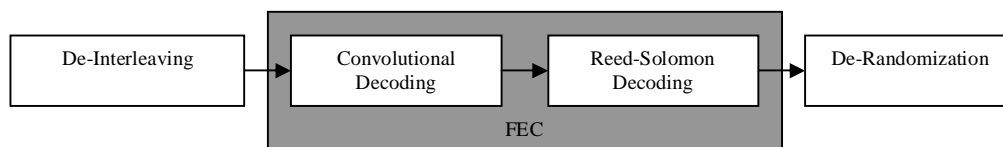


Figure 4.3: Channel Decoding Setup

4.2.1 Scrambler

The scrambler performs randomization of input data on each burst on each allocation to avoid long sequence of continuous ones and zeros. This is implemented with a Pseudo Random Binary Sequence (PRBS) generator which uses a 15-stage shift register with a generator polynomial of $1+x^{14}+x^{15}$ with XOR gates in feedback configuration as shown in figure 4.4. The implemented scrambler complies with the initialization process as specified in section 8.3.3.1 of the standard [1].

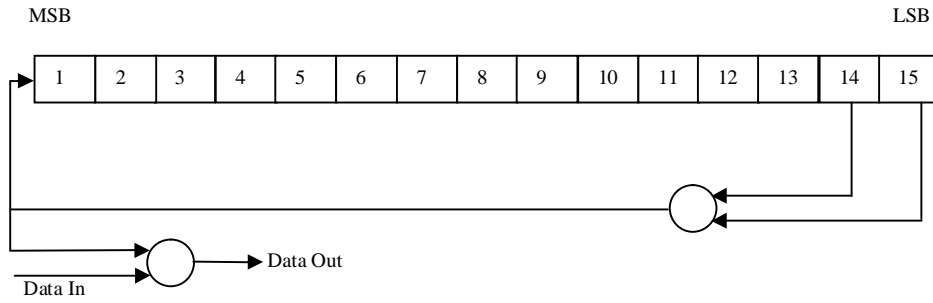


Figure 4.4: PRBS generator for randomization.

4.2.2 Reed-Solomon Encoder

The randomized data are arranged in block format before passing through the encoder and a single 0X00 tail byte is appended to the end of each burst. The implemented RS encoder is derived from a systematic RS (N=255, K=239, T=8) code using GF (2⁸). The following polynomials are used for code generator and field generator:

$$G(x) = (x+\lambda^0)(x+\lambda^1)\dots (x+\lambda^{2T-1}), \lambda = 02_{\text{HEX}} \quad (4.1)$$

$$p(x) = x^8 + x^4 + x^3 + x^2 + 1 \quad (4.2)$$

The encoder support shortened and punctured code to facilitate variable block sizes and variable error-correction capability. A shortened block of k' bytes is obtained through adding 239-k' zero bytes before the data block and after encoding, these 239-k' zero bytes are discarded. To obtain the punctured pattern to permit T' bytes to be corrected, the first 2T' of the 16 parity bytes has been retained.

4.2.3 Convolutional Encoder

The outer RS encoded block is fed to inner binary convolutional encoder. The implemented encoder has native rate of 1/2, a constraint length of 7 and the generator polynomial in Equation (4.3) and (4.4) to produce its two code bits. The generator is shown in Figure 4.5.

$$G_1 = 171_{\text{OCT}} \quad \text{For } X \quad (4.3)$$

$$G_2 = 133_{\text{OCT}} \quad \text{For } Y \quad (4.4)$$

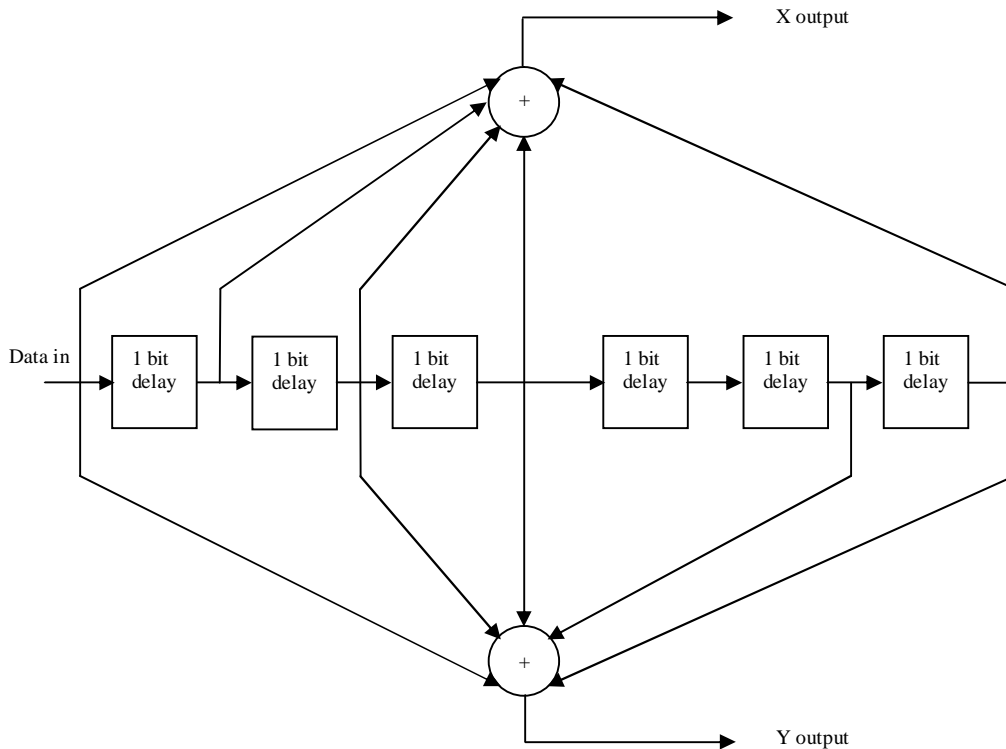


Figure 4.5: Convolutional encoder of rate $\frac{1}{2}$

In order to achieve variable code rate a puncturing operation is performed on the output of the convolutional encoder in accordance to Table 4.2. In this Table “1” denotes that the corresponding convolutional encoder output is used, while “0” denotes that the corresponding output is not used. At the receiver Viterbi decoder is used to decode the convolutional codes.

Table 4.2: Puncturing configuration of the convolutional code

| Rate | d_{FREE} | X output | Y output | XY (punctured output) |
|-------|-------------------|----------|----------|-----------------------|
| $1/2$ | 10 | 1 | 1 | X_1Y_1 |
| $2/3$ | 6 | 10 | 11 | $X_1Y_1Y_2$ |
| $3/4$ | 5 | 101 | 110 | $X_1Y_1Y_2X_3$ |
| $5/6$ | 4 | 10101 | 11010 | $X_1Y_1Y_2X_3Y_4X_5$ |

4.2.4 Interleaver

RS-CC encoded data are interleaved by a block interleaver. The size of the block is depended on the numbers of bit encoded per subchannel in one OFDM symbol, N_{cbps} . In IEEE 802.16, the interleaver is defined by two step permutation. The first ensures that adjacent coded bits are mapped onto non-adjacent subcarriers. The second permutation ensures that adjacent coded bits are mapped alternately onto less or more significant bits of the constellation, thus avoiding long runs of unreliable bits [1].

The Matlab implementation of the interleaver was performed calculating the index value of the bits after first and second permutation using Equation (4.5) and (4.6) respectively.

$$f_k = (N_{cbps}/12).k_{\text{mod}12} + \text{floor}(k/2) \quad k = 0,1,2,\dots,N_{cbps}-1 \quad (4.5)$$

$$s_k = s.\text{floor}(f_k/s) + (m_k + N_{cbps} - \text{floor}(12.m_k/N_{cbps}))_{\text{mod}(s)} \quad k=0,1,2,\dots,N_{cbps}-1 \quad (4.6)$$

where $s = \text{ceil}(N_{cpc}/2)$, while N_{cpc} stands for the number of coded bits per subcarrier, i.e., 1,2,4 or 6 for BPSK, QPSK 16-QAM, or 64-QAM, respectively.

The default number of subchannels i.e 16 is used for this implementation.

The receiver also performs the reverse operation following the two step permutation using equations (4.7) and (4.8) respectively.

$$f_j = s.\text{floor}(j/s) + (j + \text{floor}(12.j/N_{cbps}))_{\text{mod}(s)} \quad j=0,1,\dots,N_{cbps}-1 \quad (4.7)$$

$$s_j = 12.f_j - (N_{cbps} - 1).\text{floor}(12.f_j/N_{cbps}) \quad j=0,1,2,\dots,N_{cbps}-1 \quad (4.8)$$

4.2.5 Constellation Mapper

The bit interleaved data are then entered serially to the constellation mapper. The Matlab implemented constellation mapper support BPSK, grey-mapped QPSK, 16-QAM, and 64-QAM as specified in Figure 203 of the standard [1]. The complex constellation points are normalized with the specified multiplying factor for different modulation scheme so

that equal average power is achieved for the symbols. The constellation mapped data are assigned to all allocated data subcarriers of the OFDM symbol in order of increasing frequency offset index.

4.2.6 IFFT

The grey mapped data are then sent to IFFT for time domain mapping. Mapping to time domain needs the application of Inverse Fast Fourier Transform (IFFT). In our case we have incorporated the MATLAB 'ifft' function to do so. This block delivers a vector of 256 elements, where each complex number element represents one sample of the OFDM symbol.

4.2.7 Cyclic Prefix Insertion:

A cyclic prefix is added to the time domain samples to combat the effect of multipath. Four different duration of cyclic prefix are available in the standard. Being G the ratio of CP time to OFDM symbol time, this ratio can be equal to $1/32$, $1/6$, $1/8$ and $1/4$

4.3 Channel Model:

In order to evaluate the performance of the developed communication system, an accurate description of the wireless channel is required to address its propagation environment. The radio architecture of a communication system plays very significant role in the modeling of a channel. The wireless channel is characterized by:

- .. Path loss (including shadowing)
- .. Multipath delay spread
- .. Fading characteristics
- .. Doppler spread
- .. Co-channel and adjacent channel interference

All the model parameters are random in nature and only a statistical characterization of them is possible, i.e. in terms of the mean and variance value. They are dependent upon terrain, tree density, antenna height and beamwidth, wind speed and time of the year.

Path loss:

Path loss is affected by several factors such as terrain contours, different environments (urban or rural, vegetation and foliage), propagation medium (dry or moist air), the distance between the transmitter and the receiver, the height and location of their antennas, etc. It has only impact on the link budget [11], that is why we will not consider it in our channel modeling.

Multipath Delay Spread:

Due to the non line of sight (NLOS) propagation nature of the WirelessMAN OFDM, we have to address multipath delay spread in our channel model. It results due to the scattering nature of the environment. Delay spread is a parameter used to signify the effect of multipath propagation. It depends on the terrain, distance, antenna directivity and other factors. The rms delay spread value can span from tens of nano seconds to microseconds.

Fading characteristics:

In a multipath propagation environment, the received signal experiences fluctuation in its amplitude, phase and angle of arrival. The effect is described by the term multipath fading. Due to fixed deployment of transmit and receive antenna, we just have to address the small-scale fading in our channel model. Small-scale fading refers to the dramatic changes in signal amplitude and phase that can be experienced as a result of small changes (as small as a half wavelength) in the spatial positioning between a receiver and a transmitter.

Small-scale fading is called Rayleigh fading if there are multiple reflective paths that are large in number and there is no line-of-sight signal component; the envelope of such a received signal is statistically described by a Rayleigh pdf. When a dominant non fading

signal component is present, such as a line-of-sight propagation path, the small-scale fading envelope is described by a Rician pdf [14]. In other words, the small-scale fading statistics are said to be Rayleigh whenever the line-of-sight path is blocked, and Rician otherwise.

In our channel model we will consider Rician fading distribution. The key parameter of this distribution is the K-factor, defined as the ratio of the direct component power and the scatter component power.

Doppler Spread:

In fixed wireless access, a doppler frequency shift is induced on the signal due to movement of the objects in the environment. Doppler spectrum of fixed wireless channel differs from that of mobile channel [12]. It is found that the doppler is in the 0.1-2 Hz frequency range for fixed wireless channel. The shape of the spectrum is also different than the classical Jake's spectrum for mobile channel.

Along with the above channel parameters, coherence distance, co-channel interference, antenna gain reduction factor should be addressed for channel modeling.

Having the primary requirements for our channel model, we have two options to go with. Either we can use mathematical model for each of them or we can choose an empirical model that care of the above requirements. We opted for the later one and chose the Stanford University Interim (SUI) channel model for our simulation.

4.3.1 Stanford University Interim (SUI) Channel Models

SUI channel models are an extension of the earlier work by AT&T Wireless and Erceg et al [14]. In this model a set of six channels was selected to address three different terrain types that are typical of the continental US [13]. This model can be used for simulations,

design, development and testing of technologies suitable for fixed broadband wireless applications [12]. The parameters for the model were selected based upon some statistical models. The tables below depict the parametric view of the six SUI channels.

Table 4.3: Terrain type for SUI channel

| Terrain Type | SUI Channels |
|---|--------------|
| C (Mostly flat terrain with light tree densities) | SUI-1, SUI-2 |
| B (Hilly terrain with light tree density or flat terrain with moderate to heavy tree density) | SUI-3, SUI-4 |
| A (Hilly terrain with moderate-to-heavy tree density) | SUI-5, SUI-6 |

Table 4.4: General characteristics of SUI channels

| Doppler | <i>Low delay spread</i> | <i>Moderate delay spread</i> | <i>High delay spread</i> |
|---------|----------------------------------|------------------------------|--------------------------|
| Low | SUI-1,2 (High K-Factor) SUI-3 | | SUI-5 |
| High | | SUI-4 | SUI-6 |

We assume the scenario [12] with the following parameters:

- .. Cell Size: 7Km
- .. BTS antenna height: 30 m
- .. Receive antenna height: 6m
- .. BTS antenna beamwidth: 120^0
- .. Receive antenna beamwidth: omnidirectional
- .. Polarization: Vertical only
- .. 90% cell coverage with 99.9% reliability at each location covered

For the above scenario, the SUI channel parameters are tabulated in Table 4.5, 4.6 and 4.7 according to [12].

Table 4.5: Delay spread of SUI channels

| <i>Channel model</i> | <i>Tap 1</i> | <i>Tap 2</i> | <i>Tap 3</i> | <i>Rms delay spread</i> |
|----------------------|---------------|--------------|--------------|-------------------------|
| | μs | | | |
| SUI-1 | 0 | 0.4 | 0.9 | 0.111 |
| SUI-2 | 0 | 0.4 | 1.1 | 0.202 |
| SUI-3 | 0 | 0.4 | 0.9 | 0.264 |
| SUI-4 | 0 | 1.5 | 4 | 1.257 |
| SUI-5 | 0 | 4 | 10 | 2.842 |
| SUI-6 | 0 | 14 | 20 | 5.240 |

Table 4.6: Tap power(omni directional antenna) of SUI channels

| <i>Channel model</i> | <i>Tap 1</i> | <i>Tap 2</i> | <i>Tap 3</i> |
|----------------------|--------------|--------------|--------------|
| | <i>dB</i> | | |
| SUI-1 | 0 | -15 | -20 |
| SUI-2 | 0 | -12 | -15 |
| SUI-3 | 0 | -5 | -10 |
| SUI-4 | 0 | -4 | -8 |
| SUI-5 | 0 | -5 | -10 |
| SUI-6 | 0 | -10 | -14 |

Table 4.7: 90% K factor (omni directional antenna) of SUI channels

| <i>Channel model</i> | <i>Tap 1</i> | <i>Tap 2</i> | <i>Tap 3</i> |
|----------------------|--------------|--------------|--------------|
| | | | |
| SUI-1 | 4 | 0 | 0 |
| SUI-2 | 2 | 0 | 0 |
| SUI-3 | 1 | 0 | 1 |
| SUI-4 | 0 | 0 | 0 |
| SUI-5 | 0 | 0 | 0 |
| SUI-6 | 0 | 0 | 0 |

In the next section we will discuss about how these parameters have been incorporated to implement SUI channel model for our simulation.

4.3.2 SUI channel models Implementation:

The goal of the model implementation is to simulate channel coefficients. Channel coefficients with the specified distribution and spectral power density are generated using the method of filtered noise [34]. A set of complex zero-mean Gaussian distributed number is generated with a variance of 0.5 for the real and imaginary part for each tap to achieve the total average power of this distribution is 1. In this way, we get a Rayleigh distribution (equivalent to Rice with $K=0$) for the magnitude of the complex coefficients. In case of a Ricean distribution ($K>0$), a constant path component m has to be added to the Rayleigh set of coefficients. The K -factor specifies the ratio of powers between this constant part and the variable part. The distribution of the power is shown below:

total power P of each tap:

$$p = |m|^2 + \sigma^2 \quad (4.9)$$

where m is the complex constant and σ^2 the variance of the complex Gaussian set

the ratio of power is :

$$k = \frac{|m|^2}{\sigma^2} \quad (4.10)$$

From the above two equations, the power of the complex Gaussian:

$$\sigma^2 = p \cdot \frac{1}{k+1} \quad (4.11)$$

and the power of the constant part as:

$$|m|^2 = p \cdot \frac{k}{k+1} \quad (4.12)$$

The SUI channel model address a specific power spectral density (PSD) function for the scatter component channel coefficients which is given by:

$$S(f) = \begin{cases} 1 - 1.72f_0^2 + 0.785f_0^4 & |f_0| \leq 1 \\ 0 & |f_0| > 1 \end{cases} \quad (4.13)$$

Where, the function is parameterized by a maximum Doppler frequency f_m and $f_0 = f/f_m$.

To generate a set of channel coefficients with this PSD function, the original coefficients are correlated with a filter which amplitude frequency response is:

$$|H(f)| = \sqrt{S(f)} \quad (4.14)$$

For efficient implementation, a non-recursive filter and frequency-domain overlap-add method has been used.

There are no frequency components higher than f_m (for the construction formula of $S(f)$): so the channel can be represented with a minimum sampling frequency of $2f_m$ according to the Nyquist theorem. For this reason we chose the sampling frequency equal to $2f_m$.

The power of the filter has to be normalized to 1, so that the total power of the output signal is equal to the input one.

Chapter 5

Simulation Results

In this chapter the simulation results are shown and discussed. In the following sections, first we will present the structure of the implemented simulator and then we will present the simulation results both in terms of validation of implementation and values for various parameters that characterize the performance of the physical layer.

5.1 The Simulator

We have developed the simulator in Matlab™ using modular approach. Each block of the transmitter, receiver and channel is written in separate 'm' file. The main procedure call each of the block in the manner a communication system works. The main procedure also contains initialization parameters, input data and delivers results. The parameters that can be set at the time of initialization are the number of simulated OFDM symbols, CP length, modulation and coding rate, range of SNR values and SUI channel model for simulation. The input data stream is randomly generated. Output variables are available in Matlab™ workspace while BER and BLER values for different SNR are stored in text files which facilitate to draw plots. Each single block of the transmitter is tested with its counterpart of the receiver side to confirm that each block works perfectly.

5.2 Physical layer performance results

The objective behind simulating the physical layer in Matlab™ was to study BER and BLER performance under different channel conditions and varying parameters that characterize the performance. But, in order to rely on any results from PHY layer simulation we must have some results that can do some validation in terms of general trends. The next section presents a set of scatter plot to identify trends in reception quality as we vary different parameters.

5.2.1 Scatter Plots

Figure 5.1 to 5.7 shows the scatter plots for different coding and modulation schemes as SNR values are changed on SUI-1 channel model. The '+' symbol denotes the transmitted data and the '*' symbol denotes the received data. These plots are obtained by sending the same frame data from transmitter to receiver through the channel repeatedly 1000 times. The input frame was taken from section 8.3.3.5.1 of IEEE standard 802.16d. But, this does not confirm the presence of all constellation points, as it can be seen from the scatter plot of 64-QAM modulation (Figure. 5.6 and 5.7) where few constellation points are missing.

It can be observed from these plots that spread reduction is taking place with the increasing values of SNR. This scenario validates the implementation of channel model. It is also very important to note that the scatter spread gives a strong hint about the BER/BLER statistics as SNR values are varied.

In Figure 5.8, we have observed the effect of channel model on scatter plot at an SNR of 35 dB. It can be seen that severe variation is introduced in SUI-4,5,6 channel model even at high SNR value. It is clear that equalization is required for those three channel models. Figure 5.9 shows the effect of CP length on scatter plot with fixed SNR value. The differences are clearly visible that the scatter plots are less scattered for higher values of CP length. Because, the capabilities to absorb multipath effects increases with higher value of CP length.

These results provide some interaction of the PHY layer with channel model. In the following subsections we will observe error rate statistics in the form of BER and BLER from our simulation. We will also observe the performance of different error correction capabilities of the implemented simulator.

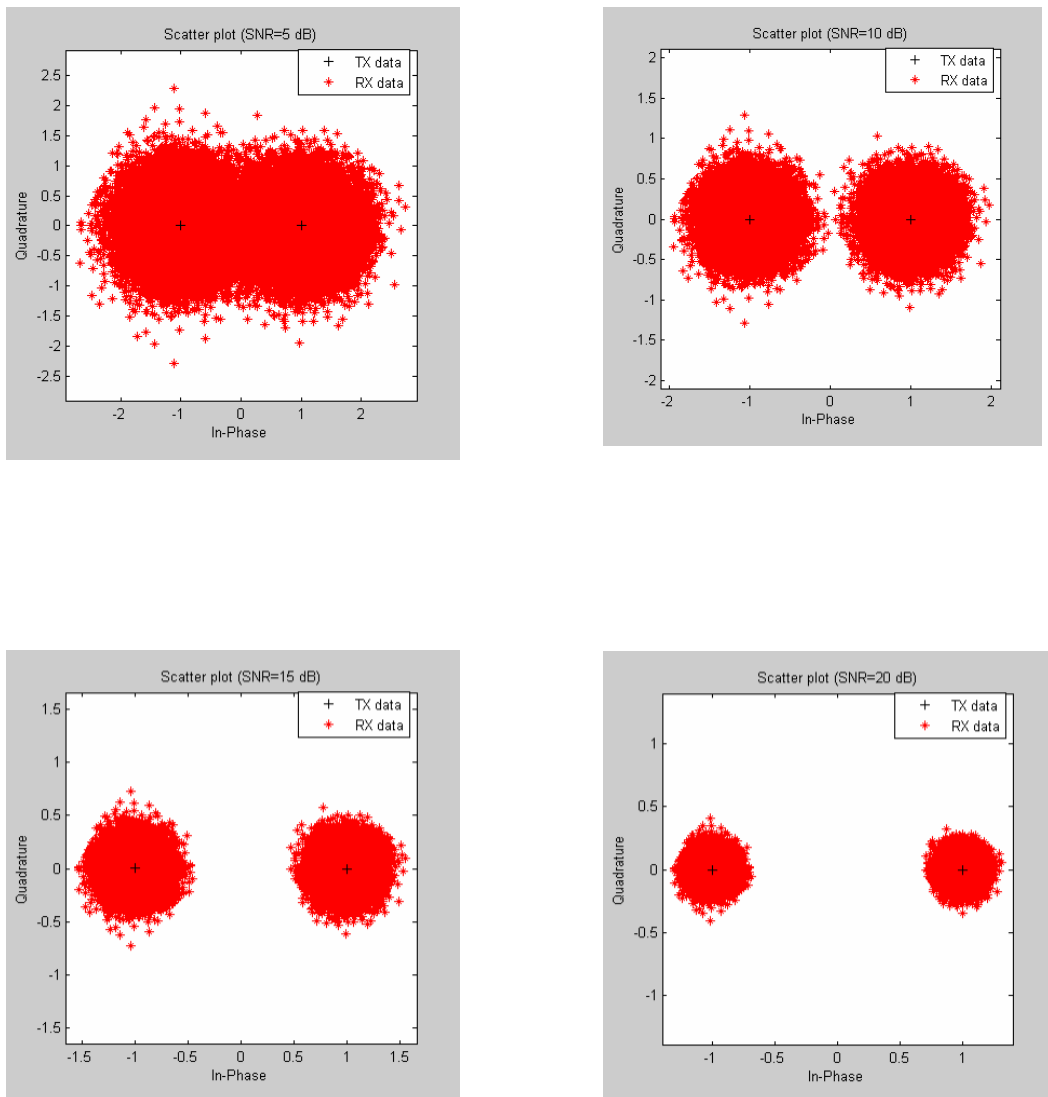


Figure 5.1: Scatter Plots for BPSK modulation (RS-CC 1/2) in SUI-1 channel model

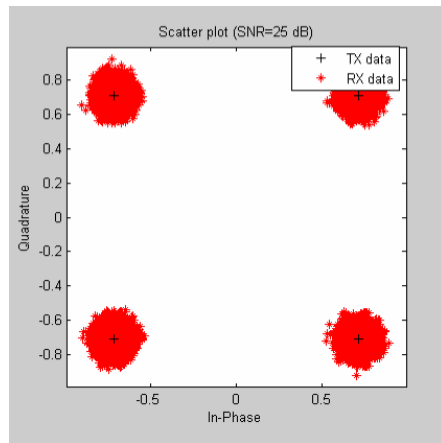
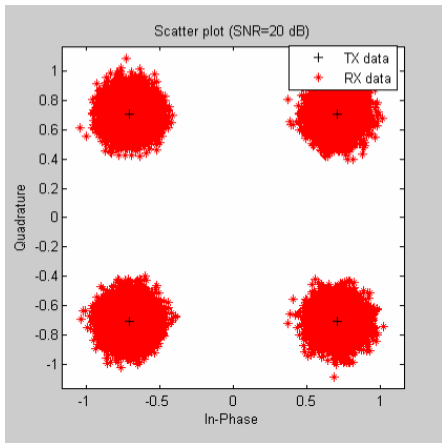
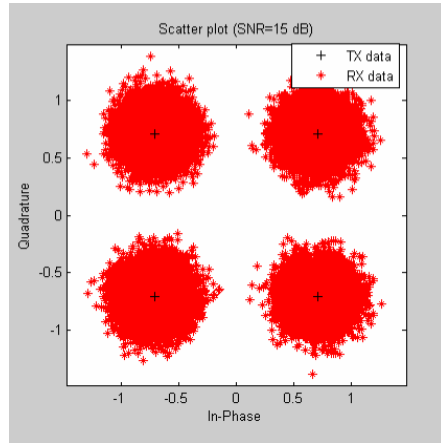
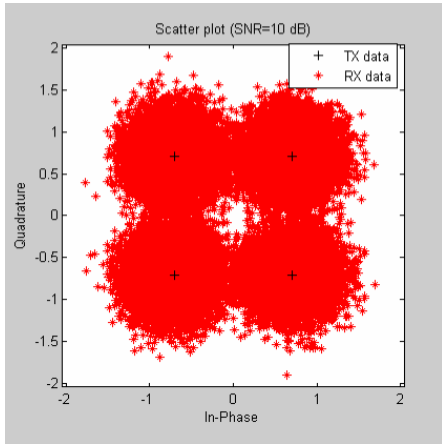


Figure 5.2: Scatter Plots for QPSK modulation (RS-CC 1/2) in SUI-1 channel model

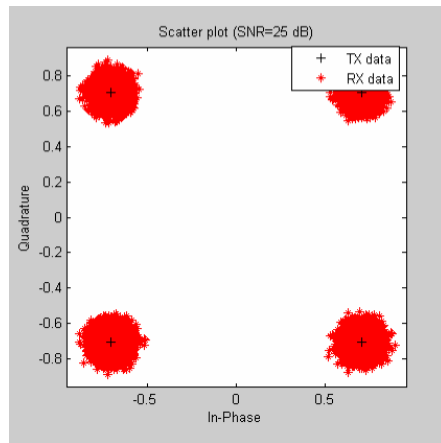
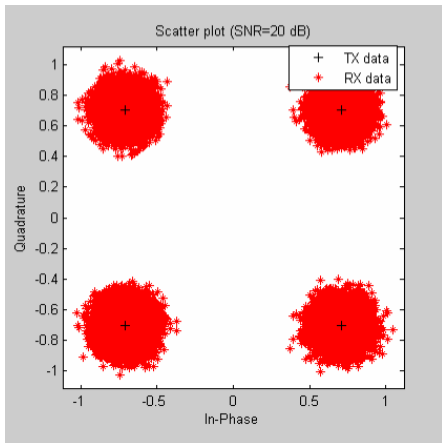
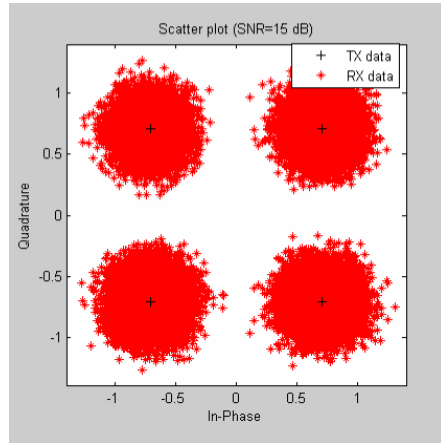
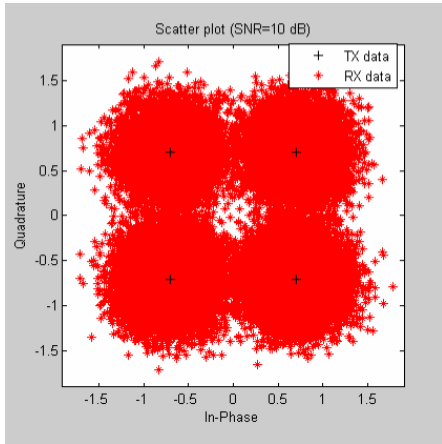


Figure 5.3: Scatter Plots for QPSK modulation (RS-CC 3/4) in SUI-1 channel model

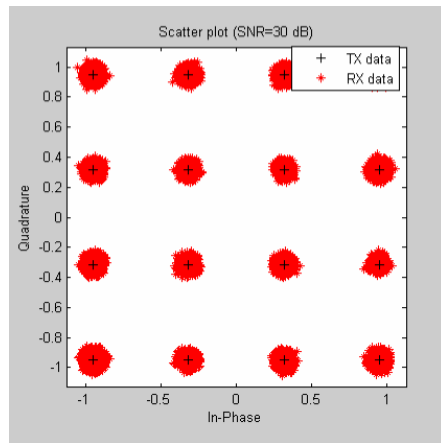
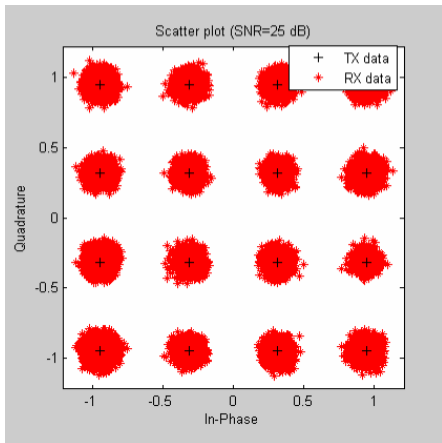
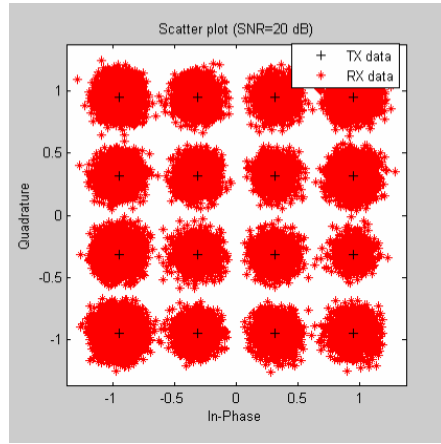
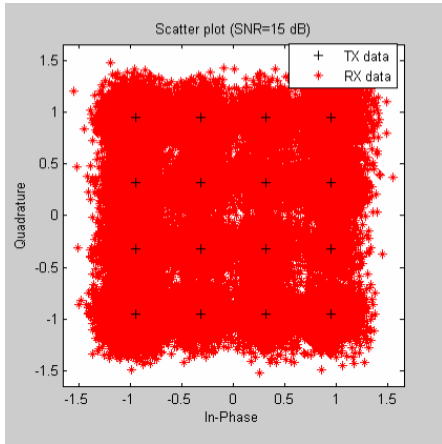


Figure 5.4: Scatter Plots for 16-QAM modulation (RS-CC 1/2) in SUI-1 channel model

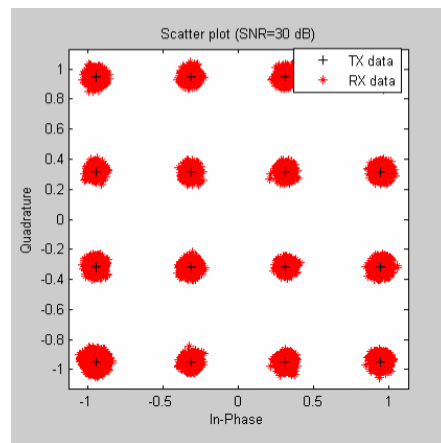
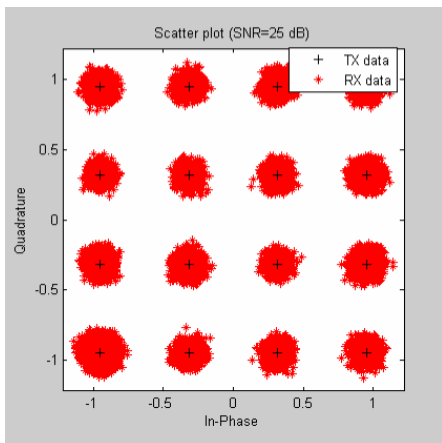
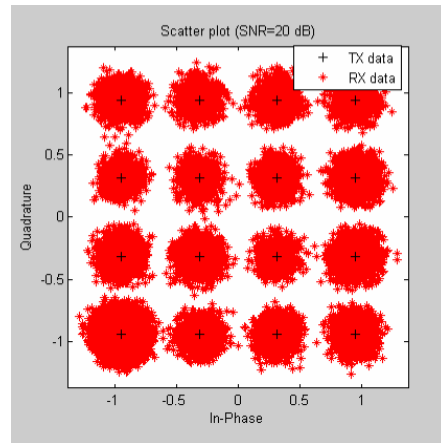
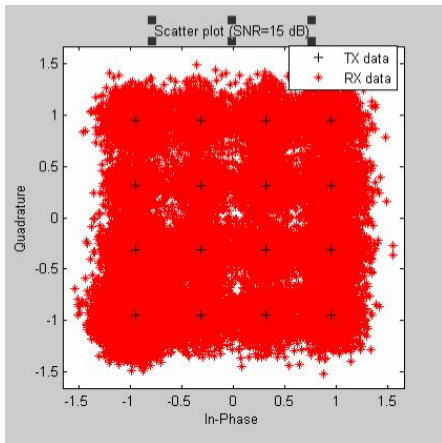


Figure 5.5: Scatter Plots for 16-QAM modulation (RS-CC 3/4) in SUI-1 channel model

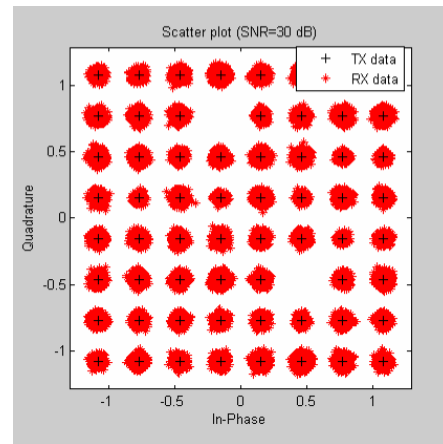
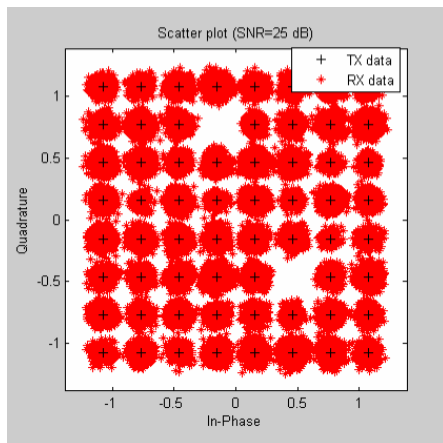
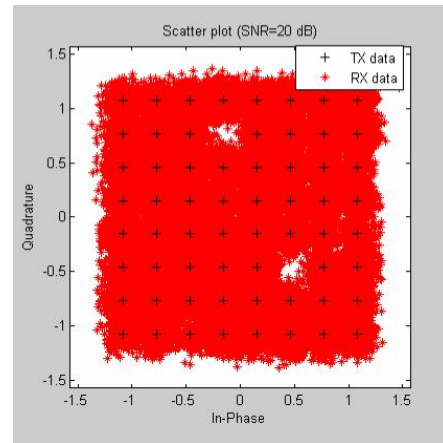
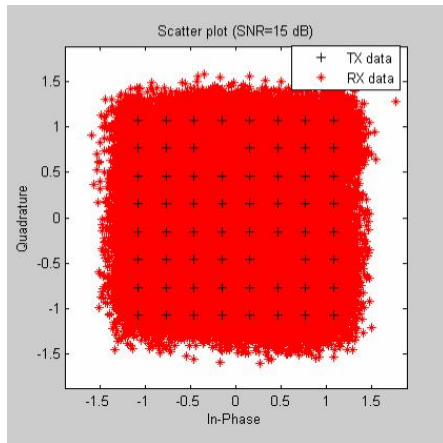


Figure 5.6: Scatter Plots for 64-QAM modulation (RS-CC 2/3) in SUI-1 channel model

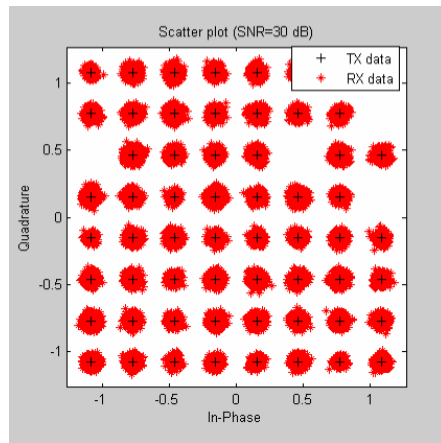
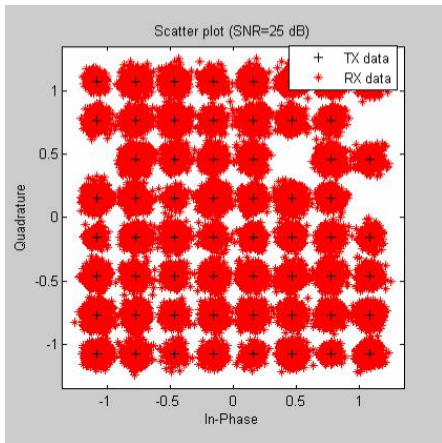
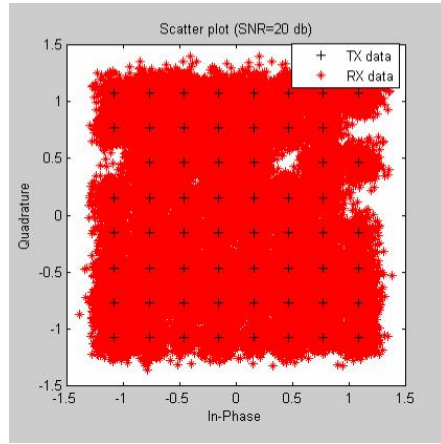
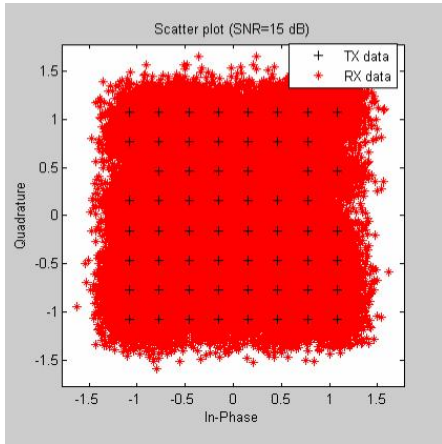


Figure 5.7: Scatter Plots for 64-QAM modulation (RS-CC 3/4) in SUI-1 channel model

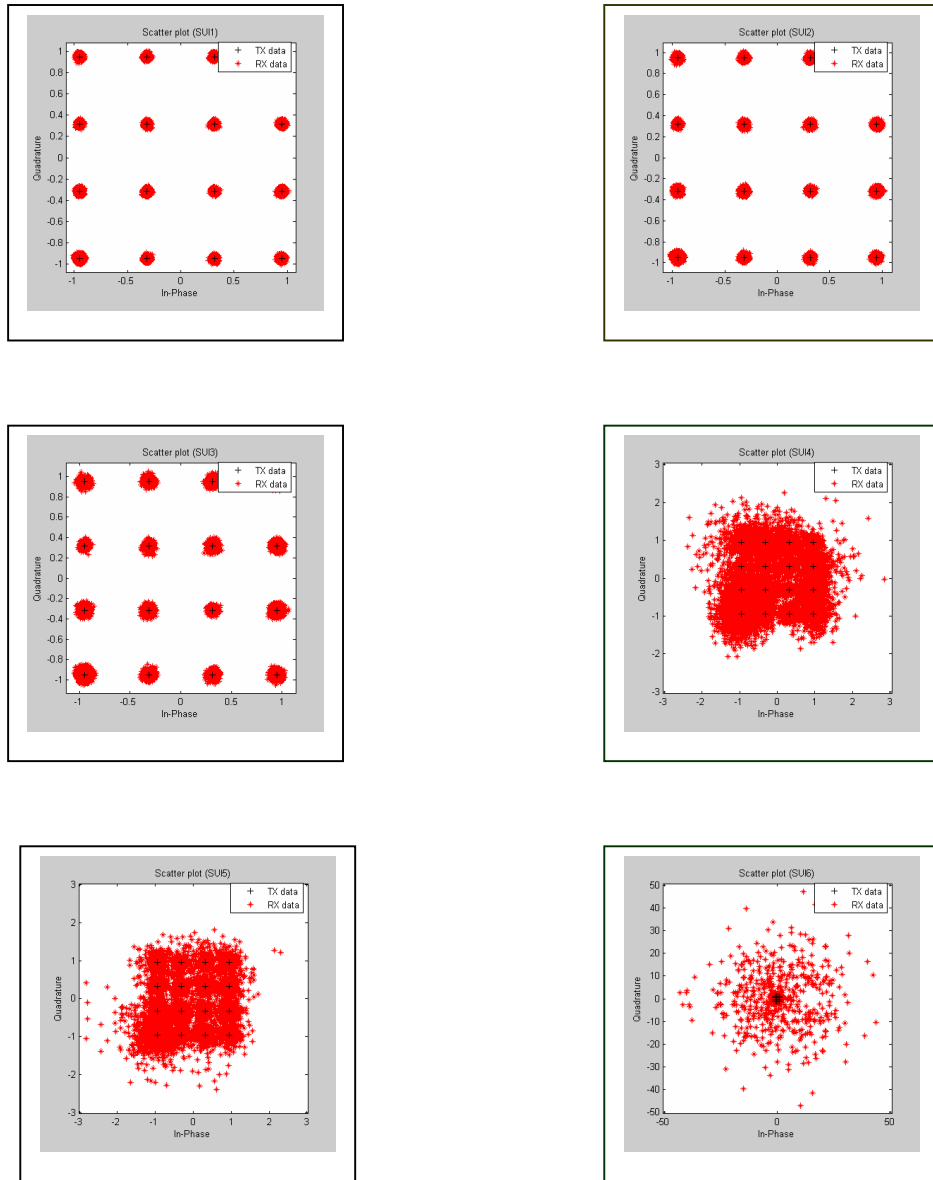


Figure 5.8: Scatter Plots for 64-QAM modulation (RS-CC 2/3) in different SUI channel model

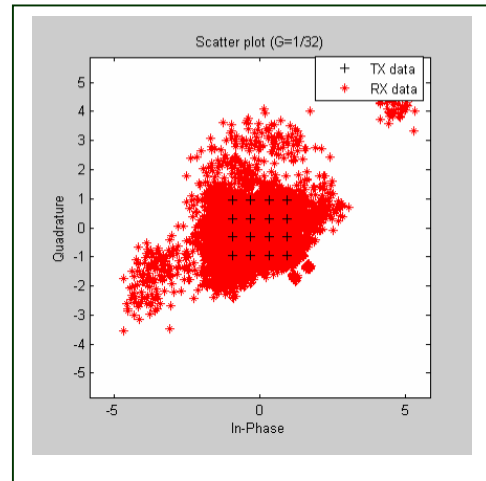
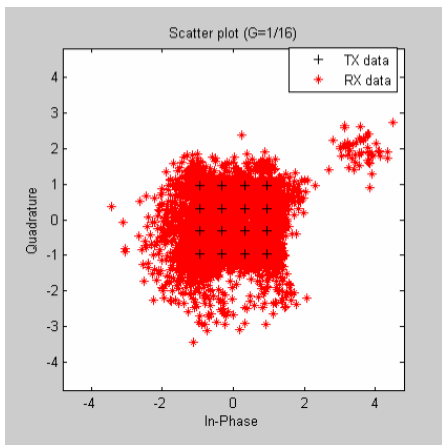
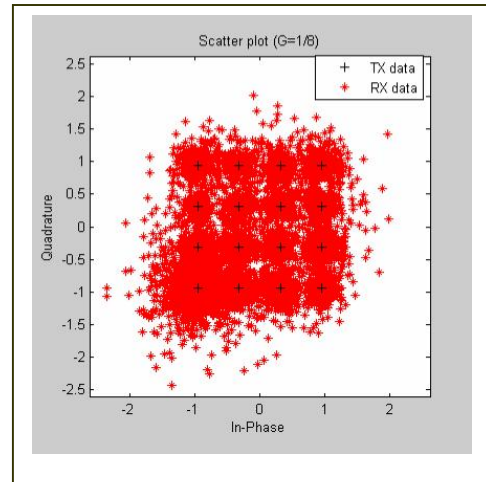
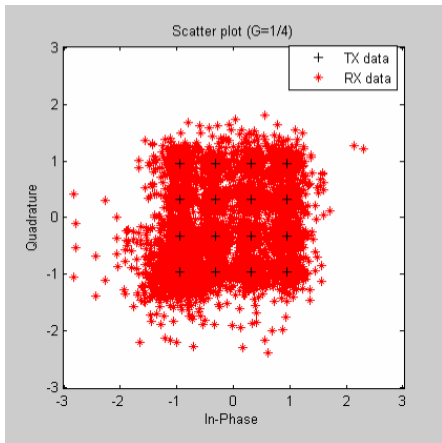


Figure 5.9: Scatter plot for 16-QAM with different CP length on SUI-5 channel model

5.2.2 BER Plots

In this section we have presented various BER vs. SNR plots for all the mandatory modulation and coding profiles as specified in the standard on same channel models. Figure 5.10, 5.11 and 5.12 show the performance on SUI-1, 2 and 3 channel models respectively. It can be seen from this figures that the lower modulation and coding scheme provides better performance with less SNR. This can be easily visualized if we look at their constellation mapping; larger distance between adjacent points can tolerate larger noise (which makes the point shift from the original place) at the cost of coding rate. By setting threshold SNR, adaptive modulation schemes can be used to attain highest transmission speed with a target BER. SNR required to attain BER level at 10^{-3} are tabulated in Table 5.1.

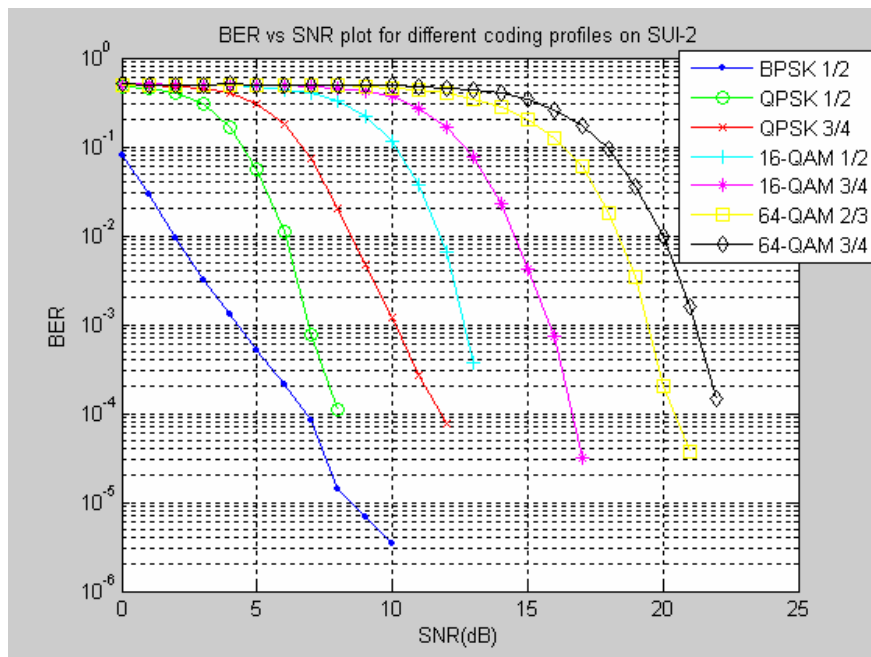


Figure 5.10: BER vs. SNR plot for different coding profiles on SUI-1 channel

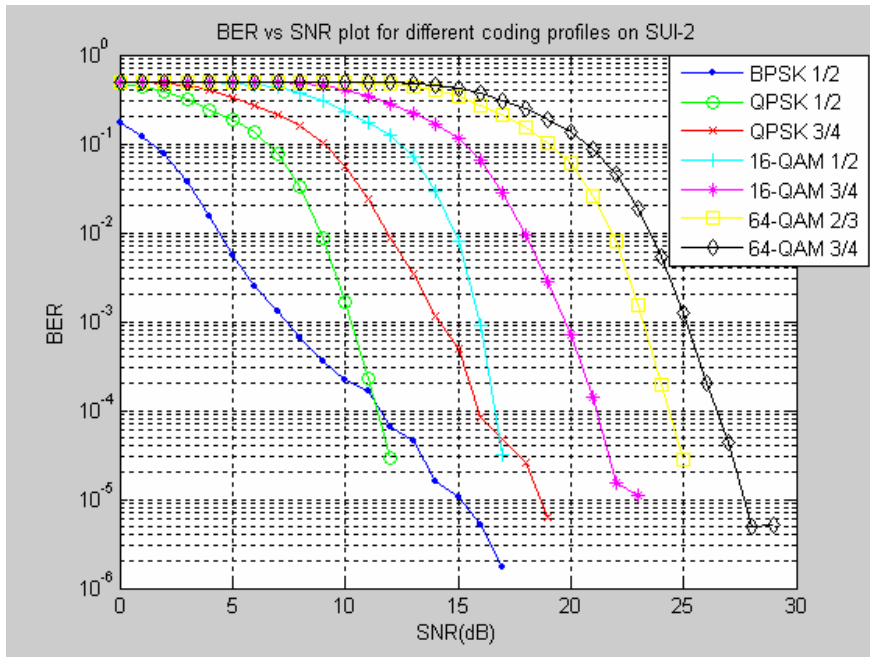


Figure 5.11: BER vs. SNR plot for different coding profiles on SUI-2 channel

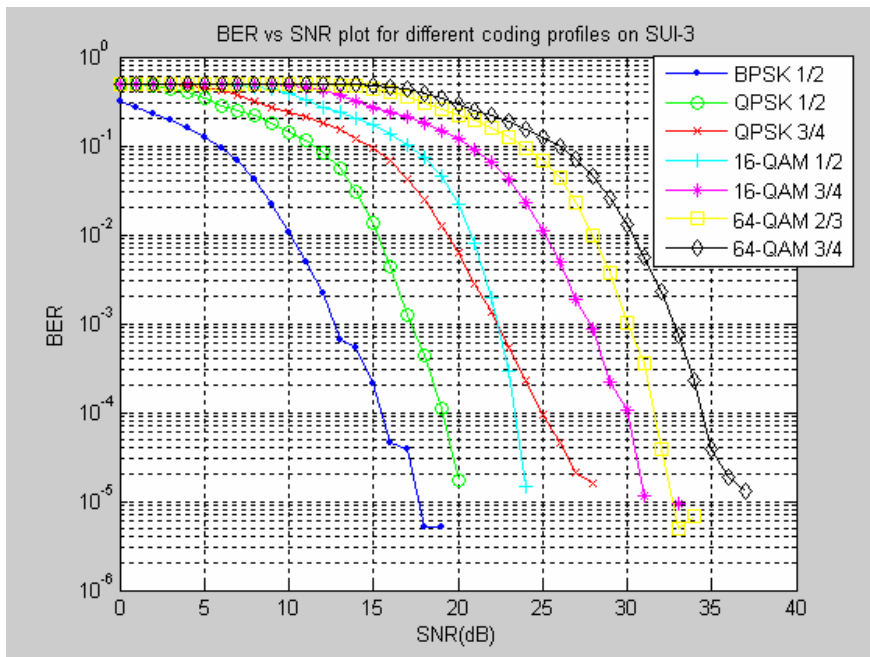


Figure 5.12: BER vs. SNR plot for different coding profiles on SUI-3 channel

Table 5.1: SNR required at BER level 10^{-3} for different modulation and coding profile

| Mod. | BPSK | QPSK | QPSK | 16-QAM | 16-QAM | 64-QAM | 64-QAM |
|-----------|---------------------------------|------|------|--------|--------|--------|--------|
| Code rate | 1/2 | 1/2 | 3/4 | 1/2 | 3/4 | 2/3 | 3/4 |
| Channel | SNR (dB) at BER level 10^{-3} | | | | | | |
| SUI-1 | 4.3 | 6.6 | 10 | 12.3 | 15.7 | 19.4 | 21.3 |
| SUI-2 | 7.5 | 10.4 | 14.1 | 16.25 | 19.5 | 23.3 | 25.4 |
| SUI-3 | 12.7 | 17.2 | 22.7 | 22.7 | 28.3 | 30 | 32.7 |

Having observed the performance of different profiles under same channel models, let us observe the variations with the change in channel conditions. Figure 5.13 shows the performance of 16-QAM $\frac{1}{2}$ on SUI-1, 2 and 3 channel models. It can be seen from the figure that the severity of corruption is highest on SUI-3 and lowest in SUI-1 channel model. The order of the severity of corruption can be easily understood by analyzing the tap power and delays of the channel models, since the doppler effect is reasonably small for fixed deployment. All the three models have same amount of delays for corresponding tap except tap 3 of SUI-2 models has $0.2 \mu\text{s}$ larger than the corresponding tap of the other two models. But, in this case tap power dominates in determining the order of severity of corruption. SUI-3 has highest tap power value and SUI-1 has lowest value.

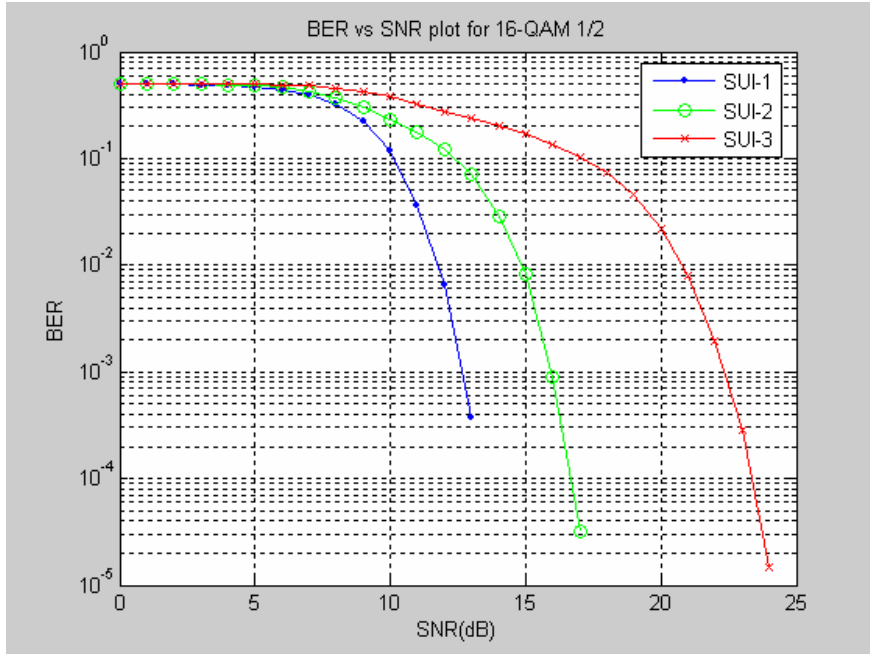


Figure 5.13: BER vs. SNR plot for 16-QAM 1/2 on different SUI channel

5.2.3 BLER Plots

BLER results play a very important role in the study of PHY layer performance analysis. Fig. 5.14, 5.15 and 5.16 show the BLER performance of all the modulation and coding profiles on SUI-1, 2 and 3 channel models respectively. The results are consistent with the BER performance which we have observed in the previous section. In case of SUI-1 channel condition, QPSK modulation requires 3dB more SNR for 1/4 code rate improvement at BLER level 10^{-2} . The same amount of SNR is required for 1/4 code rate improvement for 16-QAM modulation while 1.7 dB more SNR is required for 1/12 code rate improvement for 64 QAM. SNR level required to attain 10^{-2} BLER level for all the modulation and coding profile on different SUI channels are tabulated in Table 5.2. Figure 5.17 shows the performance of 64-QAM 2/3 on SUI-1, 2 and 3 channel models. The severity of corruption is also consistent with the BER performance. 4 dB SNR improvement is observed in SUI-1 channel condition compared to SUI-2 channel and 9 dB improvement compared to SUI-3 channel at BLER level of 10^{-2} .

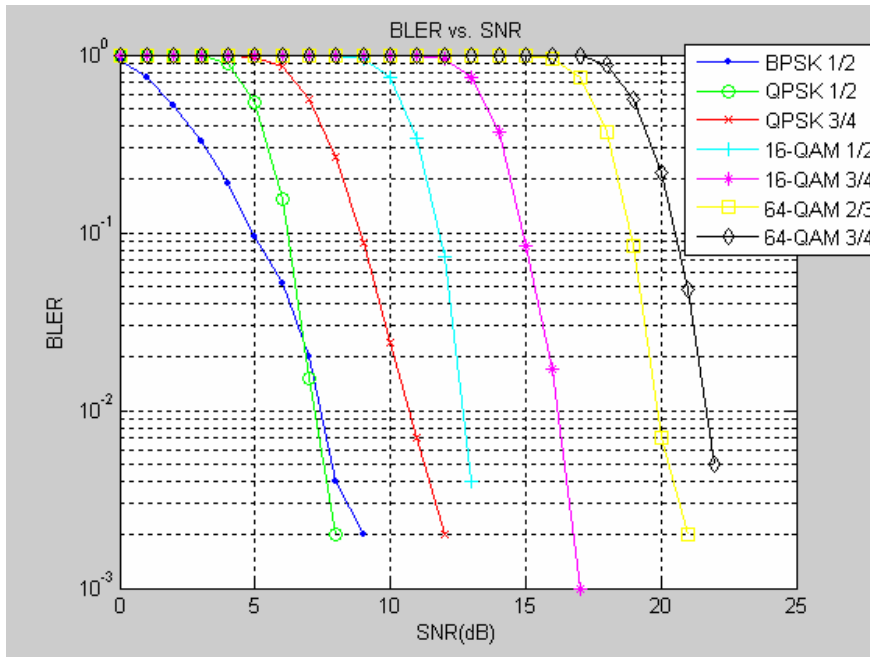


Figure 5.14: BLER vs. SNR plot for different modulation and coding profile on SUI-1

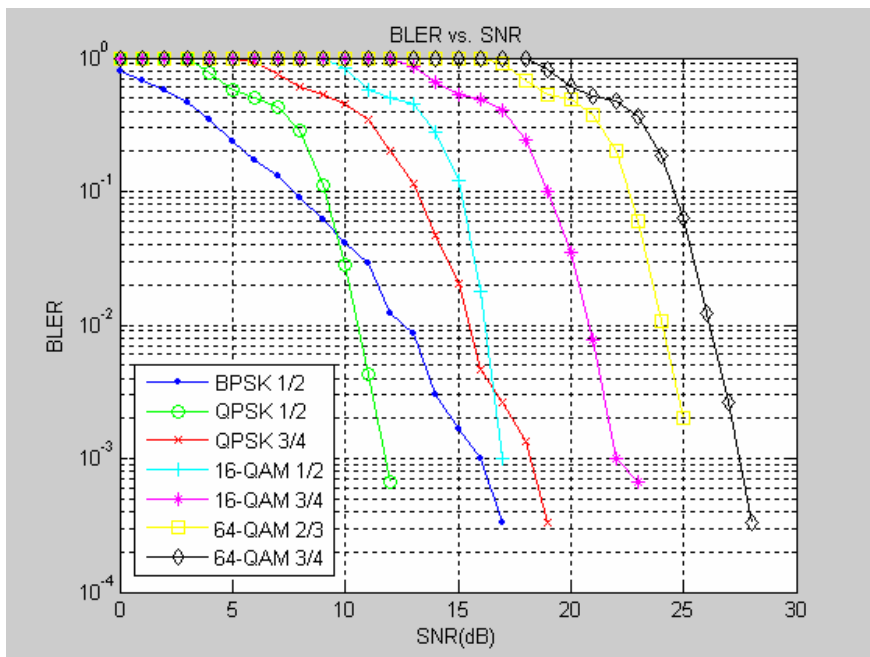


Figure 5.15: BLER vs. SNR plot for different modulation and coding profile on SUI-2

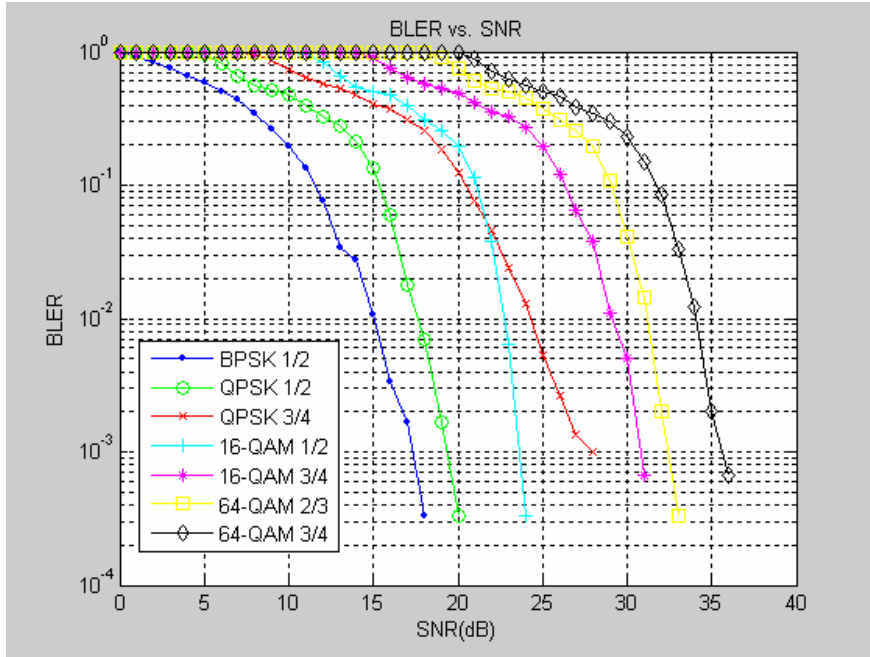


Figure 5.16: BLER vs. SNR plot for different modulation and coding profile on SUI-3

Table 5.2: SNR required at BLER level 10^{-2} for different modulation and coding profile

| Mod. | BPSK | QPSK | QPSK | 16-QAM | 16-QAM | 64-QAM | 64-QAM |
|-----------|----------------------------------|------|------|--------|--------|--------|--------|
| Code Rate | 1/2 | 1/2 | 3/4 | 1/2 | 3/4 | 2/3 | 3/4 |
| Channel | SNR (dB) at BLER level 10^{-2} | | | | | | |
| SUI-1 | 7.3 | 7 | 11 | 12.6 | 15.6 | 19.6 | 21.3 |
| SUI-2 | 10.7 | 12.7 | 15.4 | 16.5 | 20.8 | 23.8 | 26.1 |
| SUI-3 | 15 | 17.7 | 22.7 | 24.4 | 28.8 | 31.2 | 33.8 |

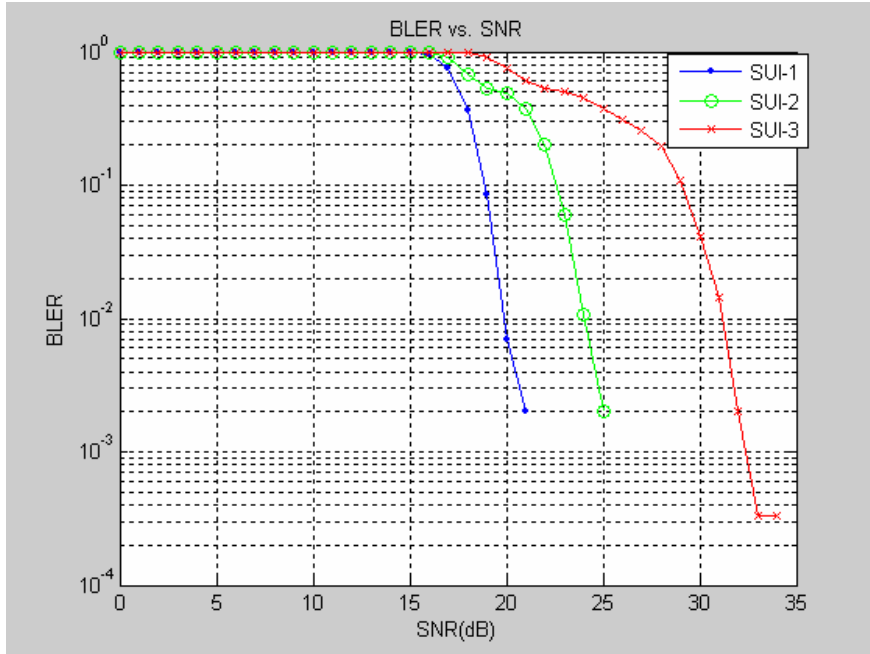


Figure 5.17: BLER vs. SNR plot for 64-QAM 2/3 modulation and coding profile on different SUI channel

5.2.4 Effect of Forward Error Correction

An interesting simulation of FEC is that without the concatenated Reed-Solomon and Convolutional coder, how much performance degradation will appear in this design. To figure out how much improvement of the concatenated code, the QPSK 1/2 modulation and coding profile is chosen on SUI-3 channel model. Figure 5.18 shows the performance of RS-CC compared to no FEC. FEC improves the BER performance by almost 6dB at BER level of 10^{-3} . Figure 5.19 shows the BLER performance for the same scenario. 10 dB SNR improvement is observed at BLER level of 10^{-2} .

The observations made in Figure 5.18 and Figure 5.19 is repeated for 16-QAM 1/2 and 64-QAM 2/3 modulation and coding profiles also. It can be seen from the Figure 5.20 and 5.21 that FEC gains 7 dB improvement at BER level of 10^{-3} while 11.8 dB improvement at BLER level of 10^{-2} . In case of 64-QAM 2/3, Figure 5.22 shows 4.5 dB improvement is observed at BER level of 10^{-3} and Figure 5.23 shows 10 dB improvement is observed at BLER level of 10^{-2} .

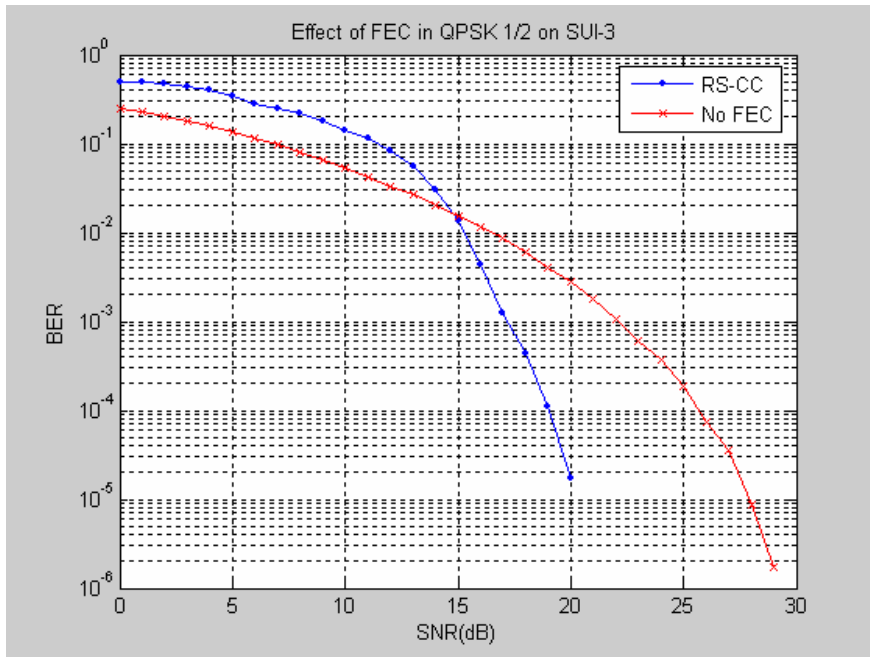


Figure 5.18: Effect of FEC in QPSK 1/2 on SUI-3 channel model

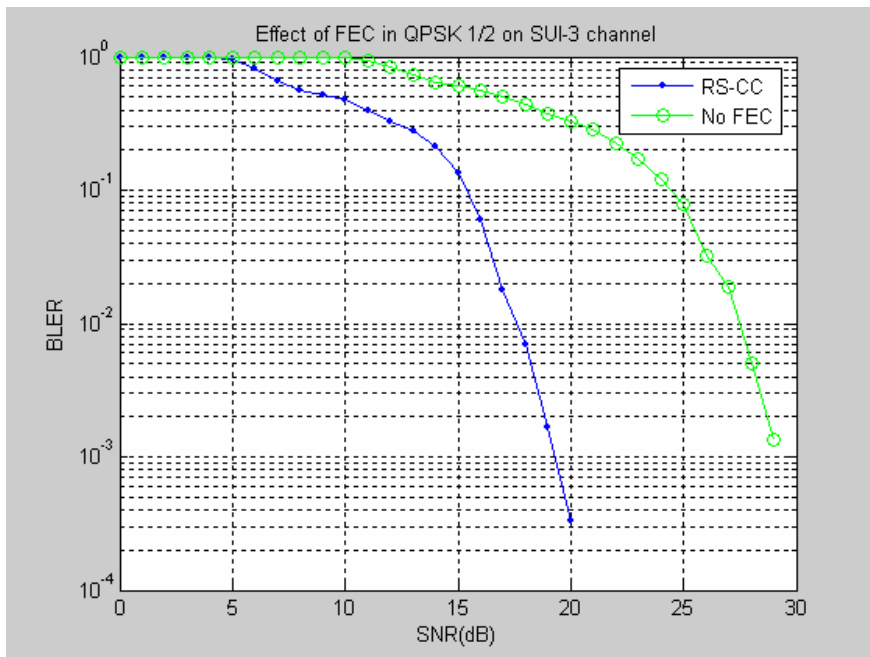


Figure 5.19: Effect of FEC in QPSK 1/2 on SUI-3 channel model

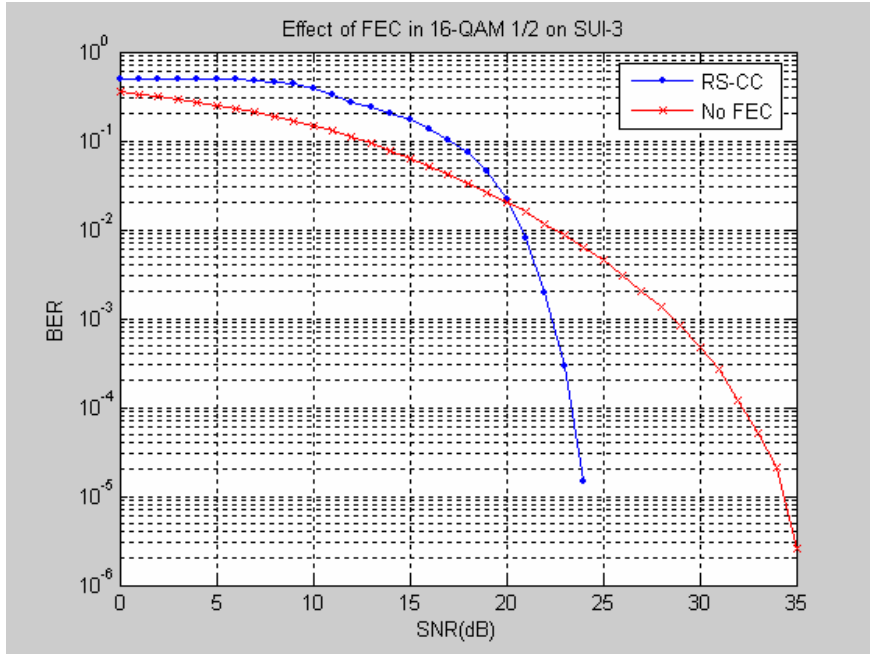


Figure 5.20: Effect of FEC in 16-QAM 1/2 on SUI-3 channel model

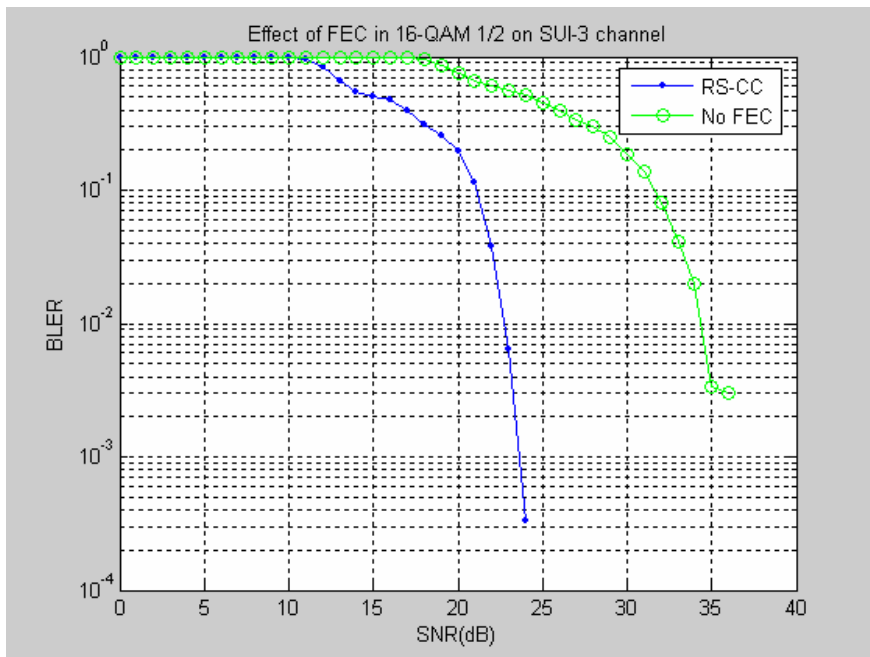


Figure 5.21: Effect of FEC in 16-QAM 1/2 on SUI-3 channel model

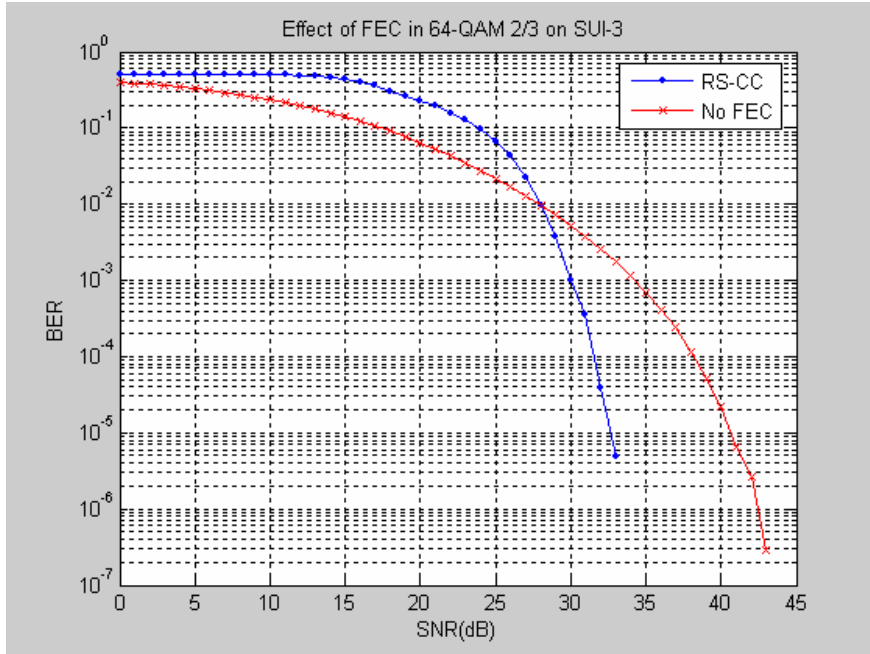


Figure 5.22: Effect of FEC in 64-QAM 2/3 on SUI-3 channel model

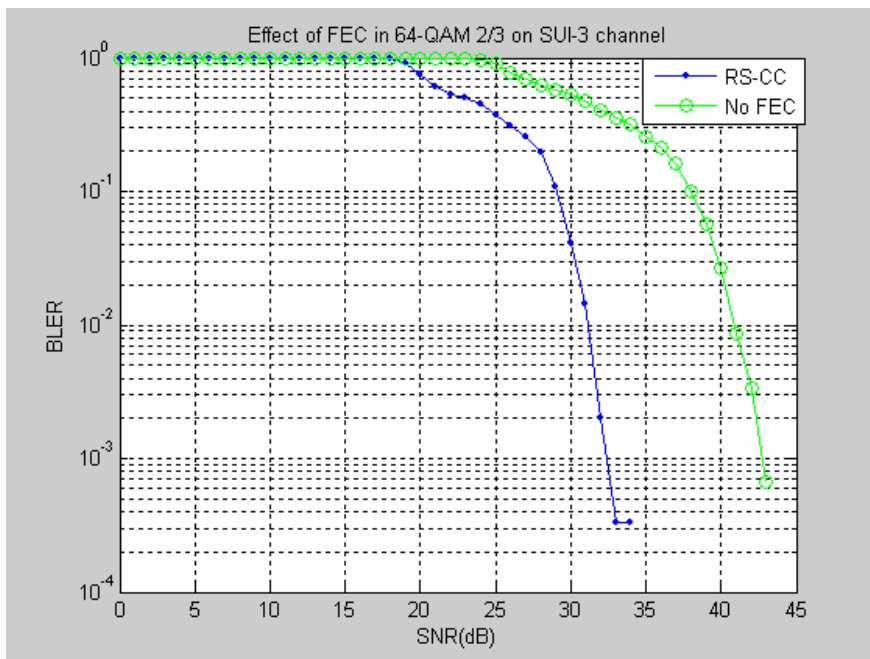


Figure 5.23: Effect of FEC in 64-QAM 2/3 on SUI-3 channel model

5.2.5 Effect of Reed-Solomon Encoding

Another interesting simulation of FEC is that without the Reed-Solomon encoder, how much performance degradation will appear in this design. The performance improvement due to RS codec on different modulation and coding profiles has been observed on SUI-3 channel model. The performance can be observed from Figure 5.24 to 5.29. The SNR improvement due to RS codec for different schemes is tabulated in Table 5.3.

Table 5.3: Performance improvement due to RS Coding

| Modulation | QPSK | 16-QAM | 64-QAM |
|---------------------------|------|--------|--------|
| Code Rate | 1/2 | 1/2 | 2/3 |
| SNR(dB) at BER 10^{-3} | 1 | 1.2 | 1.4 |
| SNR(dB) at BLER 10^{-2} | 3 | 4.5 | 5 |

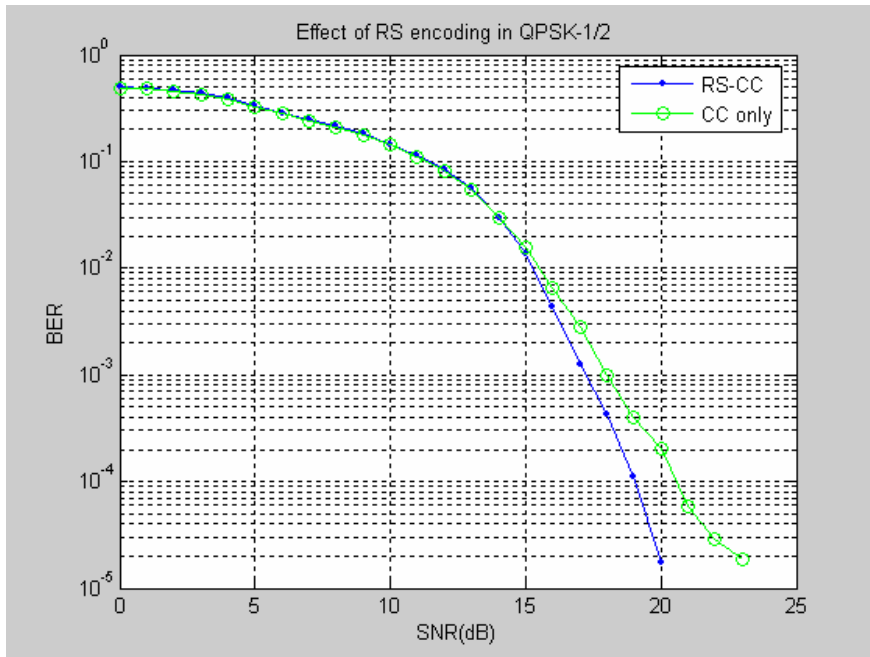


Figure 5.24: Effect of Reed Solomon encoding in QPSK $\frac{1}{2}$ on SUI-3 channel model

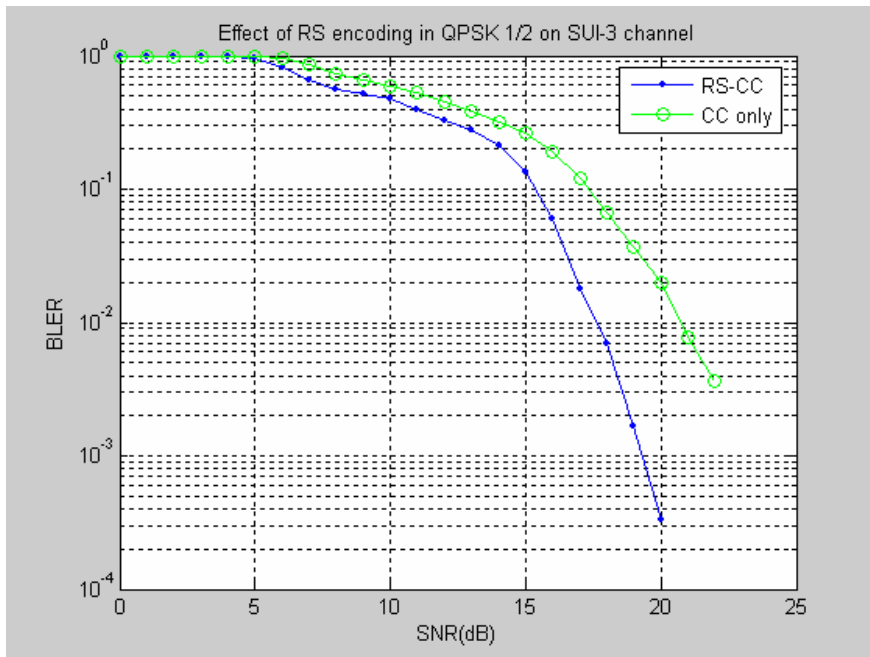


Figure 5.25: Effect of Reed Solomon encoding in QPSK $\frac{1}{2}$ on SUI-3 channel model

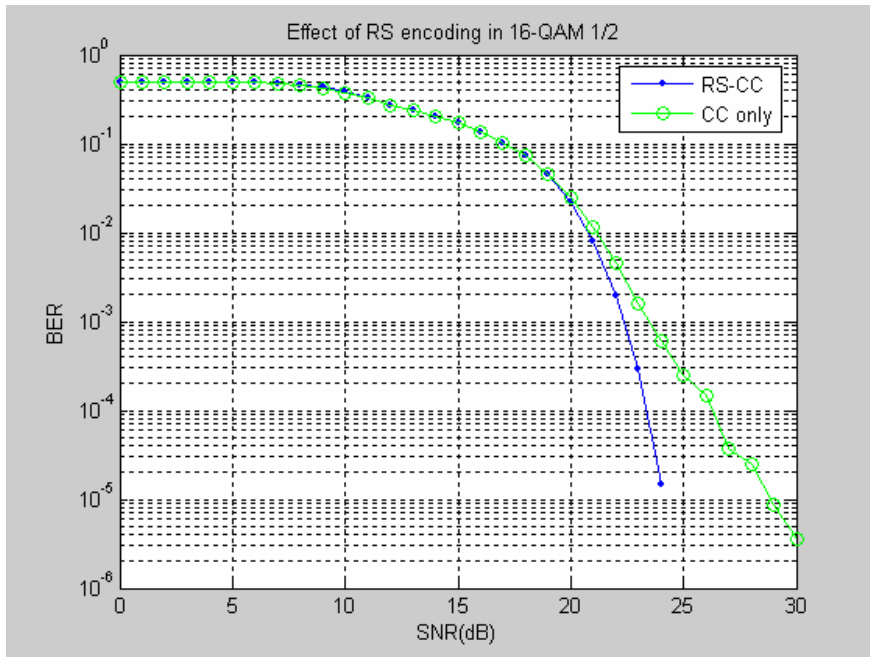


Figure 5.26: Effect of Reed Solomon encoding in 16-QAM $\frac{1}{2}$ on SUI-3 channel model

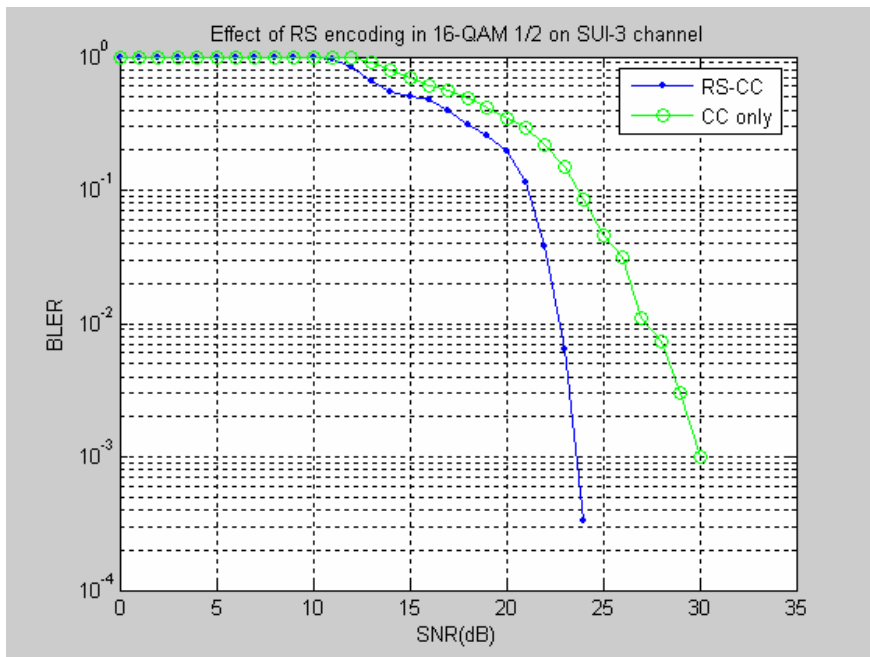


Figure 5.27: Effect of Reed Solomon encoding in 16-QAM $\frac{1}{2}$ on SUI-3 channel model

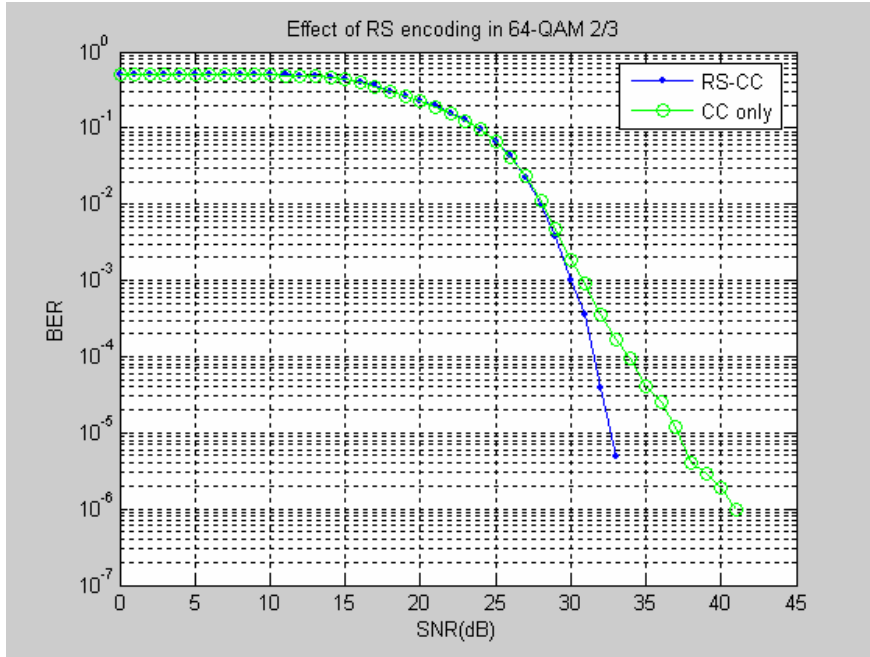


Figure 5.28: Effect of Reed Solomon encoding in 64-QAM 2/3 on SUI-3 channel model

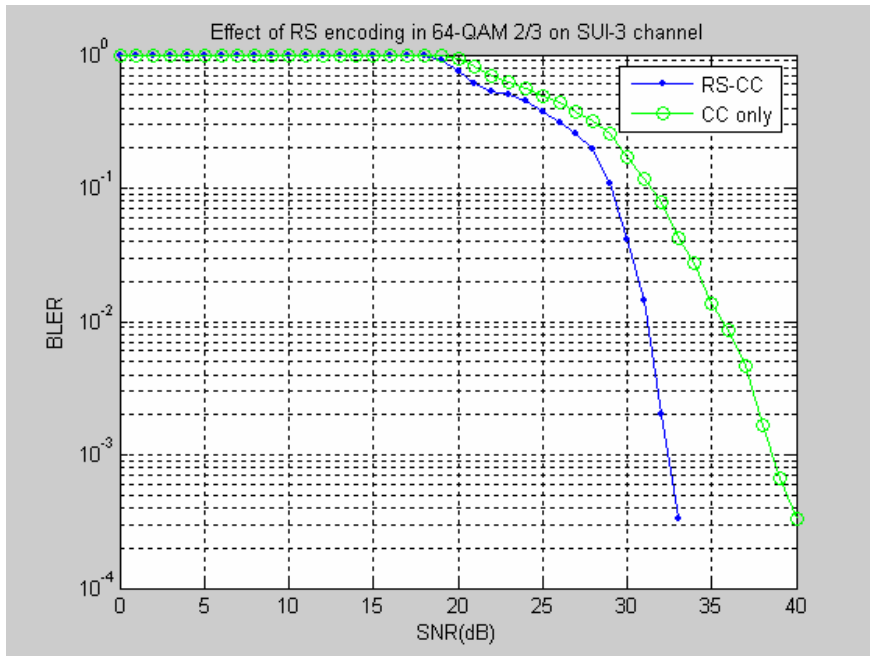


Figure 5.29: Effect of Reed Solomon encoding in 64-QAM 2/3 on SUI-3 channel model

5.2.6 Effect of Bit interleaver

The effect of bit interleaving on the performance of different modulation and coding schemes has been observed here. It can be seen from the Figure 5.30 and 5.31 that bit interleaver gains 2.2 dB SNR improvement at BER level of 10^{-3} and 1 dB improvement at BLER level of 10^{-2} for BPSK. Figure 5.32 to Figure 5.37 show the performance improvement due to bit interleaver for QPSK $\frac{1}{2}$, 16-QAM $\frac{1}{2}$ and 64-QAM $\frac{2}{3}$. The SNR improvement observed from the figures are tabulated in Table 5.4. In this case, we have conducted all the simulation on SUI-2 channel model.

Table 5.4: Performance improvement due to bit interleaving

| Modulation | BPSK | QPSK | 16-QAM | 64-QAM |
|------------------------------|------|------|--------|--------|
| Code Rate | 1/2 | 1/2 | 1/2 | 2/3 |
| SNR(dB) at BER 10^{-3} | 2.2 | 0.8 | 1.4 | 2.2 |
| SNR(dB) at BLER 10^{-2} | 1 | 1.2 | 1.7 | 2.5 |

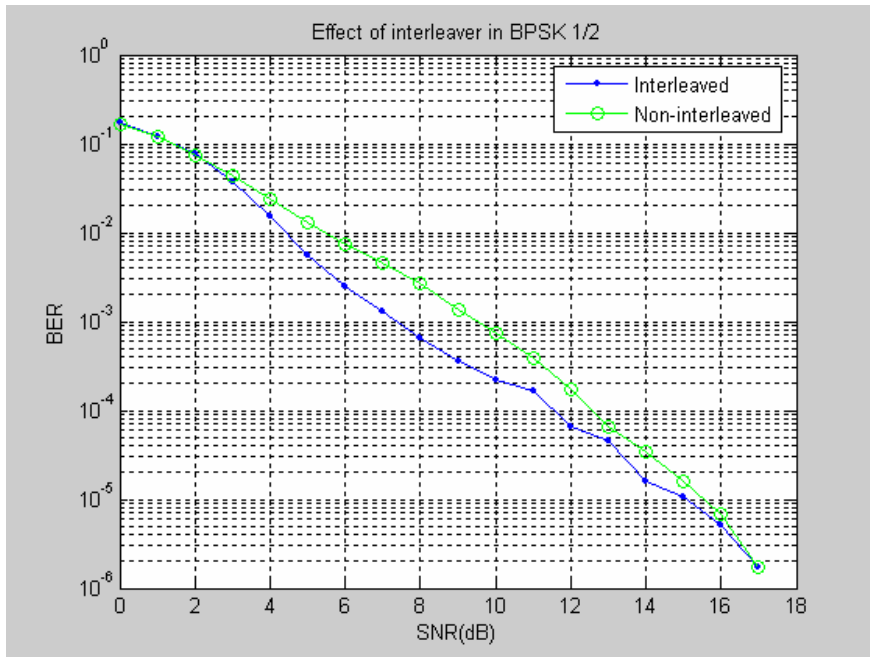


Figure 5.30: Effect of Block interleaver in BPSK $\frac{1}{2}$ on SUI-2 channel model

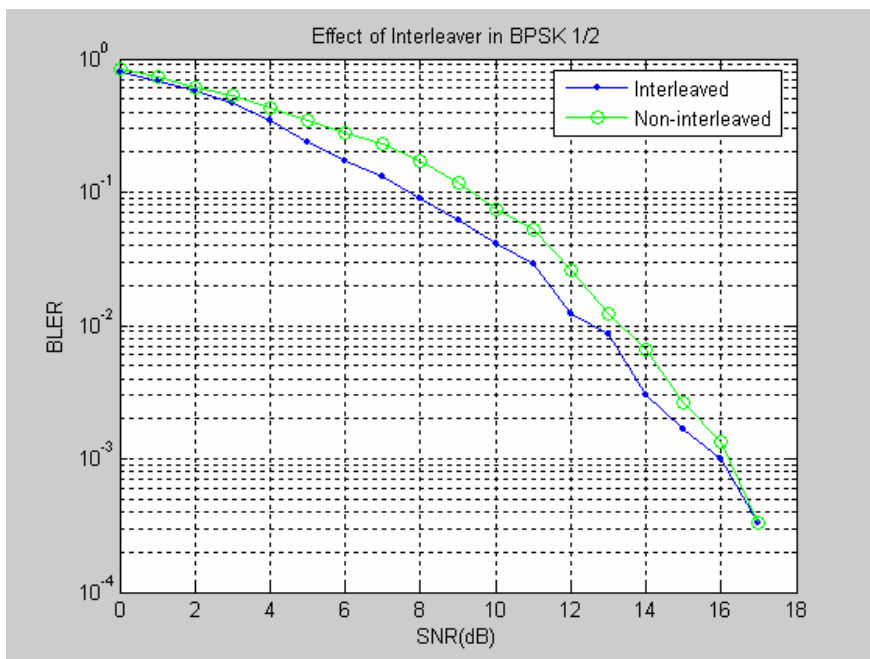


Figure 5.31: Effect of Block interleaver in BPSK $\frac{1}{2}$ on SUI-2 channel model

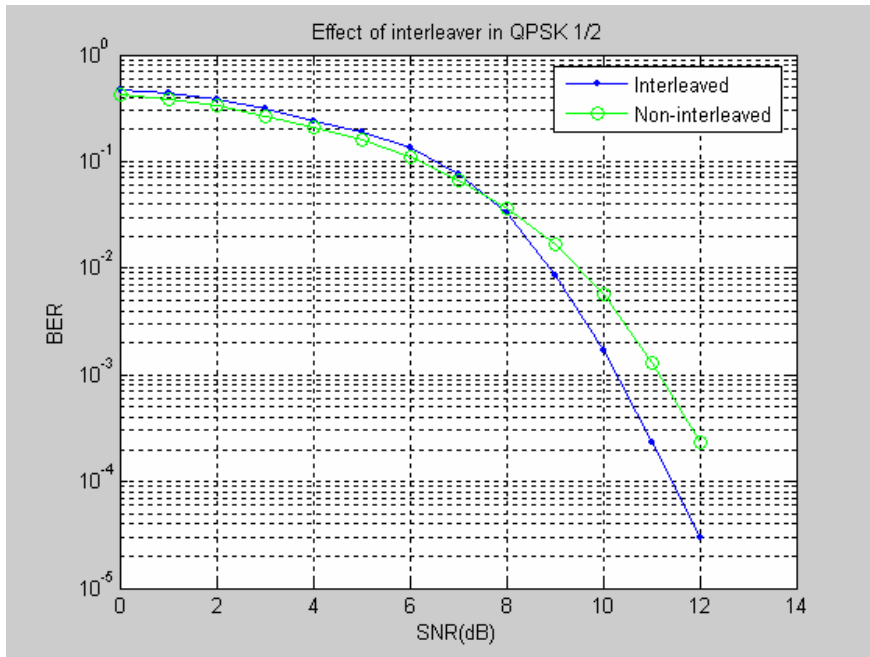


Figure 5.32: Effect of Block interleaver in QPSK 1/2 on SUI-2 channel model

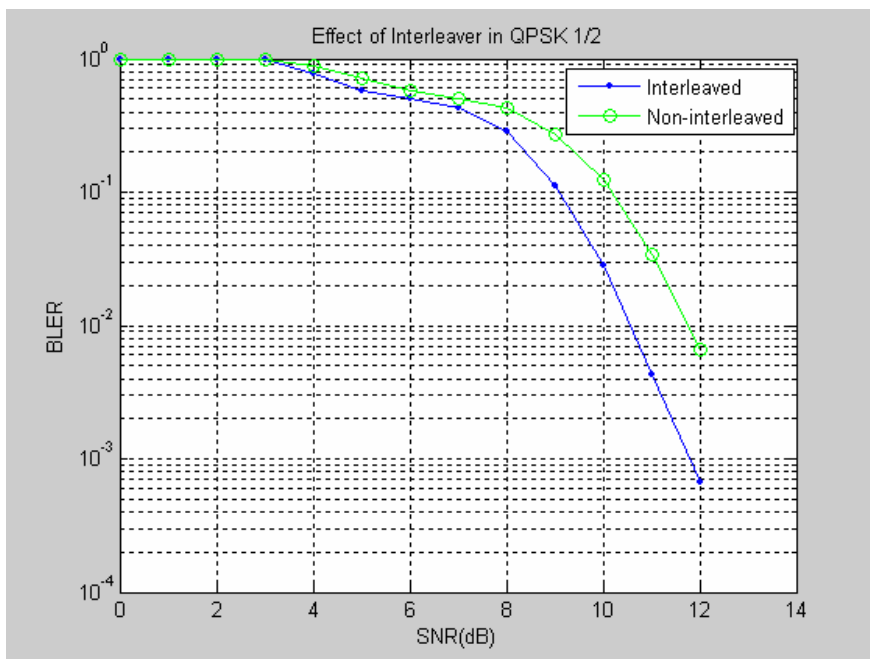


Figure 5.33: Effect of Block interleaver in QPSK 1/2 on SUI-2 channel model

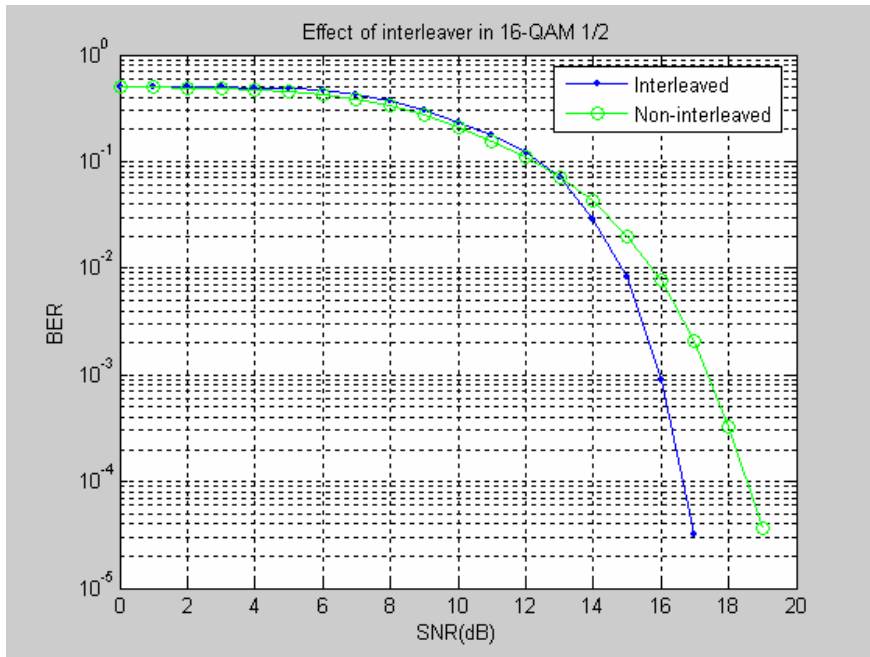


Figure 5.34: Effect of Block interleaver in 16-QAM $\frac{1}{2}$ on SUI-2 channel model

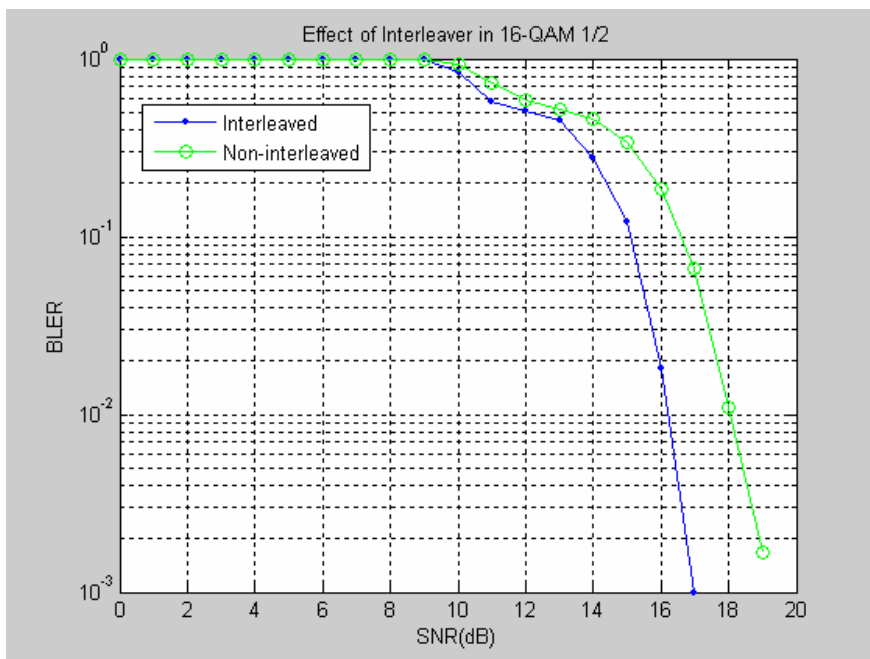


Figure 5.35: Effect of Block interleaver in 16-QAM $\frac{1}{2}$ on SUI-2 channel model

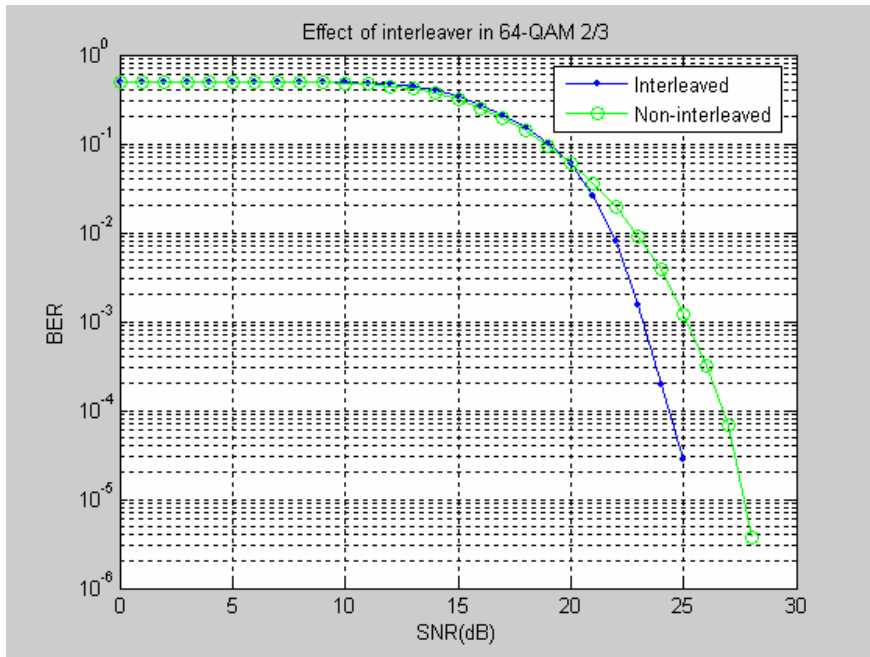


Figure 5.36: Effect of Block interleaver in 64-QAM 2/3 on SUI-2 channel model

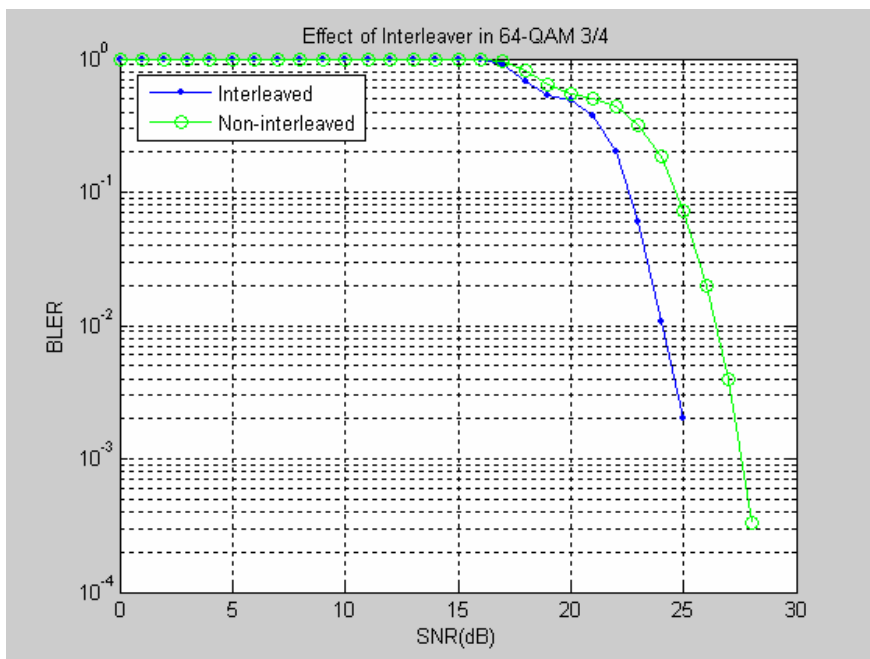


Figure 5.37: Effect of Block interleaver in 64-QAM 2/3 on SUI-2 channel model

5.2.7 Spectral Efficiency

The spectral efficiency of all the modulation and coding profile on SUI-1 channel model is shown in Figure 5.38. The spectral efficiency is presented in many ways in the literature. We derived the spectral efficiency using the relation [15],

$$\eta = (1 - p_e)^n m r \quad 6.1$$

Here,

P_e -the bit error rate

n - the number of bits in the block

m - the number of bits per symbol and

r - the code rate

Figure 5.39 shows the spectral efficiency of QPSK ¾ on SUI-1, 2 and 3 channel models.

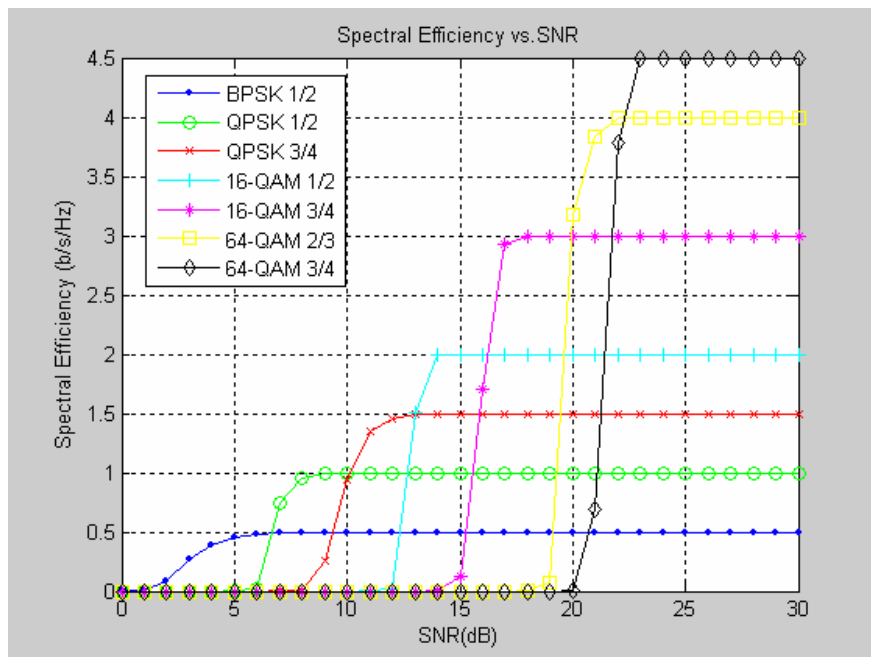


Figure 5.38 Spectral efficiency of different modulation and coding profile on SUI-1 channel model

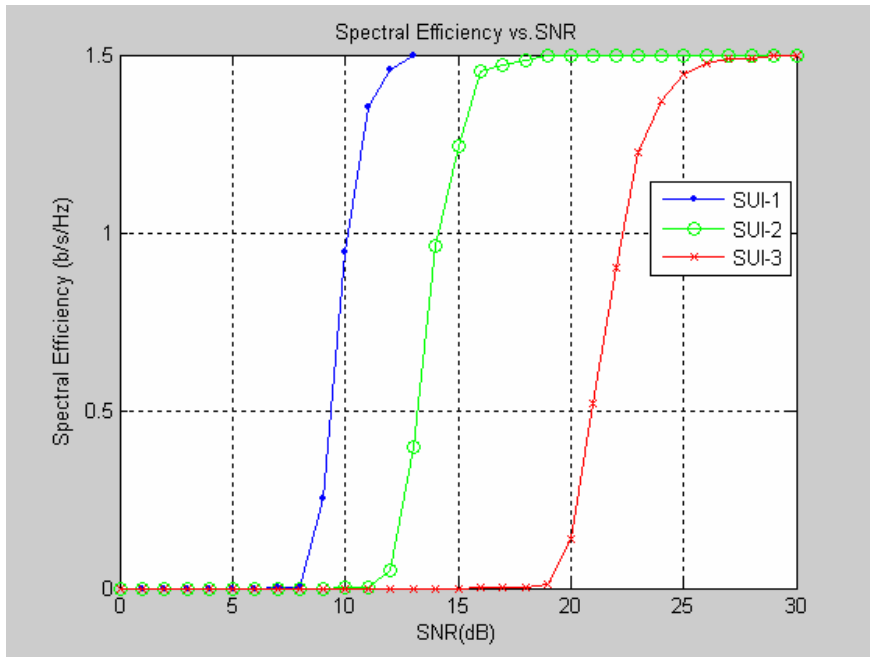


Figure 5.39: Spectral efficiency of QPSK $3/4$ on SUI-1, 2 and 3 channel model.

Chapter 6

Conclusion and Future Work

6.1 Conclusion

The key contribution of this thesis was the implementation of the IEEE 802.16 OFDM PHY layer using MATLAB in order to evaluate the PHY layer performance under reference channel model. The implemented PHY layer supports all the modulation and coding schemes as well as CP lengths defined in the specification. To keep matters simple we avoided doing over-sampling of the data samples before using the channel model. Though, that can be implemented by minor modifications. On the receiver side, we have assumed perfect channel estimation to avoid the effect of any particular estimation method on the simulation results, though insertion of pilot subcarriers in the OFDM symbols makes use of any comb-type estimator possible. The developed simulator can be easily modified to implement new features in order to enhance the PHY layer performance.

Simulation was the methodology used to investigate the PHY layer performance. The performance evaluation method was mainly concentrated on the effect of channel coding

on the PHY layer. The overall system performance was also evaluated under different channel conditions. Scatter plots were generated to validate the model in terms of general trends in reception quality as we vary different parameters. A key performance measure of a wireless communication system is the BER and BLER. The BER and BLER curves were used to compare the performance of different modulation and coding scheme used. The effects of the FEC and interleaving were also evaluated in the form of BER and BLER. These provided us with a comprehensive evaluation of the performance of the OFDM physical layer for different states of the wireless channel.

6.2 Future Works

The implemented PHY layer model still needs some improvement. The channel estimator can be implemented to obtain a depiction of the channel state to combat the effects of the channel using an equalizer.

The IEEE 802.16 standard comes with many optional PHY layer features, which can be implemented to further improve the performance. The optional Block Turbo Coding (BTC) can be implemented to enhance the performance of FEC. Space Time Block Code (STBC) can be employed in DL to provide transmit diversity.

Reference

- [1] IEEE 802.16-2004, ” *IEEE Standard for Local and Metropolitan Area Networks - Part 16: Air Interface for Fixed Broadband Wireless Access Systems*”, 1 October, 2004
- [2] Ghosh, A.; Wolter, D.R.; Andrews, J.G.; Chen, R., “*Broadband wireless access with WiMax/802.16: current performance benchmarks and future potential*”, Communications Magazine, IEEE, Vol.43, Iss.2, Feb. 2005,Pages: 129- 136
- [3] IEEE 802.16 and WiMAX, “http://www.wimax-industry.com/wp/papers/intel_80216_wimax.pdf”, last accessed on 15.05.07
- [4] Koffman, I.; Roman, V.,”*Broadband wireless access solutions based on OFDM access in IEEE 802.16*” Communications Magazine, IEEE, Vol.40, Iss.4, April 2002,Pages:96-103
- [5] ETSI Broadband Radio Access Networks (BRAN); HIPERMAN; Physical (PHY) Layer. Standard TS 102 177, 2003.
- [6] “*IEEE Standard 802.16 for Global Broadband Wireless Access,*” http://ieee802.org/16/docs/03/C80216-03_14.pdf” last accessed 15.05.07
- [7] IEEE Std 802.16-2001,”*IEEE Std. 802.16-2001 IEEE Standard for Local and Metropolitan area networks Part 16: Air Interface for Fixed Broadband Wireless Access Systems*”, December 2001
- [8] IEEE Std 802.16e-2005 and IEEE Std 802.16-2004/Cor 1-2005 (Amendment and Corrigendum to IEEE Std 802.16-2004),”*IEEE Standard for Local and metropolitan area networks Part 16: Air Interface for Fixed and Mobile Broadband Wireless Access Systems Amendment 2: Physical and Medium Access Control Layers for Combined Fixed and Mobile Operation in Licensed Bands and Corrigendum 1*”, February 2006
- [9] IEEE Std 802.16a-2003 (Amendment to IEEE Std 802.16-2001), “*IEEE Standard for Local and metropolitan area networks --- Part 16: Air Interface for Fixed Broadband Wireless Access Systems--- Amendment 2: Medium Access Control Modifications and Additional Physical Layer Specifications for 2-11 GHz*”, January 2003
- [10] Derrick D. Boom, “*Denial Of Service Vulnerabilities In IEEE 802.16 Wireless Networks*”, Master’s Thesis at Naval Postgraduate School Monterey, California,USA, 2004
- [11] Hikmet Sari, “*Characteristics and Compensation of Multipath Propagation in Broadband Wireless Access System*”, ECPS 2005 Conference, 15-18 March, 2005

- [12] V. Erceg, K.V.S. Hari, M.S. Smith, D.S. Baum et al, “*Channel Models for Fixed Wireless Applications*”, IEEE 802.16.3 Task Group Contributions 2001, Feb. 01
- [13] V. Erceg et. al, “*An empirically based path loss model for wireless channels in suburban environments*,” IEEE JSAC, vol. 17, no. 7, July 1999, pp. 1205-1211.
- [14] Bernard Sklar, “*Digital Communications: Fundamentals and Applications, 2nd Edition*,” January 11, 2001
- [15] S. Catreux, V. Erceg, D. Gesbert, and R. Heath, “*Adaptive Modulation and MIMO Coding for Broadband Wireless Data Networks*,” IEEE Communications Magazine, pp.108-115, June 2002.
- [16] WiMAX Forum Certification of Broadband Wireless Systems, http://www.wimaxforum.org/technology/downloads/Certification_FAQ_final.pdf , last accessed 15.05.2007
- [17] Fixed, nomadic, portable and mobile applications for 802.16-2004 and 802.16e WiMAX networks , http://www.wimaxforum.org/technology/downloads/Applications_for_802.16-2004_and_802.16e_WiMAX_networks_final.pdf , last accessed on 15.05.2007
- [18] Mobile WiMAX – Part I: A Technical Overview and Performance Evaluation, http://www.wimaxforum.org/technology/downloads/Mobile_WiMAX_Part1_Overview_and_Performance.pdf , last accessed on 15.10.2007
- [19] Sweeney, Daniel, “*WiMAX Operator’s Manual: Building 802.16 Wireless Networks*”, Apress Publishing, May 2004
- [20] Alamouti, S.M. , ”*A simple transmit diversity technique for wireless communications*” IEEE Journal on Selected Areas in Communications, Vol.16, Iss.8, Oct 1998, Pages:1451-1458
- [21] Wu, Zhongshan, “*MIMO-OFDM Communication Systems: Channel Estimation and Wireless Location*”, Ph.D Thesis, Dept. of Electrical & Computer Engineering, Louisiana State University, USA, May 2006
- [22] J.W. Cooley and J.W. Tukey, “*An Algorithm for the Machine Calculation of Complex Fourier Series*”, Math. Computation, vol. 19, pp. 297 - 301, 1965.
- [23] M. Rahman , S. Das , F. Fitzek, “*OFDM based WLAN systems*”, Technical Report, Aalborg University, Denmark, February 2005
- [24] R.V. Nee & R. Prasad, *OFDM for Wireless Multimedia Communications*. Artech House Publishers, 2000.

- [25] Rohling, M.; May, T.; Bruninghaus, K.; Grunheid, R., “*Broad-band OFDM radio transmission for multimedia applications*”, proceedings of the IEEE, Vol.87, Iss.10, Oct 1999, Pages:1778-1789
- [26] John A. C. Bingham, “*Multicarrier Modulation for Data Transmission: An Idea Whose Time Has Come*”, IEEE Communications Magazine, pp. 5 - 14, May 1990.
- [27] H. Sari, G. Karam, and I. Jeanclaude, “*Transmission techniques for digital terrestrial TV broadcasting*” *IEEE Communications Magazine*, pp.100–109, Feb. 1995.
- [28] C. Eklund, “*IEEE Standard 802.16: A Technical Overview of the WirelessMAN™ Air Interface for Broadband Wireless Access*,” IEEE Commun. Mag., pp. 98-107, June 2002
- [29] IEEE Std 802.11a-1999(R2003), “*Part 11: Wireless LAN Medium Access Control (MAC) and Physical Layer (PHY) specifications: High-speed Physical Layer in the 5 GHz Band*”, June 2003
- [30] IEEE Std 802.11g, “*Part 11: Wireless LAN Medium Access Control (MAC) and Physical Layer (PHY) specifications Amendment 4: Further Higher Data Rate Extension in the 2.4 GHz Band*”, June 2003
- [31] ETSI TS 101 475, ” *Broadband Radio Access Networks (BRAN); HIPERLAN Type 2; Physical (PHY) layer*”, April 2000
- [32] J.M. Cioffi., “*A multicarrier primer*”. Stanford University, “<http://www.stanford.edu/group/cioffi/documents/multicarrier.pdf>”, last accessed on 15.05.2007
- [33] What does WiMAX Forum Certified™ mean?, “<http://www.wimaxforum.org/technology/faq/>”, last accessed on 02.06.2007
- [34] Daniel S. Baum, “*Simulating the SUI Channel Models*”, IEE 802.163c-01_53

Appendix

Matlab code for IEEE 802.16 OFDM transmitter, receiver and SUI channel model.

```
% IEEE 802.16 TX
```

```
% randomizer
function randomized_data = randomizer(data)
% randomizer(data): randomizes each allocation of data block as specified in
% 802.16

global IEEE80216params;

%initialization value for PRBS generator
if (IEEE80216params.Link.DIUC == 0 ) && (IEEE80216params.Link.direction == 'Dlink')
    seed_value=[0 0 0 0 0 0 1 0 1 0 1 0 0 1];
else
    % At the start of each burst except burst#1, the randomizer shall
    % be initialized with the following seed_value
    seed1=de2bi(IEEE80216params.Link.BSID,4,'left-msb');
    seed2=de2bi(IEEE80216params.Link.DIUC,4,'left-msb');
    seed3=de2bi(IEEE80216params.Link.FrameNo,4,'left-msb'); % The frame number
    %used for initialization refers to the frame in which the downlink burst is transmitted

    seed_value= horzcat(seed1,horzcat([1 1],horzcat(seed2,horzcat([1],seed3))));
end;

% data randomization

for i=1:size(data,2)

    % XORing of bit X15 and bit X14
    xor_out= bitxor(seed_value(15), seed_value(14));
    %randomized data value
    randomized_data(i)= bitxor(xor_out, data(i));
    %new seed value
    seed_value=[xor_out seed_value(1:14)];
end
randomized_data;
clear seed_value
clear data

% RS encoder
function rs_encoded_data=rs_encoder(data)

%% rs_encoder(data):Shortend and punctured RS encoder to enable variable block sizes and
%% variable error correction capability
%% Has been derived from a systematic RS(N=255,K=239,T=8)code using GF(2^8)
global IEEE80216params;

%get parameters for RS encoder
```

```

generator=IEEE80216params.RS.generator;
N=IEEE80216params.RS.N;
K=IEEE80216params.RS.K;
T=IEEE80216params.RS.T;

%Data manipulation for RS CODER Input
num_bits=size(data,2); % number of bit in data block
num_bytes=num_bits/8;% number of byte
clear num_bits;

%convert from binary to uint8
bytes=(bi2de(reshape(data,8,num_bytes).','left-msb').');

%get number of block required to fit data
num_blocks=ceil(num_bytes/K);

%if we have multiple of block number of bytes then insert and extra block to
%have a trailing 0x00
if(num_blocks==floor(num_bytes/K))
    num_blocks=num_blocks+1;
end

bytes(num_bytes+1:num_blocks*K-1)=255;
clear num_bytes;
%last byte in the bust is 0x00
bytes=[bytes 0];

%now do the encoding
msg_block=reshape(bytes,K,num_blocks).'; %the rows are the blocks to be encoded
refl=msg_block;
clear num_blocks;
clear bytes;

%RS encoding is bypassed for BPSK modulation
if(N == K)
    rs_data=msg_block;
else

%do RS encoding for other scheme
rsenc_block=rsenc(gf(msg_block,8),N,K,[],'beginning');
rs_data=double(rsenc_block.x); % conversion of GF into Double

end
clear msg_block;
clear rsenc_block;
%conversion to binary
num_blocks=size(rs_data,1);
for i=1:num_blocks
    %get the binary data from decimal numbers
    bit_data=de2bi(rs_data(i,:),'8','left-msb').';
    rs_encoded_data(i,:)=bit_data(:);
end
clear rs_data;
clear bit_data;

```

```

%CC Encoder
function conv_encoded_data=conv_encoder(data)

%conv_encoder(data): encodes RS encoded block with puncturing pattern and
%serialization order as specified in Table 214
global IEEE80216params;

%Code Rate p/q
p=IEEE80216params.CC.p;
q=IEEE80216params.CC.q;

%determine number of blocks
num_blocks=size(data,1)

%CC encoding of each block
for i=1:num_blocks
    conv_encoded_data(i,:)=convenc(data(i,:),IEEE80216params.CC.trellis);
end
clear num_blocks;

% puncturing pattern and serialization order according to TABLE 214 of IEEE802.16-2004 Spec. (Page
433)
% for rate of (1/2)no puncturing is required.

if (p==2)&&(q==3) %X1Y1Y2:
    conv_encoded_data(:,3:4:end)=[];

else
    if (p==3)&&(q==4) %X1Y1Y2Y3
        conv_encoded_data(:,3:6:end)=[];
        conv_encoded_data(:,5:5:end)=[];
    else
        if (p==5)&&(q==6) %X1Y1Y2X3Y4X5
            conv_encoded_data(:,3:10:end)=[];
            conv_encoded_data(:,5:9:end)=[];
            conv_encoded_data(:,5:8:end)=[];
            conv_encoded_data(:,7:7:end)=[];
        end
    end
end
clear p;
clear q;

%interleaver

function interleaved_data = interleaver(data)
%% interleaver(data): interleave all encoded data with a block size
%% corresponding to the number of coded bits per the allocated subchannels
%% per OFDM symbol (Ncbps)
global IEEE80216params;
%% global phys_profile

switch (IEEE80216params.Modulation.Type) %% this will come from set phy_profile so add that as global
after making that
    case 'BPSK'
        Ncbps= 12* IEEE80216params.Modulation.subchn;

```

```

        s= ceil( 1/2 );
    case 'QPSK'
        Ncbps= 24* IEEE80216params.Modulation.subchn;
        s= ceil( 2/2 );
    case '16QAM'
        Ncbps= 48* IEEE80216params.Modulation.subchn;
        s= ceil( 4/2 );
    case '64QAM'
        Ncbps= 72* IEEE80216params.Modulation.subchn;
        s= ceil( 6/2 );
end

%% check
if ((size(data,2) < Ncbps) || (size(data,2) > Ncbps))
    error('size mismatch');
end

% first permutation accoring to eqn. 71
for k=0:Ncbps-1
    mk=(Ncbps/12)*mod(k,12)+floor(k/12);
    firstPerm_interleaved_data(:,mk+1)=data(:,k+1);
end
clear k;
clear mk;
clear punct_code;

%second permutation according to eqn. 72
for k=0:Ncbps-1
    jk=s*floor(k/s)+mod((k+Ncbps-floor(12*k/Ncbps)),s);
    interleaved_data(:,jk+1)=firstPerm_interleaved_data(:,k+1);
end
clear jk;
clear data;
clear firstPerm_interleaved_data;
clear Ncbps;

%pilot modulator
function w_k=pilot_modulator(data)

%global simulation_opts;
global IEEE80216params;

sequence_length=size(data,1);

if (IEEE80216params.Link.direction == 'Dlink')
    initialization_seq=de2bi(hex2dec('7FF'),'left-msb');
    Symbol_off=2;
else
    initialization_seq= de2bi(hex2dec('555'),'left-msb');
    Symbol_off=1;
end

for i=1:(sequence_length+Symbol_off)
    initialization_seq_msb=bitxor(initialization_seq(11),initialization_seq(9));
    initialization_seq=[initialization_seq_msb initialization_seq(1:10)];
    w_k(i)=initialization_seq_msb;

```

```

end

w_k(1:Symbol_off)=[];

%constalletaion mapper

function const_mapped_data= constellation_mapper(data,w_k)
% constellation_mapper(data,w_k) maps the data to appropriate subcarrier.
%%support only full subchannelization

%global simulation_opts;
global IEEE80216params;

num_blocks=size(data,1);% get the block size, in bits, that gets encoded
const_mapped_data=zeros(num_blocks,IEEE80216params.Ofdm.Nfft);% initialize const_mapped_data to
zero
clear num_blocks;

switch (IEEE80216params.Modulation.Type)

case 'BPSK'
    modulated_data=pskmod(data,2);

case 'QPSK'
    symbol_size=2;
    scaling_fact= sqrt(1/2);

    %convert the symbol into [0...M-1]
    for i=1:symbol_size:size(data,2)
        mod_inp(:,floor(i/symbol_size) +1)=bi2de(data(:,i:i+symbol_size-1),'left-msb');
    end
    %QPSK is implemented as 4 QAM
    %scaled modulated data
    modulated_data=scaling_fact
    *genqammod(mod_inp,IEEE80216params.Modulation.gray_map_qpsk);

case '16QAM'

    symbol_size=4;
    scaling_fact= sqrt(1/10);

    %convert the symbol into [0...M-1]
    for i=1:symbol_size:size(data,2)
        mod_inp(:,floor(i/symbol_size) +1)=bi2de(data(:,i:i+symbol_size-1),'left-msb');
    end
    %scaled modulated data
    modulated_data=scaling_fact
    *genqammod(mod_inp,IEEE80216params.Modulation.gray_map_16qam);

case '64QAM'

    symbol_size=6;
    scaling_fact= sqrt(1/42);

```

```

%convert the symbol into [0...M-1]
for i=1:symbol_size:size(data,2)
    mod_inp(:,floor(i/symbol_size)+1)=bi2de(data(:,i:i+symbol_size-1),'left-msb');
end

%scaled modulated data
modulated_data=scaling_fact
*genqammod(mod_inp,IEEE80216params.Modulation.gray_map_64qam);

end

% place the modulated data into data subcarriers
const_mapped_data(:,IEEE80216params.Map.DataSubCars)=modulated_data(:,1:end);

clear data;
clear modulated_data;

% fill in the pilot subcarriers
if (IEEE80216params.Link.direction=='Dlink')
    const_mapped_data(:,41)=complex(1-2*w_k,0);
    const_mapped_data(:,91)=complex(1-2*w_k,0);
    const_mapped_data(:,192)=complex(1-2*w_k,0);
    const_mapped_data(:,217)=complex(1-2*w_k,0);

    const_mapped_data(:,66)=complex(1-2*(1-w_k),0);
    const_mapped_data(:,116)=complex(1-2*(1-w_k),0);
    const_mapped_data(:,142)=complex(1-2*(1-w_k),0);
    const_mapped_data(:,167)=complex(1-2*(1-w_k),0);
else %Ulink
    const_mapped_data(:,41)=complex(1-2*w_k,0);
    const_mapped_data(:,91)=complex(1-2*w_k,0);
    const_mapped_data(:,192)=complex(1-2*w_k,0);
    const_mapped_data(:,217)=complex(1-2*w_k,0);
    const_mapped_data(:,142)=complex(1-2*w_k,0);
    const_mapped_data(:,167)=complex(1-2*w_k,0);

    const_mapped_data(:,66)=complex(1-2*(1-w_k),0);
    const_mapped_data(:,116)=complex(1-2*(1-w_k),0);
end

% ofdm modulator

function timedomain_data_vec = ofdm_modulator(data)

%global simulation_opts;
global IEEE80216params;

timedomain_data=ifft(data.);

```

```

%CP length
CP_len=IEEE80216params.Ofdm.G*size(timedomain_data,1);

% append the CP at the beginning of time data
timedomain_data_cp=[timedomain_data(end+1-CP_len:end,:);timedomain_data];

% time domain data vector
timedomain_data_vec=timedomain_data_cp(:).';
%IEEE 802.16 Receiver

% ofdm demodulator
function [data_sub,pilot_sub]=ofdm_demodulator(rx_signal)
%% ofdm_demodulator(rx_signal):generate frequency domain OFDM symbol
global IEEE80216params;

symbol_length=IEEE80216params.Ofdm.Nfft*(1+IEEE80216params.Ofdm.G);%symbol length
no_of_symbols=floor(size(rx_signal,2)/symbol_length);%number of symbol

for i=1:IEEE80216params.simOpts.RxDiv

    rx_data=rx_signal(i,:);

    clear rx_signal;
    ofdm_symbol=rx_data(1:no_of_symbols*symbol_length);
    ofdm_symbol=reshape(ofdm_symbol,symbol_length,no_of_symbols);

    clear rx_data;
    % separating guard
    ofdm_symbol=ofdm_symbol(symbol_length-IEEE80216params.Ofdm.Nfft+1:symbol_length,:);
    % fft operation

    freq_domain_data=fft(ofdm_symbol)/(IEEE80216params.Ofdm.Nfft/sqrt(IEEE80216params.Ofdm.Nused)
/IEEE80216params.simOpts.RxDiv);
    %separation of pilot and data symbol
    data_sub(i,:)=freq_domain_data(IEEE80216params.Map.DataSubCars,:);
    pilot_sub(i,:)=freq_domain_data(IEEE80216params.Map.PilotSubCars,:);
end

% de-mapper
function demod_bit_stream=demodulator(ofdm_demod_symbol)
% demodulator(ofdm_demod_symbol): demodulate according to the selected scheme.
% rescaling has been done since symbols were scaled before in mapping
global IEEE80216params;

switch (IEEE80216params.Modulation.Type)
case 'BPSK'
    %There is no need for scaling in BPSK
    demodulated_symbol=pskdemod(ofdm_demod_symbol,2);
    symbol_size=1;
case 'QPSK'
    %scaling
    scalin_fact=sqrt(1/2);
    ofdm_demod_symbol=ofdm_demod_symbol/scalin_fact;
    %4QAM demodulation

```

```

demodulated_symbol=genqamdemod(ofdm_demod_symbol,IEEE80216params.Modulation.gray_map_qps
k);
    symbol_size=2;
case '16QAM'
    scalin_fact=sqrt(1/10);
    ofdm_demod_symbol=ofdm_demod_symbol/scalin_fact;
    %16QAM demodulation

demodulated_symbol=genqamdemod(ofdm_demod_symbol,IEEE80216params.Modulation.gray_map_16q
am);
    symbol_size=4;

case '64QAM'
    scalin_fact=sqrt(1/42);
    ofdm_demod_symbol=ofdm_demod_symbol/scalin_fact;
    %64QAM demodulation

demodulated_symbol=genqamdemod(ofdm_demod_symbol,IEEE80216params.Modulation.gray_map_64q
am);
    symbol_size=6;
end

%symbol to bit conversion
s=size(demodulated_symbol,2);
for i=1:s
    demodulated_bit=de2bi(demodulated_symbol(:,i),symbol_size,'left-msb');
    demod_bit_stream(:,i)=demodulated_bit(:);
end

demod_bit_stream=demod_bit_stream.';

% de-interleaver
function deinterleaved_data = deinterleaver(data)
%%deinterleaver(data): deinterleaves received data based on two step
%%permutation as per specification

global IEEE80216params;

%interleaver block size on varing modulation scheme
switch (IEEE80216params.Modulation.Type)

    case 'BPSK'
        Ncbps= 12* IEEE80216params.Modulation.subchn;
        s= ceil( 1/2 );
    case 'QPSK'
        Ncbps= 24*IEEE80216params.Modulation.subchn;
        s= ceil( 2/2 );
    case '16QAM'
        Ncbps= 48* IEEE80216params.Modulation.subchn;
        s= ceil( 4/2 );
    case '64QAM'
        Ncbps= 72* IEEE80216params.Modulation.subchn;
        s= ceil( 6/2 );

```

```

end

% first permutation
for j=0:Ncbps-1
    jk=s*floor(j/s)+mod(j+floor(12*j/Ncbps),s)+1;
    firstperm_deinterleaved_data(:,jk)= data(:,j+1);
end

% second permutation
for j=0:Ncbps-1
    jl=12*j-(Ncbps-1)*floor(12*j/Ncbps)+1;
    deinterleaved_data(:,jl)=firstperm_deinterleaved_data(:,j+1);
end

% convolutional decoder

function convdecod_data=conv_decoder(data)
%conv_decoder(data): decodes received data with puncturing pattern and
%serialization order as specified in Table 214

global IEEE80216params;

%%Code Rate p/q
p=IEEE80216params.CC.p;
q=IEEE80216params.CC.q;

%mapping 0's to 1 and 1's to-1
data=-2*data +1;

%depuncturing the data as per the given in table 212

if ((p==1) && (q==2)) %puncturing is not required
    punc_pattern=[1 2];
    s=1*2;
else
if ((p==2) && (q==3))
%X1Y1Y2
punc_pattern=[1 2 4];
s=2*2;
else
if ((p==3) && (q==4))
%X1Y1Y2X3
punc_pattern=[1 2 4 5];
s=2*3;
else
%X1Y1Y2X3Y4X5
if ((p==5) &&(q==6))
punc_pattern=[1 2 4 5 8 9];
s=2*5;
end
end
end
end
end
end

```

```

syms=size(data,1);
rem_size=rem(size(data,2), length(punc_pattern));

for i=1:syms

    depunct=zeros(s,floor(size(data,2)/length(punc_pattern)));
    depunct_bits=reshape(data(i,1:end-
rem_size),length(punc_pattern),floor(size(data,2)/length(punc_pattern)));
    depunct(punc_pattern,:)=depunct(punc_pattern,:)+depunct_bits;

    if(rem_size ~=0)
        remd=zeros(1,s);
        remd_bits=data(end-rem_size+1:end);
        remd(punc_pattern(1:rem_size))=remd_bits+remd(punc_pattern(1:rem_size));

        native_code(i,:)=[depunct(:)' remd];
    else
        native_code(i,:)=depunct(:);
    end
end

%viterbi decoding of native_code
for i=1:syms
    convdecod_data(i,:)=vitdec(native_code(i,:),IEEE80216params.CC.trellis,96,'trunc','unquant');
end

%RS decoder

function [rsdecoded_data errs_corr]=rs_decoder(data)

%% rs_encoder(data):Shortend and punctured RS decoder to enable variable block sizes and
%% variable error correction capability
%% Has been derived from a systematic RS(N=255,K=239,T=8)code using GF(2^8)
global IEEE80216params;

%get parameters for RS encoder
generator=IEEE80216params.RS.generator;
N=IEEE80216params.RS.N;
K=IEEE80216params.RS.K;
T=IEEE80216params.RS.T;

%RS decoder starts here
syms=size(data,1);% number bits
num_bytes=size(data,2)/8; % number of bytes in each block

for i=1:syms
    %bit to byte conversion
    bytes=bi2de(reshape(data(i,:),8,num_bytes).','left-msb').;
    dblock(i,:)=bytes;
end

if(N == K)% bypass RS decoding for BPSK
rsdecoded_data=dblock;

```

```

errs_corr=0;
else
%decode the data and get the error correction count
[rsdecoded_data,errs_corr]=rsdec(gf(dblock,8),N,K,[],'beginning');
% GF to double conversion
rsdecoded_data=double(rsdecoded_data.x);
end

```

%% SUI- Channel

```

function rx_data=channel_sui(tx_data,ch_impulse_resp)
%channel_sui(tx_data,ch_impulse_resp): convolve the transmitted data with SUI
%channel impulse response and add noise
%
global IEEE80216params;
% initialize the receive data with zeros
rx_data=zeros(IEEE80216params.simOpts.RxDiv,size(tx_data,2)+size(ch_impulse_resp,2)-1);

%convolve tx_data with ch_impulse_response
for i=1:IEEE80216params.simOpts.RxDiv
    for j=1:IEEE80216params.simOpts.TxDiv
        rx_data(i,:)=rx_data(i,:)+conv(tx_data(j,:),ch_impulse_resp((i-
1)*IEEE80216params.simOpts.TxDiv+j,:));
    end
end

leng=size(rx_data,2);

%% AWGN NOISE
noise_varience=IEEE80216params.Ofdm.Nfft/IEEE80216params.Ofdm.Nused/(10^(IEEE80216params.si
mOpts.SNR/10))/2;

noise=sqrt(noise_varience)*(randn(IEEE80216params.simOpts.RxDiv,leng)+j*randn(IEEE80216params.si
mOpts.RxDiv,leng));

%% adding noise to rx_data
rx_data=rx_data+noise;

function [CIR,time]=cir(coeffs,time,systemtime)
% cir(coeffs,time,systemtime): generate the channel impulse response
% coeffs: channel coefficients
% time: time interval between the change of each coeff. is required
% systemtime: simulated system time

global IEEE80216params;

persistent counter;
if (isempty(counter) || (systemtime==0))
    counter=1;
end

```

```

ch_no= IEEE80216params.simOpts.TxDiv*IEEE80216params.simOpts.RxDiv; % number of antenna pairs

if(systemtime-time >=IEEE80216params.channel.Nyquist_time)
counter=mod(counter,length(coeffs))+1;
time=time+IEEE80216params.channel.Nyquist_time;
end

% initialize the CIR with zeros
CIR=zeros(ch_no,max(IEEE80216params.channel.conv_locs));
%generate CIR
for i=1:length(IEEE80216params.channel.tau)

CIR(:,IEEE80216params.channel.conv_locs(i))=CIR(:,IEEE80216params.channel.conv_locs(i))+coeffs(:,i,
counter);
end

function paths_r=ch_fading(leng)
%% %% ch_fading(leng): generates the fading coefficients

global IEEE80216params;

ch_no= IEEE80216params.simOpts.TxDiv*IEEE80216params.simOpts.RxDiv; % number of antenna pairs

L=length(IEEE80216params.channel.P); % number of taps

%% %% coeff. generation
for j=1:ch_no

paths_r(j,,:)=sqrt(1/2)*randn(L,leng)+j*randn(L,leng).*((sqrt(IEEE80216params.channel.variance))*ones(
1,leng));

    for i=1:L
        temp(1:leng)=paths_r(j,i,:);
        path=fftfilt(IEEE80216params.channel.filter(i,:),[temp
zeros(1,IEEE80216params.simOpts.DoppTaps)]);
        paths_r(j,i,:)=path(1+IEEE80216params.simOpts.DoppTaps/2:end-
IEEE80216params.simOpts.DoppTaps/2);
    end
end

%% %% Correlation Matrix
for i=1:ch_no
    for j=1:ch_no
        if (i~=j)
            correlation_matrix(i,j)=IEEE80216params.channel.AntCorlnFac;
        else
            correlation_matrix(i,j)=1;
        end
    end
end
end

correlation_matrix=sqrtm(correlation_matrix);

% correlate according to correlation matrix

```

```

for tap=1:L
    paths_r(:,tap,:)=correlation_matrix*squeeze(paths_r(:,tap,:));
end

for i=1:ch_no
    paths_r(i,:,:)=squeeze(paths_r(i,:,:));
end

for tap=1:L
    paths_r(1:end,tap,1:end)=IEEE80216params.channel.paths_c(tap)+paths_r(1:end,tap,1:end);
end

% coeff. normalization
paths_r=IEEE80216params.channel.Normfact*paths_r;

```

%% %% IEEE 802.16 model Parameters

```
function IEEE80216params=IEEE80216_params()
```

```

%% %% OFDM SYMBOL PARAMETERS
%% %% primitive OFDM symbol parameter

```

```

IEEE80216params.Ofdm.BW=1.75*10^6 % nominal channel bandwidth
IEEE80216params.Ofdm.Nused=200; % number of used subcarrier
%% sampling factor
BW=IEEE80216params.Ofdm.BW/(10^6);
if (rem(BW,1.75)==0)
    IEEE80216params.Ofdm.n=8/7;
else if (rem(BW,1.5)==0)
    IEEE80216params.Ofdm.n=86/75;
else if (rem(BW,1.25)==0)
    IEEE80216params.Ofdm.n=144/125;
else if (rem(BW,2.75)==0)
    IEEE80216params.Ofdm.n=316/275;
else if (rem(BW,2.0)==0)
    IEEE80216params.Ofdm.n=57/50;
else % otherwise
    IEEE80216params.Ofdm.n=8/7;
end
end
end
end
end
end

```

```
IEEE80216params.Ofdm.G=1/4 % ratio of CP time to useful time
```

```

%%% derived OFDM symbol parameter

IEEE80216params.Ofdm.Nfft=256; % smallest power of 2 greater than Nused
% sampling frequency
IEEE80216params.Ofdm.Fs=floor((IEEE80216params.Ofdm.n*IEEE80216params.Ofdm.BW)/8000)*8000;
% subcarrier spacing
IEEE80216params.Ofdm.del_f=IEEE80216params.Ofdm.Fs/IEEE80216params.Ofdm.Nfft;
% useful symbol time
IEEE80216params.Ofdm.Tb=1/(IEEE80216params.Ofdm.del_f);
% CP time
IEEE80216params.Ofdm.Tg=IEEE80216params.Ofdm.G*IEEE80216params.Ofdm.Tb;
% symbol time
IEEE80216params.Ofdm.SymbolTime=IEEE80216params.Ofdm.Tg+IEEE80216params.Ofdm.Tb;
% sampling time
IEEE80216params.Ofdm.SampleTime=IEEE80216params.Ofdm.Tb/IEEE80216params.Ofdm.Nfft;
% number of pilot carrier
IEEE80216params.Ofdm.Npilot=8;
% number of data carrier
IEEE80216params.Ofdm.Ndata=IEEE80216params.Ofdm.Nused- IEEE80216params.Ofdm.Npilot;

%MAPPING Parameters : full subchannelization
IEEE80216params.Map.DataSubCars=[29:40 42:65 67:90 92:115 117:128 130:141 143:166 168:191
193:216 218:229];
IEEE80216params.Map.PilotSubCars=[41 66 91 116 142 167 192 217];
IEEE80216params.Map.GuardSubCars=[1:28 230:256];
IEEE80216params.Map.UsedSubCars=[29:128 130:229];

% Link Parameters
IEEE80216params.Link.direction='Dlink'; %always model applies to this
IEEE80216params.Link.DIUC=7;
IEEE80216params.Link.BSID=1;
IEEE80216params.Link.FrameNo=1 % transmission start from frame number 1
IEEE80216params.Link.Frames=250; % number of frames to be sent
IEEE80216params.Link.FrameTime=4*10^(-3);

IEEE80216params.Link.Alloc_frac=0.1;
IEEE80216params.Link.BurstTime=IEEE80216params.Link.Alloc_frac*IEEE80216params.Link.FrameTime
% RS encoder parameter
IEEE80216params.RS.generator=rsgenpoly(255,239,[],0); % RS field and code generator

%CC encoder parameter
IEEE80216params.CC.trellis=poly2trellis(7,[171 133]);% CC trellis as per specification
IEEE80216params.CC.tblen=32; %the traceback length

%MODULATION params
IEEE80216params.Modulation.subchn=16; % full subchannelization
% gray coded mappings
graymap_16=['1101'
'1100'
'1110'
'1111'
'1001'
'1000'

```

```
'1010'  
'1011'  
'0001'  
'0000'  
'0010'  
'0011'  
'0101'  
'0100'  
'0110'  
'0111'];
```

```
graymap_64=['111011'
```

```
'111010'  
'111000'  
'111001'  
'111101'  
'111100'  
'111110'  
'111111'  
'110011'  
'110010'  
'110000'  
'110001'  
'110101'  
'110100'  
'110110'  
'110111'  
'100011'  
'100010'  
'100000'  
'100001'  
'100101'  
'100100'  
'100110'  
'100111'  
'101011'  
'101010'  
'101000'  
'101001'  
'101101'  
'101100'  
'101110'  
'101111'  
'001011'  
'001010'  
'001000'  
'001001'  
'001101'  
'001100'  
'001110'  
'001111'  
'000011'  
'000010'  
'000000'  
'000001'  
'000101'
```

```

'000100'
'000110'
'000111'
'010011'
'010010'
'010000'
'010001'
'010101'
'010100'
'010110'
'010111'
'011011'
'011010'
'011000'
'011001'
'011101'
'011100'
'011110'
'011111'];

% binary to decimal conversion
mapping_16qam=bin2dec(graymap_16).';
mapping_64qam=bin2dec(graymap_64).';
mapping_qpsk= [ 2 3 0 1];

clear graymap_16;
clear graymap_64;

% QPSK - implemented as 4 QAM
constell_qpsk=qammod([0:3],4);
IEEE80216params.Modulation.gray_map_qpsk(mapping_qpsk(:)+1)=constell_qpsk(:);
% 16QAM
constell_16qam=qammod([0:15],16);
IEEE80216params.Modulation.gray_map_16qam(mapping_16qam(:)+1)=constell_16qam(:);
% 64QAM
constell_64qam=qammod([0:63],64);
IEEE80216params.Modulation.gray_map_64qam(mapping_64qam(:)+1)=constell_64qam(:);
clear mapping_qpsk;
clear mapping_16qam;
clear mapping_64qam;
clear constell_qpsk;
clear constell_16qam;
clear constell_64qam;

IEEE80216params.simOpts.TxDiv=1;
IEEE80216params.simOpts.RxDiv=1;

IEEE80216params.simOpts.DoppTaps=256 % taps in doppler filter

IEEE80216params.simOpts.ChanModel='SUI2'

switch(IEEE80216params.simOpts.ChanModel)
case 'SUI1'
    IEEE80216params.channel.P=[0 -15 -20];

```

```
IEEE80216params.channel.K=[4 0 0];  
IEEE80216params.channel.tau=[0 0.4 0.9];  
IEEE80216params.channel.Dop=[0.4 0.3 0.5];  
IEEE80216params.channel.AntCorr=0.7;  
IEEE80216params.channel.Fnorm=-0.1771;  
IEEE80216params.channel.Trms=0.111;
```

case 'SUI2'

```
IEEE80216params.channel.P=[0 -12 -15];  
IEEE80216params.channel.K=[2 0 0];  
IEEE80216params.channel.tau=[0 0.4 1.1];  
IEEE80216params.channel.Dop=[0.2 0.15 0.25];  
IEEE80216params.channel.AntCorr=0.5;  
IEEE80216params.channel.Fnorm=-0.393;  
IEEE80216params.channel.Trms=0.202;
```

case 'SUI3'

```
IEEE80216params.channel.P=[0 -5 -10];  
IEEE80216params.channel.K=[1 0 0];  
IEEE80216params.channel.tau=[0 0.4 0.9];  
IEEE80216params.channel.Dop=[0.4 0.3 0.5];  
IEEE80216params.channel.AntCorr=0.4;  
IEEE80216params.channel.Fnorm=-1.5113;  
IEEE80216params.channel.Trms=0.264;
```

case 'SUI4'

```
IEEE80216params.channel.P=[0 -4 -8];  
IEEE80216params.channel.K=[0 0 0];  
IEEE80216params.channel.tau=[0 1.5 4];  
IEEE80216params.channel.Dop=[0.2 0.15 0.25];  
IEEE80216params.channel.AntCorr=0.3;  
IEEE80216params.channel.Fnorm=-1.9218;  
IEEE80216params.channel.Trms=1.257;
```

case 'SUI5'

```
IEEE80216params.channel.P=[0 -5 -10];  
IEEE80216params.channel.K=[0 0 0];  
IEEE80216params.channel.tau=[0 4 10];  
IEEE80216params.channel.Dop=[2 1.5 2.5];  
IEEE80216params.channel.AntCorr=0.3;  
IEEE80216params.channel.Fnorm=-1.5113;  
IEEE80216params.channel.Trms=2.842;
```

case 'SUI6'

```
IEEE80216params.channel.P=[0 -10 -14];  
IEEE80216params.channel.K=[0 0 0];  
IEEE80216params.channel.tau=[0 14 20];  
IEEE80216params.channel.Dop=[0.4 0.3 0.5];  
IEEE80216params.channel.AntCorr=0.3;  
IEEE80216params.channel.Fnorm=-0.5683;  
IEEE80216params.channel.Trms=5.240;
```

```

end

%%% fading
IEEE80216params.channel.P=10.^(IEEE80216params.channel.P/10);% db to linear scale
IEEE80216params.channel.variance=IEEE80216params.channel.P./(IEEE80216params.channel.K+1);% variance
IEEE80216params.channel.meanp=IEEE80216params.channel.P.*(IEEE80216params.channel.K./(IEEE80216params.channel.K+1));
IEEE80216params.channel.m=sqrt(IEEE80216params.channel.meanp);
IEEE80216params.channel.paths_c=IEEE80216params.channel.m;

IEEE80216params.channel.Nyquist_freq=2*max(IEEE80216params.channel.Dop);% Nyquist freq. of channel
IEEE80216params.channel.Nyquist_time=(1/IEEE80216params.channel.Nyquist_freq);

IEEE80216params.channel.conv_locs=1+round(IEEE80216params.channel.tau/(IEEE80216params.Ofdm.SampleTime*10^6));

%%% channel filter

IEEE80216params.channel.filter=zeros(length(IEEE80216params.channel.P),IEEE80216params.simOpts.DoppTaps);
for i=1:length(IEEE80216params.channel.P)
    D=IEEE80216params.channel.Dop(i)/max(IEEE80216params.channel.Dop)/2;

f0=[0:floor(IEEE80216params.simOpts.DoppTaps*D)]/(floor(IEEE80216params.simOpts.DoppTaps*D));
    PSD = 0.785*f0.^4 - 1.72*f0.^2 + 1.0;
    filter=[PSD(1:end-1) zeros(1,IEEE80216params.simOpts.DoppTaps-2*floor(IEEE80216params.simOpts.DoppTaps*D)) PSD(end:-1:2) ];
    filter=sqrt(filter);
    filter=ifftshift(fft(filter));
    filter= real(filter);
    filter=filter/sqrt(sum(filter.^2));
    IEEE80216params.channel.filter(i,:)=filter;
end

IEEE80216params.channel.Normfact=10^(IEEE80216params.channel.Fnorm/20);

%%% channel coding profile selection

function IEEE80216params=ch_coding_profile(ch_cod_prof_no,IEEE80216params)
%%%ch_coding_profile(ch_cod_prof_no,IEEE80216params): set the modulation
%%%scheme and the parameter for RS-CC coder

%select profile
switch(ch_cod_prof_no)
case 1
    IEEE80216params.Modulation.Type='BPSK';
    IEEE80216params.RS.N=12;
    IEEE80216params.RS.K=12;
    IEEE80216params.RS.T=0;

```

```

        IEEE80216params.CC.p=1;
        IEEE80216params.CC.q=2;
case 2
    IEEE80216params.Modulation.Type='QPSK';
    IEEE80216params.RS.N=32;
    IEEE80216params.RS.K=24;
    IEEE80216params.RS.T=4;
    IEEE80216params.CC.p=2;
    IEEE80216params.CC.q=3;
case 3
    IEEE80216params.Modulation.Type='QPSK';
    IEEE80216params.RS.N=40;
    IEEE80216params.RS.K=36;
    IEEE80216params.RS.T=2;
    IEEE80216params.CC.p=5;
    IEEE80216params.CC.q=6;
case 4
    IEEE80216params.Modulation.Type='16QAM';
    IEEE80216params.RS.N=64;
    IEEE80216params.RS.K=48;
    IEEE80216params.RS.T=8;
    IEEE80216params.CC.p=2;
    IEEE80216params.CC.q=3;
case 5
    IEEE80216params.Modulation.Type='16QAM';
    IEEE80216params.RS.N=80;
    IEEE80216params.RS.K=72;
    IEEE80216params.RS.T=4;
    IEEE80216params.CC.p=5;
    IEEE80216params.CC.q=6;
case 6
    IEEE80216params.Modulation.Type='64QAM';
    IEEE80216params.RS.N=108;
    IEEE80216params.RS.K=96;
    IEEE80216params.RS.T=6;
    IEEE80216params.CC.p=3;
    IEEE80216params.CC.q=4;
case 7
    IEEE80216params.Modulation.Type='64QAM';
    IEEE80216params.RS.N=120;
    IEEE80216params.RS.K=108;
    IEEE80216params.RS.T=6;
    IEEE80216params.CC.p=5;
    IEEE80216params.CC.q=6;
otherwise
    error('Not a valid profile number: valid range[1:6]');
end

%based on this profile decide on the data length
Nosyms=floor(IEEE80216params.Link.BurstTime/IEEE80216params.Ofdm.SymbolTime);
IEEE80216params.Link.Dataleng=IEEE80216params.RS.K*Nosyms -1; % number of bytes
IEEE80216params.Link.Dataleng=IEEE80216params.Link.Dataleng*8; % number of bytes

```